Institut für Veterinärbiochemie und Molekularbiologie
der Vetsuisse-Fakultät Universität Zürich

Direktor: Prof. Dr. Dr. Michael O. Hottiger

Posttranslational Modification of Histone 1.4 by SET7/9 and ARTD1

Inaugural-Dissertation

zur Erlangung der Doktorwürde der
Vetsuisse-Fakultät Universität Zürich

vorgelegt von

Marc André Barandun

Tierarzt
von Feldis GR

genehmigt auf Antrag von

Prof. Dr. Dr. Michael O. Hottiger, Referent
Prof. Dr. Hanspeter Nägeli, Korreferent

2014

Table of Contents

1. Zusammenfassung

Proteine sind sehr wichtig für die Steuerung von biochemischen Prozessen und verleihen den Zellen ihre Struktur und Funktion. Proteine werden nach ihrer Bildung (d.h. posttranslational) meist zusätzlich chemisch modifiziert, um deren Funktion und enzymatische Aktivität zu regulieren.

In der vorliegenden Arbeit wurde gezeigt, dass die Monomethyltransferase SET7/9 spezifisch die C-terminale Domäne der Histonvariante H1.4 an bestimmten Lysinen modifiziert (K121, K129, K159, K171, K177 und K192). Die Lysine befinden sich jeweils am Ende der Konsensus-Sequenz KAK. Ausserdem verhinderte die Zugabe von DNS zur Methylierungsreaktion die Modifikation von H1.4 durch SET7/9. Die Expressionsanalyse von GFP fusioniert mit dem ganzen H1.4 oder nur mit dessen C- oder N-terminalen Domäne in U2OS Zellen zeigte, dass alle drei Fusionsproteine entweder im Hetero- oder Euchromatin des Nukleus lokalisiert sind.

Zudem wurde gezeigt, dass H1.4 an etlichen Positionen durch die ADP-Ribosyltransferase ARTD1 modifiziert wird. Die durch ARTD1 vermittelte ADP-Ribosylierung wurde vor allem in der C-terminalen Domäne gefunden und unterdrückte die durch SET7/9 vermittelte Methylierung von H1.4.

Dieser gegenseitige Ausschluss dieser zwei posttranslationalen Modifikationen bestärkt die Hypothese, dass posttranslationale Modifikationen von strukturnahen Aminosäuren sich gegenseitig beeinflussen und so die Funktionalität des Proteins regulieren können.

2 Summary

Proteins are important for the regulation of biochemical processes and are crucial for the structure and function of cells. Proteins are post-translationally often chemically modified, which regulates their function and enzymatic activities.

The work presented in this thesis shows that the mono-methyltransferase SET7/9 modifies the linker histone H1.4 only at the C-terminal domain. Several lysine residues (K121, K129, K159, K171, K177 and K192) were identified to be methylated. SET7/9 only modified lysine residues at the terminal position of a given KAK motif. Also, the addition of DNA to the methylation reaction inhibited the modification of H1.4 by SET7/9. Expression analysis of GFP-tagged full length H1.4 or its C-terminal or N-terminal fragments in U2OS cells suggested that all fusion proteins localize to either hetero- or euchromatin in the nucleus.

Furthermore, the ADP-ribosyltransferase ARTD1 modified several amino acid residues in the C-terminal domain of H1.4, a process that inhibited SET7/9-dependent methylation. This mutual exclusion of the two modifications suggests that post-translational modification of structurally close amino acids can influence each other and thereby regulate the functionality of proteins.

3 Abbreviations

3-AB	3-aminobenzamide
aa	Amino acid(s)
ADP	Adenosine diphosphate
AMD	Automodification domain
AMPK	AMP-activated protein kinase
ARH	ADP-ribosyl hydrolase
ARTD	ADP-ribosyltransferase diphtheria toxin-like
ATP	Adenosine triphosphate
bp	base pairs
BB	Binding buffer
BRCT	BRCA1 C-terminus
BSA	Bovine serum albumin
CDK	Cyclin-dependent kinase
Cl	Cluster
CTD	Carboxy-terminal domain
DBD	DNA binding domain
DNA	Deoxyribonucleic acid
DNS	Desoxyribonukleinsäure
dNTP's	deoxy Nucleotide-Tri-Phosphates
DSB	DNA double-strand break
EB	Elution buffer
Ezh2	Enhancer of zeste homolog 2
FL	Full-length
Fr	Fragment
GFP	Green fluorescence protein
GST	Glutathione S-transferase
H1	Histone 1
H2A	Histone 2A
H2B	Histone 2B
H_2O_2	Hydrogen peroxide
H3	Histone 3
H4	Histone 4
HIF	Hypoxia inducible factor
His	Polyhistidine
HMG	High mobility group
HP1	Heterochromatin protein 1
HR	Homologous recombination
K	Lysine
KMT	Lysine methyl transferas
LPS	Lipopolysaccharide
LSD	Lysine specific demethylase
ml	Milliliter
mM	Millimolar
NAD^+	Nicotinamide adenine dinucleotide
nCi	Nanocurie
NEB	New England Biolabs
NF-κB	Nuclear factor κB

ng	Nanogramm
NLS	Nuclear localization signal
NTD	Amino-terminal domain
PAR	Poly(ADP-ribose)
PARG	Poly(ADP-ribose) glycohydrolase
PARP	Poly(ADP-ribose) polymerase
PARylation	Poly(ADP-ribosyl)ation
PBS	Phosphate buffered saline
PCR	Polymerase Chain Reaction
pH	Power of hydrogen
PRMT	Arginine methyl transferase
R	Arginine
SAM	S-adenosylmethionine
SDS-PAGE	Sodium-dodecyl-sulfate polyacrylamide gel electrophoresis
SET	Su(var)3-9, Enhancer-of-zeste, Trithorax
TBS	Tris buffered saline
TBS-T	Tris buffered saline Tween 20
WB	Washing buffer
WGR	Tryptophan-glycine-arginine motif
wt	Wild type
ZBD	Zinc binding domain
ZF	Zinc finger
µl	Microliter
µM	Micromolar

4 Introduction

4.1 Chromatin

The human genome consists of $3.2x10^9$ nucleotide bases that form a linear chain of around 2 m in length (roughly 100'000 times the size of a cell) [1]. To fit into the nucleus of the cell, the DNA thus has to be tightly compacted. Since each eukaryotic cell contains exactly one copy of the entire genome, the condensation of the DNA is absolutely required. The compaction of the DNA is controlled through structural arrangements of the DNA with histones and non-histone proteins, which together form the chromatin [2] (Fig. 1).

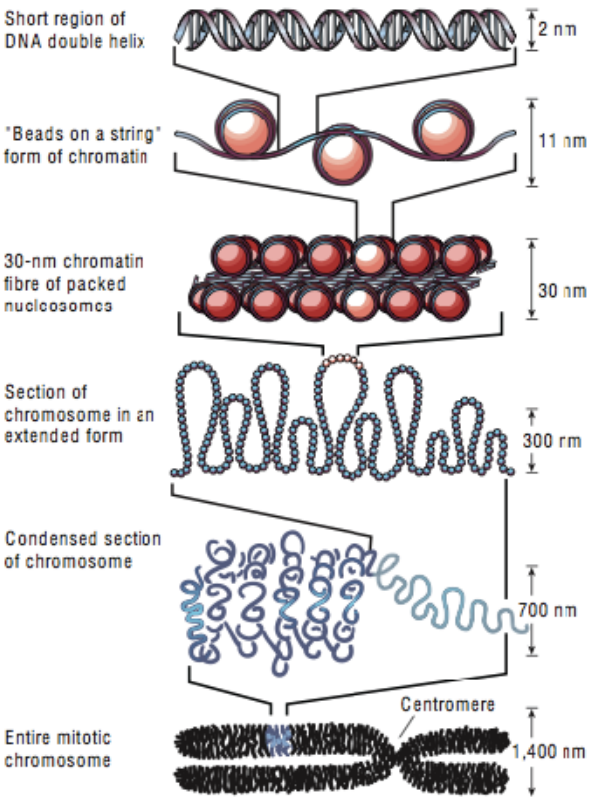

Figure 1: DNA compaction within the interphase nucleus occurs through different histone-dependent interactions. The 'beads on a string' structure (10 nm fiber) is formed by wrapping DNA around nucleosomes. Histone tail-mediated nucleosome-nucleosome interactions induce the formation of the 30 nm fiber and an even higher compaction is accomplished through tail-mediated association of individual fibers [3].

This chromatin structure is a drawback for genomic activities such as replication, transcription, repair or recombination, because it restricts the accessibility of the DNA. Hence, there has to be a mechanism that makes the DNA more accessible in response to different stimuli. Exchanging or chemically modifying histones can mediate this needed change of the chromatin structure [2]. There are two major states of chromatin: euchromatin

and heterochromatin. Euchromatin constitutes the less condensed chromatin that is more accessible for regulatory proteins. Heterochromatin, on the other hand, represents the compact state of chromatin, which is tightly folded and inaccessible. These distinct states are each associated with a special set of histone modifications [4]. Beyond that, we observe additional chromatin states with intermediate condensation levels.

4.1.1 Structure and Organization of Chromatin

Nucleosomes are the most basic unit of the chromatin and consist of DNA that is wrapped around histones. One nucleosome has a diameter of 10 nm and achieves a 7-fold compaction of the DNA [2,5]. The nucleosome consists of the four core histones H2A, H2B, H3, H4 and the linker histone H1, which are the most abundant proteins in chromatin [2]. Histones are basic proteins and contain many positively charged amino acids, which allows them to interact with the negatively charged DNA. The variable linker region between two nucleosomes can be bound by histone H1, which seals two rounds of DNA at its entry/exit site on the surface of the nucleosome core [6]. In the presence of the linker histone H1, six nucleosomes from the 'beads on a string' conformation condense to form the 30 nm fiber, which represents a higher level of DNA condensation. This leads to an overall compaction of the linear DNA by factor of 30 to 40 [7]. With the help of additional factors such as non-histone and nuclear scaffold proteins, large chromatin loop domains can be established. Those are further compacted to generate interphase and mitotic chromosomes [2]. At the end, chromonema fibers represent the highest organized state of chromatin [8]. These chromatin alterations achieve a very moldable structure, which allow cellular DNA-associated processes to be performed, while maintaining the capability of cell division and equal distribution of the DNA to the daughter cells.

4.1.2 Non-histone Proteins

One-third of the mass of mitotic chromosomes is comprised of chromatin-associated non-histone proteins, of which some even remain associated with the chromatin after removal of the histones [9]. Non-histone proteins comprise many different types, such as high mobility group (HMG) proteins, scaffold proteins, DNA topoisomerases and DNA polymerases. All of these proteins regulate different functions that assure the maintenance of the chromosomal structure and integrity. Furthermore, non-histone proteins play a role in mitotic events such

as chromosomal condensation, sister chromatid separation and interaction of the chromosomes with the cytoskeleton during spindle formation [9].

4.2 Histone Proteins

The five different histones (H2A, H2B, H3, H4 and H1) in mammalian cells are mostly expressed during S-phase and incorporated into chromatin in a DNA replication-dependent manner. It is proposed that core and linker histones may have evolved from totally different genes of eubacteria and archaea. Their variation is thus reflecting the increasing complexity during eukaryotic evolution [10].

Each histone is structured into one core domain, which is flanked by two tail domains. The core domain allows protein-protein interactions and induces compaction of the DNA [11]. Not only the N- but also the C-terminal tails can be altered by posttranslational modifications and thereby regulate the interaction with DNA [6]. Histone modifications can neutralize the positive charge of the histone tails, which results in a reduced interaction with the negatively charged phosphate backbone of the DNA. Therefore, modified chromatin (e.g., acetylated lysine residues) is often less compacted and better accessible for proteins involved in processes such as DNA-repair, recombination, replication or transcription [4].

4.2.1 Core Histones

The nucleosome core particle consists of 2 copies of each core histone H2A, H2B, H3, and H4, which form dimers and assemble into an octamer that is enwrapped by 145-147 base pairs of DNA [12] (Fig 2).

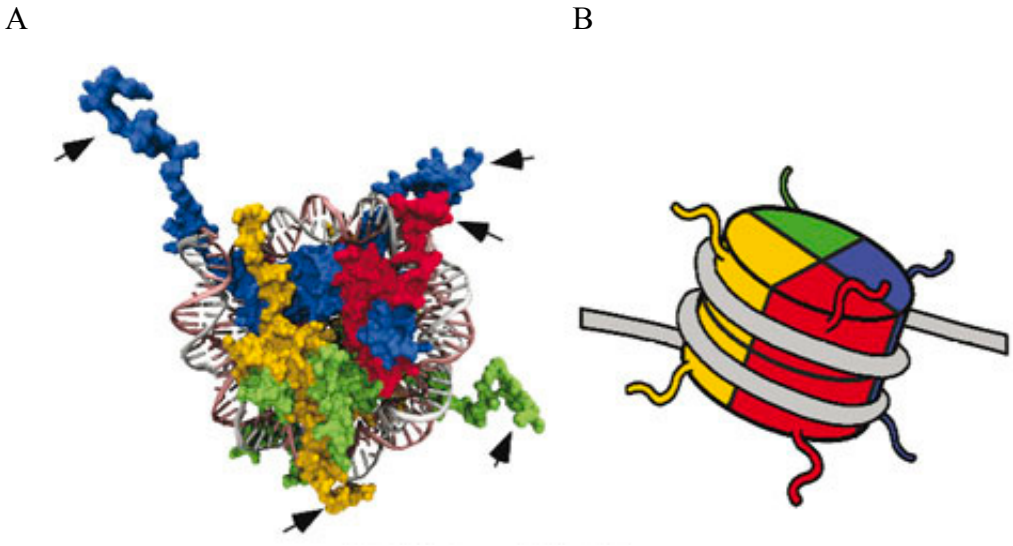

Figure 2: A nucleosome with core histone proteins H2A (orange), H2B (green), H3 (blue) and H4 (red) and a 147-bp DNA strand. **A:** 1.9-Å nucleosome core particle structure with the DNA strand shown in silver and red. The black arrows mark the N-terminal rails of the histone proteins, which are targets of many post-translational modifications. **B:** A cartoon diagram to clearly illustrate the positions of the core histone proteins [13].

The H3-H4 tetramer strongly interacts with the nucleosomal DNA and the N-terminal tails of the histones H3 and H4 leave the nucleosomal core close to where DNA enters or exits the nucleosome [4]. In contrast, the histones H2A and H2B associate more weakly with the DNA of the nucleosome [14] and are frequently displaced from nucleosomes [11]. Therefore, post-translational modifications on these histones play a less important role than on histones H3 and H4 [15].

4.2.2 Core Histone Variants

Throughout evolution, the general structure of chromatin has been conserved. However, histone variants, which can be incorporated into nucleosomes to regulate the chromatin barrier, have evolved in vertebrates [16]. Histone variants differ only in a few amino acids from their original counterparts and are mainly expressed in different cell cycle phases. Incorporation into the chromatin happens mainly in a DNA replication-independent

manner [17]. In core histones, histone H2B and H4 are mostly invariant, whereas H2A and H3 are exchanged more frequently.

Histone H2A variants can be grouped into the replicative histone variants H2A.1 and H2A.2, synthesized in S-phase in a replication-coupled manner, and the replacement variants H2Av (H2A.X/H2A.Z), Htz1 (H2A.Z), macroH2A and H2ABbd, which are expressed either constitutively throughout the cell cycle or outside of S-phase [18]. H2A.X, the best-studied variant, is phosphorylated at its C-terminal SQ (E/D) motif upon treatment with DNA-double-strand break inducing agents [19]. This phosphorylation of H2A.X is crucial for the recruitment of DNA-repair proteins [20]. MacroH2A is much larger than the other H2As, because it contains a non-histone macro-domain at the C-terminus [21]. Nucleosomes containing macroH2A participate only weakly in ADP-dependent remodeling, chaperone-mediated histone exchange, transcription factor binding or transcriptional activation by Pol II [22]. Another histone variant, H2A.Z, is more prominent at promoters, which are competent for transcriptional activation [23]. Rapid eviction of H2A.Z is needed for full transcriptional activation and elongation, since H2A.Z containing nucleosomes are resistant to chromatin remodeling and modifications [24]. H2ABbd activates transcription and is found on active X-chromosomes and autosomes [17].

The group of histone H3 variants consists of H3.1 and H3.2, which are the replicative variants, and the replacement variants H3.3 and CENP-A. The major H3 variant is CENP-A that is found in centromere-regions of chromosomes and is essential for centrosome function. Other variants, for example H3.3, are generally expressed in transcriptionally active chromatin and involved in the regulation of transcription [25].

4.2.3 Linker Histone H1

The linker histone H1 is less evolutionarily conserved than the core histones. Multiple non-allelic variants are expressed in eukaryotes and can even be tissue specific. Eleven different subtypes have been identified in mammals, but very little is known about their specific functions. Much data suggest that H1 has a critical role in controlling the higher order chromosomal structure [26]. It was shown that H1 is required for normal morphology of replicated mitotic chromosomes [27]. Histone H1 is rather involved in the regulation of specific genes and in specific processes than producing global effects on transcription. Depletion of H1.2 and H1.4 resulted in an arrest of cell proliferation, while the loss of H1.0, H1.3 or H1.5 had no effect on cell growth [6,28].

4.2.4 Linker Histone H1 Variants

The vast variety of H1 variants (7 are somatic (H1.1-H1.5, H1.0 and H1x), 4 are expressed in germ cells (H1t, H1T2, HILS1, H1oo)), and the fact that some are only expressed in specific tissues or at certain stages of development, led to the suggestion that these defined patterns may have specific functions [29].

In general, H1.2 to H1.5 are found in nearly all cells, while H1.2 and H1.4 are the main variants in most somatic cells [30]. H1oo is only expressed in oocytes, starting from the primordial follicle stage to early embryogenesis. H1t, H1T2 and the variant HILS1 are only found in sperm cells [6,31], while H1x has been found in different cell types [32]. Some cell types depend on linker histone H1.0 for their terminal differentiation [33]. However, mice lacking the H1.0 protein did not exhibit impaired growth or reproduction and the stoichiometry of H1 to nucleosome did not change. This result suggests that the other main histone H1 types compensated the loss of H1.0. The same outcome was observed when the pachytene specific subtype H1t was deleted [34] or when the main type H1.1 was depleted [35]. Even after deletion of two of the three main histone H1 types, there was no phenotypic change [36]. The deletion of all three H1 subtype genes led to decondensation of chromatin and changes in core histone modification and the mice died around mid-gestation [37,38].

A functional role of individual histone H1 subvariants, in addition to their structural impact on chromatin, is well supported, but more studies are needed to determine these differential functions of individual histone variants. The structural function seems to be subtype independent, since the single deletion of distinct linker histones genes can be compensated [6].

4.2.5 Structure of the Linker Histone H1

The three-domain structure of the core histones is also found in histone H1. With a length of 20-35 amino acids, the N-terminal tail is relatively short and enriched in basic amino acids. The first half of the N-terminus is highly hydrophobic [26]. The central domain of H1 consists of 75 amino acids, is highly conserved among all the subtypes, and has a globular conformation [39]. Forming the extended part of the histone with approximately 100 amino acids, the C-terminal domain is highly enriched in lysine, alanine and proline. It varies significantly between the different subtypes and species [26] (Fig. 3).

Figure 3: H1 variants vary the most in the C-terminal domain. Alignment of the H1 variants H1.2, H1.4 and H1t. Functionally similiar amino acids are marked in the same color.

This C-terminal domain acquires a specific secondary structure when bound to DNA [40], stabilizes the folding of the nucleosome array into chromatin fibers, and is needed for the high-affinity binding to chromatin [41].

4.2.6 Linker Histone and binding to Chromatin

H1 histones promote tighter packing of chromatin, condensation from the 'beads on a string' conformation to the 30 nm fiber, and limit the access for regulatory proteins to nucleosomal components [42]. Through the globular domain, histone H1 binds the entering and exiting DNA at the surface of the nucleosome at least twice and thus stabilizes the DNA wrapping [39]. Two contradictory models suggested different positioning characteristics of H1 based on studies of formation of nucleosomes on DNA in vitro. One model proposes that the globular H1 domain bridges two DNA duplexes between the dyad and one of the chromosomal DNA ends [43]. According to the alternative hypothesis, the globular H1 domain is placed 65 base pairs away from the nucleosome dyad inside of one of two chromosomal DNA turns [44]. Newer studies indicated a two site-model, in which one α-helix of the winged helix element of the globular domain interacts with DNA at a distance of approximately one helical turn away from the nucleosomal dyad. About 15 nucleotide pairs away from the nucleosomal core DNA is the second proposed site [39].

According to the structure, the N-terminal H1 domain has only minimal effects on chromatin binding and is not expected to bind to the DNA [45]. The most divergent part of H1, the C-terminal domain, is at the same time the main determinant of the binding of H1

subtypes to chromatin [41]. Specific subdomains of the C-terminal linker histone domain mediate this effect [6]. An interaction between the linker histone and the C-terminal tail of the core histone H2A was found, but the precise binding sites are still unknown. However, identifying interaction partners of H2A by mass spectrometry only revealed peptides corresponding to H1.1 and H1.2, while no peptides corresponding to core histones were detected. Further experiments suggest that the H2A C-terminus is required for efficient H1 binding to the nucleosome *in vivo* [46].

H1 limits the mobility of nucleosomes and the accessibility of chromosomal DNA for chromatin remodeling complexes through its interaction with chromatin (Fig 4).

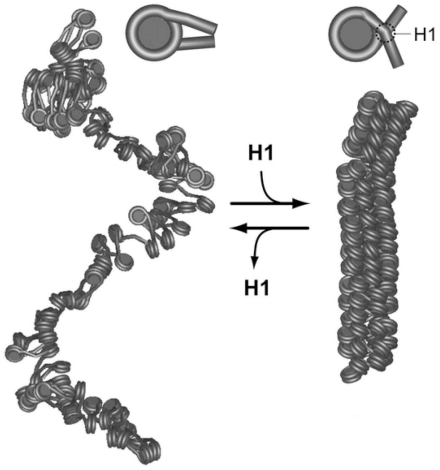

Figure 4: Chromatin compaction induced by linker histone H1. A more closed conformation of the linker DNA and overall of chromatin is achieved when H1 binds to nucleosomes.

Nevertheless, H1 was identified as a highly mobile chromatin element in comparison to the core histones. Interactions between H1 and the nucleosome are transient and last only for 3 to 4 minutes before histone H1 dissociates and quickly interacts with another binding site [47,48]. Thus, linker histone H1 travels more slowly than most other chromatin binding proteins and is influenced by competition with other proteins, for example of the high mobility group [42]. The binding affinity of the different H1 subtypes correlates with the length of the C-terminal domain. The most mobile subtypes are H1.1 and H1.2, H1.0 and H1.3 exhibit moderate affinity, and H1.4 and H1.5 have the highest affinity [45]. Additional modulation of the kinetics of H1 exchange can be achieved by H1 modification and by interaction of H1 with other structural protein components of chromatin. For example, it was shown that ongoing phosphorylation is needed for histone H1 mobility [48].

4.3 Posttranslational Modification (PTM)

Posttranslational protein modifications are reversible modifications that are added after the translation of proteins. Specific chemical groups are enzymatically attached and thereby affect the structure, function and biological activity of the modified proteins. The core histones are modified at over 60 different amino acids on their N-terminal tails [4]. The highest number of modifications has been recorded for H3, followed by H4, H2B and H2A. The C-terminal tails of these core histones and their non-tail regions are modified to a lesser extent.

Various modifications such as acetylation, methylation, phosphorylation, ubiquitination, sumoylation, ADP-ribosylation, N-formylation, deamination and proline isomerization have been reported for all five histones [4]. The multitude of posttranslational modifications creates immense possibilities for the regulation of functional responses within the cell, which is an important mechanism in epigenetics [49]. The proposed "histone code" greatly regulates the access to the information of the genetic code. The covalent modifications of histone proteins can modify chromatin structure, thereby changing between transcriptional active or silent chromatin states [50]. Here, only PTMs on histone H1 are discussed, due to the focus on the linker histone.

4.3.1 Epigenetics

Epigenetics is defined as heritable changes in gene expression or cellular phenotype that occur without changes in the underlying DNA sequence. The genetic information encoded in DNA is the basis for the phenotype of an organism, but the definite genesis of this phenotype is controlled by the accessibility of the DNA sequence (i.e., transcription of genes). This regulation can either be transient or stably imprinted by biochemical modifications. DNA methylation and histone modifications by acetylation, methylation, phosphorylation, ubiquitination, ADP-ribosylaion and others are reactions that lead to such a regulation [51]. These modifications are targeted at specific sites in multiple ways.

More and more evidence suggests that the epigenetic information from the combination of different histone modifications and various histone variants is fundamental [52]. Thus, the research of histone proteins and their posttranslational modifications has received

progressively more attention as further results confirm the importance of chromosomal proteins.

4.3.2 Posttranslational Modifications of the Linker Histone H1

In the linker histone H1, the N-terminal tail (aa 1-36) can be modified, but to a lesser extent than the globular domain (aa 37-113) and the C-terminal tail (aa 114-219)[49]. The most abundant modifications found in H1 are phosphorylation, acetylation, methylation, ubiquitination and the recently discovered N-formylation [53]. Phosphorylation of histone H1 is the best-studied modification and progressively increases during the cell cycle. The majority of the H1 phosphorylation sites lie within the cycline-dependent kinase (CDK) motif (S/T)PX(K/R), which is important for DNA binding of H1 [54]. The number of CDK motifs, the degree of phosphorylation, and the functional outcome during the cell cycle differ within the variants of H1 [55]. During late G2 and mitosis, phosphorylation becomes maximal and decreases again towards the end of mitosis in telophase [56]. This led to the belief that phosphorylation of H1 decondensates DNA as a precondition for DNA replication [57]. It has also been shown that H1 phosphorylation increases its dynamic exchange in chromatin [48]. Therefore, H1 dephosphorylation and the consequential tighter binding between H1 and DNA are also considered important for the process of differentiation [39,41]. Nevertheless, phosphorylation not only affects the interaction of histone H1 with the core nucleosome, but also with heterochromatin proteins [58].

The most frequent covalent modifications in core histones are acetylation and methylation of lysine or arginine. Deacetylation of the strongly conserved lysine-26 in H1.4 leads to the formation of heterochromatin [59] and methylation of the same lysine promotes repression of transcription [60]. Activation of transcription is generally related with acetylation of core histones, while methylation is either seen at sites of activation or at repressed locations of the genome [17]. The same results were observed for the linker histone H1, which demonstrates that histone H1 also contributes to the ‘histone code’ just as the core histones do.

4.4 Lysine Methylation

Methylation of histones regulates the formation and maintenance of heterochromatin, X-chromosome inactivity, transcription, DNA repair and genomic imprinting [61]. Depending

on the site and the degree, histone methylation can be an activating or repressing mark [62,63]. For example, methylation of K4, K36 and K79 on histone 3 is associated with transcriptionally active chromatin, while methylation of K9 and K27 on H3 or K20 on H4 are rather found with compacted chromatin [62].

Methylation does not change the charge of the acceptor, but impacts its basicity, hydrophobicity and the affinity of molecules such as transcription factors towards DNA [61]. In all cases, methyl groups are transferred to the target site by using S-adenosylmethionine (SAM) as a co-substrate [64]. Histone methylation occurs on lysine (mono-, di-, or trimethylated) (Fig 5) or arginine (mono- or dimethylated) residues and is catalyzed by histone methyltransferases (HMTs) [65].

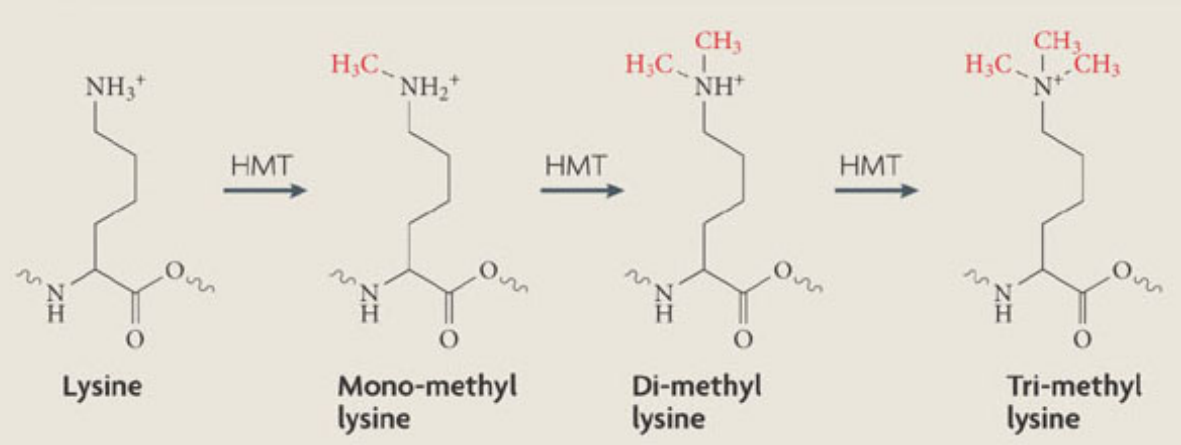

Figure 5: Methylation of lysine in histones can occur as mono-, di- or tri-methylation by histone methyltransferases (HMT). The methyl-groups are marked in red [66].

Three different enzyme groups are able to methylate histones: SET domain lysine methyltransferases, non-SET domain lysine methyltransferases, and arginine methyltransferases [51]. Histone methyltransferases are generally specific for the acceptor amino acids, as their name suggests, but several of them target also non-histone protein substrates. Thus, their proposed high specificity is debatable [51].

Lysine methylation is a reversible modification. The recently discovered lysine specific demethylase 1 (LSD1) is part of a histone modification complex, which controls cell specific gene expression [67]. The demethylase can remove the methyl group from nucleosomes, which proves that protein lysine methylation is a reversible posttranslational modification [67-69]. Both, LSD1 and the closely related LSD2 [70] remove the methyl group from lysines by forming of an imine intermediate, which undergoes hydrolysis to complete the

demethylation. This pathway only allows the demethylation of mono- and dimethylated lysines [71]. On the other hand, Jumonji-C domain containing demethylases are also able to demethylate trimethylated lysine residues [72].

4.5 Lysine Methyltransferase (KMT) SET7/9

SET7/9 was discovered as a histone methyltransferase that catalyzes mono-methylation of histone 3 lysine 4 (H3K4), but it shows only a weak activity on nucleosomes, which implies that the main targets of the enzyme are non-histone proteins [73-75] (Fig. 6). Protein dimethylation by SET7/9 has been described in some cases, but the enzyme mostly acts as a mono-methyltransferase [76,77].

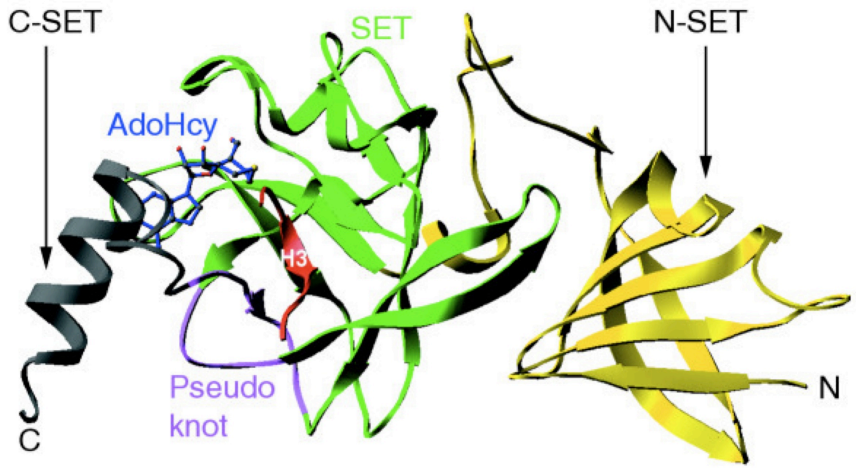

Figure 6: Crystal structure of human SET7/9. The C-SET, SET and N-SET domains of the human SET7/9 are shown as well as the pseudo knot, which is formed by two conserved SET motifs. Also, a bound H3 is indicated as well as the reaction byproduct AdoHcy [78].

In agreement with this hypothesis, numerous non-histone proteins such as Dnmt1 (reduction in stability), p53 (activation and stabilization), TAF10 (increased affinity for polymerase II), estrogen receptor α (activation and stabilization), pRb, p65 and Tat protein of HIV1 are methylated by SET7/9 [79-87]. In addition, a recent study identified up to 90 new non-histone target peptides and a strong methylation of free H2A and H2B tails [76]. Hence, the targeting of SET7/9 to different substrates suggests a low specificity of the enzyme.

SET7/9 prefers positively charged substrates and methylates the last lysine residue in the motif [K>R][S>KYARTPN][K^{me}] [76]. Peptides that do not perfectly match this sequence can be methylated to a lesser extent. In the cell, a strong interaction of acceptor proteins with the SET7/9 methyltransferase can stimulate the transfer of a methyl group to weak target sites.

Therefore, a weaker methylation does not have to imply a lower biological importance [76]. Serine phosphorylation of histone tails and non-histone proteins inhibits the methylation of those proteins by SET7/9 [76]. This implies a universal crosstalk between phosphorylation and SET7/9 induced methylation [88].

4.6 Poly-ADP-Ribosylation

ADP-ribosylation is a reversible posttranslational modification of proteins. The target amino acids in eukaryotes are lysine, arginine, glutamate, aspartate, cysteine, phosphor serine and asparagine residues [89]. Mono-ADP-ribosylation involves the addition of one ADP-ribose moiety to specific amino acids. This unit can then serve as an acceptor for additional modifications and thus give rise to linear or branched polymers of ADP-ribose (PAR) and thereby lead to a poly-ADP-ribosylated protein [90]. In cells, mono-ADP-ribosylation is mainly found outside the nucleus and is more common than poly-ADP-ribosylation (PARylation), which mostly occurs on nuclear proteins [91,92].

ADP-ribosyltransferases (ARTs) attach either a single or multiple ADP-ribose units to themselves (= automodification) or to different target proteins. They use nicotinamide adenine dinucleotide (NAD^+) as a substrate, which is transferred onto specific amino acid side chains or attached to pre-existing protein-linked ADP-ribose units under the release of nicotinamide as a byproduct [93] (Fig. 7).

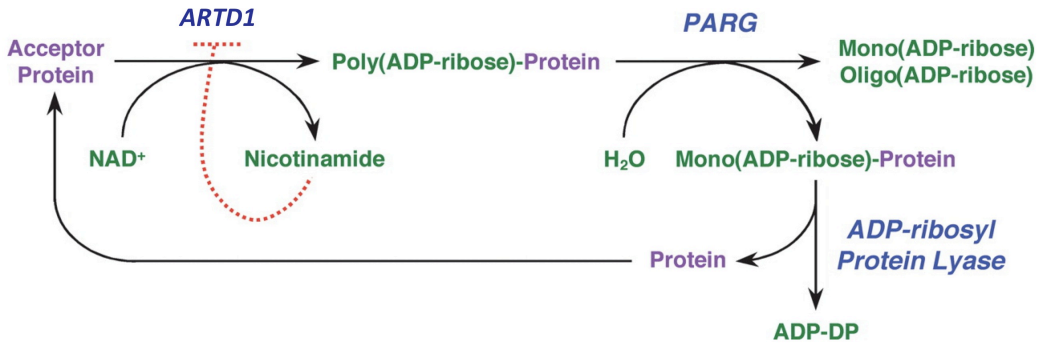

Figure 7: Synthesis and degradation of PAR on a target protein by ARTD1. ARTD1 induces the polymerization of ADP-ribose units from NAD^+ molecules on acceptor proteins, which leads to the formation of PAR. PARG induces the hydrolysis of the ADP-ribosylation leading to free mono and oligo(ADP-ribose). ADP-ribosyl protein lyase releases the last ADP-ribose monomer from the acceptor protein, freeing ADP-3″-deoxypentose-2″-ulose (ADP-DP). Modified from [94].

PAR formation requires three enzyme-catalyzed steps: initiation of mono-ADP-ribosylation, elongation, and branching of the polymer [95]. The chain length is variable and can reach up to 400 units *in vitro*. Long polymers are consecutively branched after a linear section of 20 to 50 units of ADP-ribose [96]. As mentioned, *in vivo* the level of PARylation is determined by the opposing activities of ARTs and PAR-degrading enzymes. The glycosidic bond between two ADP-ribose units can be hydrolyzed by Poly(ADP-ribose) glycohydrolases (PARGs) and ADP-ribosyl hydrolases (ARHs) [97,98]. In mice, PARG knock out leads to embryonic lethality due to the increased PAR accumulation, indicating the importance of PARG as the major PAR-degrading factor in cells [99].

Modification of proteins by ADP-ribosylation adds negative charge to the acceptor protein. In the case of PAR chains, this can be substantial and thus affect the target protein structure, enzymatic activity, or interaction with other proteins [100]. Different types of conserved PAR binding modules interact with PAR in a non-covalent way. This includes a PAR binding zinc finger domain [101], macrodomains [102], and a short PAR-binding motif consisting of basic and hydrophobic amino acids, which can be found in many DNA checkpoint proteins [103].

4.6.1 ADP-Ribosyltransferase Diphtheria Toxin-like (ARTD) Family

There are three families of mammalian proteins, which catalyze mono- and or poly-ADP-ribosylation. The sirtuins, NAD^+-dependent protein deacetylases [104], the ARTCs (formerly ecto-ARTs) with a homology to cholera C2 and C3 toxin [97], and the ARTDs (formerly poly(ADP-ribose) polymerases (PARPs)) with sequence homology to bacterial diphtheria toxin [105]. Among the family of ARTDs are both mono- and poly-ADP-ribosyltransferases, whereas the other two families are believed to catalyze only mono-ADP-ribosylation.

So far, 18 ARTD proteins have been found in humans [89]. The best-studied member of the ARTD family is ARTD1, a nuclear, chromatin-associated enzyme, which is responsible for around 90% of the cellular PAR generation [106,107]. All ARTDs share a highly conserved 50 amino acid motif within their catalytic domain, which allows the binding of NAD^+ [108]. An evolutionary conserved H-Y-E catalytic triad is responsible for the PARylation activity [89,109]. For the ADP-ribose chain elongation, the catalytic glutamate residue E988 is needed [110,111], and for NAD^+ binding the histidine and tyrosine residues are important. ARTD1 to 6 contain a complete H-Y-E motif and have putative PARylation activity. Members lacking only the

glutamate residue (ARTD8 and 10) have putative mono-ADP-ribosyltransferase activity. ARTD9 and 13, which miss the histidine and glutamate residues, are catalytically inactive [109].

Most probably, only members of the ARTD family are able to ADP-ribosylate histones. ARTD1, ARTD2 and ARTD3 are the only ARTs exclusively found in the nucleus, whereas ARTD4, ARTD5, ARTD6, ARTD9 and ARTD10 are localized in the nucleus and the cytoplasm [105]. ARTD1 and 3 are known to poly-ADP-ribosylate individual histones, while ARTD10 only results in mono-ADP-ribosylated histones [109,112,113]. Because only a few percent of the total histones are ADP-ribosylated, it is difficult to detect and identify specific acceptor sites [114]. However, all core histones and the linker histone H1 are potential acceptors of ADP-ribose and can for example be modified during or shortly after their synthesis in the cytoplasm, during transport into the nucleus, while bound to chaperons, or after their integration into chromatin [90].

Based on in vitro and in vivo results, chromatin-associated histone H1 is the major PAR acceptor, followed by H2B, whereas the rest of the core histones are weakly modified [115,116]. A PAR chain length of up to 15 ADP-ribose units has been seen for histone H1 [117], whereas core histone are modified with shorter oligomers [118].

4.7 ADP-Ribosyltransferase Diphtheria Toxin-like 1 (ARTD1)

ARTD1 is a 113 kDa protein, formed by 1014 amino acids, and holds three main functional units. The N-terminal DNA-binding domain (DBD) contains three zinc finger domains (ZF I, ZF II and ZBD III) for the DNA-dependent activation and a nuclear localization sequence (NLS). The central automodification domain (AMD) comprises three confirmed modification sites (K498, K521, K524) [95] and a BRCT (BRCA1 C-terminus) motif for protein-protein interaction, which is found in various DNA damage response proteins. The C-terminal catalytic domain includes a W-G-R motif and a NAD^+ binding fold for the enzymatic activity of ARTD1 (Fig. 8).

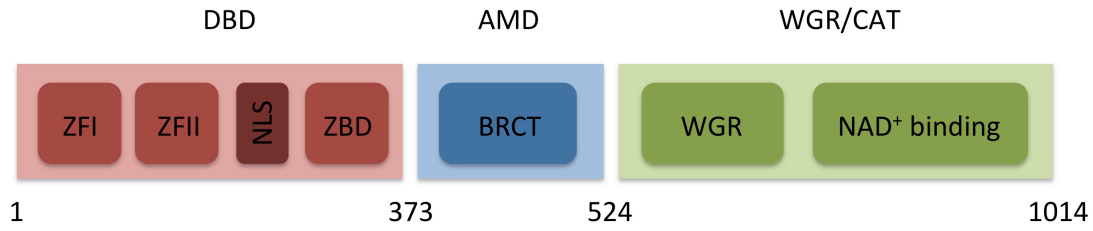

Figure 8: Structural features of ARTD1**.** DBD: DNA binding domain with zinc fingers ZFI, ZFII, a nuclear localization signal (NLS) and a zinc binding domain (ZBD). AMD: automodification domain with the BRCA1 C-terminus (BRCT). CAT: catalytic domain with the WGR motif and the NAD^+ binding domain.

ARTD1 is involved in cellular processes such as the DNA damage response, cell cycle regulation, gene expression, differentiation and aging. It modifies nuclear proteins including core and linker histones, DNA repair proteins and transcription factors, but first and foremost ARTD1 targets itself. Under normal conditions, the activity of ARTD1 is low, but as soon as the enzyme binds to DNA strand breaks, the activity is greatly increased and PAR levels rise (up to 10 to 500 fold) [119].

As mentioned previously, ARTD1 plays a critical role in many physiological and pathophysiological processes. ADP-ribosylation by ARTD1 affects inter- and intracellular signaling, cell cycle regulation, chromatin remodeling, DNA replication, transcription, DNA repair, somatic recombination, regulation of telomere length, inflammation and cell death via apoptosis or necrosis [105,120]. The deletion of ARTD1 renders mice hypersensitive to ionizing radiation and thus cells are more sensitive to alkylating agents. However, these mice are viable and their phenotype supports the importance of ARTD1 for the maintenance of genomic integrity [119,121-123].

The modification of core and linker histones by the enzymatic activity of ARTD1 induces decondensation of higher order chromatin structures [107,124,125]. However, there is contradictory data regarding the compactness of chromatin. In vivo condensation and in vitro decondensation was reported after ARTD1 treatment [116,126,127]. Further, ARTD1 might function as a substitute for H1, as the enzyme was concentrated at actively transcribed gene promoters and H1 showed a reciprocal chromatin binding pattern to ARTD1. Upon ARTD1 depletion, H1 was also enriched at ARTD1-regulated genes [128]. Nuclear factor kappa B (NF-κB) regulates transcription of inflammatory and cell survival genes, where ARTD1 co-activator function is also involved [129]. Upon extracellular inflammatory stimuli such as LPS or TNFα, a synergistic co-activation of NF-κB dependent gene expression through ARTD1,

the acetyltransferase p300, the arginine methyltransferase 1 (CARM1) and the protein arginine methyltransferase 1 (PRMT1) takes place [129,130].

The enzymatic activity of ARTD1 is allosterically induced upon binding to single and double strand breaks, cruciform, crossovers and supercoils [131]. Because of this and of the rapid recruitment to sites of DNA damage *in vivo*, which is essential for accumulation of repair factors like XRCC and the MRN complex [132,133], ARTD1 was mainly regarded as a DNA damage response protein. Also, many DNA repair factors have PAR-binding domains and are recruited to DNA damage sites in a PAR-dependent manner [101,103,127,134]. Hence, ARTD1 and PAR are thought to play an important role in various DNA repair pathways, particularly in base excision repair [135-137]. Nevertheless, ARTD1 seems to be redundant for DNA repair under normal physiological conditions, as DNA repair pathways are effective in cells lacking ARTD1 [138-140] and knockout mice are viable, fertile and without increased tumor risk [141].

Oxidative stress induces hyperactivation of ARTD1, which results in a depletion of cellular NAD^+ and ATP levels and thereby induces cell death [142,143]. Hyperactivation of the nuclear ARTD1 activity leads to accumulation of PAR in the cytosol. Cytoplasmic PAR then binds the apoptosis inducing factor (AIF). Due to the PAR binding, AIF is subsequently released from the mitochondrial membrane and relocalized to the nucleus, where it induces DNA fragmentation and caspase-independent cell death [144]. During apoptosis, ARTD1 is cleaved and thus inactivated by caspases to prevent a deleterious activation of the enzyme in response to the DNA fragmentation. This should preserve the cellular ATP levels, which is needed for apoptosis [145]. Nevertheless, knock in mice with a caspase-resistant, non-cleavable ARTD1 (D214N) develop normally, which suggests that ARTD1 cleavage is not an absolute requirement for apoptosis [146].

4.7.1 Posttranslational Modifications of ARTD1

NAD^+-dependent automodification of ARTD1 within the DBD and AMD is one of its most important post-translational modifications [95]. Interaction with DNA activates the enzymatic activity of ARTD1. Auto-PARylation leads to repulsion from the DNA due to the negative charge of the modified ARTD1 and the DNA [95]. This negative feedback loop reduces the overproduction of PAR.

Also, trans-modification of ARTD1 takes place. ARTD1 is phosphorylated by the mitogen-activated protein kinases ERK1/2 at the S372 and T373 sites, which enhances the

DNA damage induced enzymatic activity of ARTD1 [147]. Phosphorylation by JNK1 leads to sustained ARTD1 activation during H_2O_2 exposure [148], AMPK increases ARTD1 activity [149], whereas protein kinase C decreases ARTD1 DNA binding and enzymatic activity [150]. Another modification is acetylation by p300/CBP at five different lysine residues (K498, K505, K508, K521, K524), which allows interaction with p50 and the co-activator function for NF-κB-dependent gene expression [151].

Furthermore, ARTD1 is a target of covalent addition of polypeptides such as ubiquitin and small ubiquitin-like modifier (SUMO). SUMO E3 ligase PIASγ modifies ARTD1 at K486 and thereby interferes with its co-activator function in HIF1-dependent gene expression [152].

Interestingly, various post-translational modifications target the same or neighboring amino acids within the AMD, which allows crosstalk between the different modifications. For instance, automodification of ARTD1 is likely reduced by acetylation, as it modifies three amino acids that are important for PARylation of the enzyme.

4.8 PARP Inhibitors

Cell lines deficient in homologous recombination (HR), which is an essential, error-free DSB repair mechanism, display high lethality when treated with pharmacological ARTD inhibitors (PARP inhibitors) [153,154]. Tumor suppressor proteins BRCA1 and BRCA2 are required for HR and are mutated in many cases of heritable breast, ovarian and prostate cancer. Therefore, the treatment of these and other types of cancer with PARP inhibitors, alone or in combination with chemotherapy, is presently tested in clinical trials. The hypothesis is that ARTD1 inhibition should slow down the repair of single strand breaks. Endogenously generated SSBs would add up and then be altered into DSBs during replication. HR deficient cancer cells would not be able to repair these defects and die. However there have to be other mechanisms that contribute to the lethal effect of PARP inhibitors, as different studies did not detect an increase in DNA strand breaks in treated cells [155,156]. It is believed that the negative influence of PARP inhibitors on NF-κB-dependent anti-apoptotic gene expression could be one of these factors [157,158].

There are other pathophysiological settings, where the clinical relevance of PARP inhibitors is further elucidated. During cerebral ischemia/reperfusion in patients suffering a stroke or in inflammatory disorders, the suppression of an ARTD1 hyperactivation could lead to a better outcome [159,160].

Most PARP inhibitors are unspecific nicotinamide analogs and thus target not only ARTD1 but also other NAD^+ dependent enzymes including other ARTD family members. One of the first substances that were used to inhibit ARTD1 *in vivo* and *in vitro* was 3-aminobenzamide (3-AB). However, its potency and specificity were too low for therapeutic uses. Nowadays, several newly developed PARP inhibitors with increased potency and less off-target effects are in clinical trails [161]. Olaparip (AstraZeneca) and ABT-888 (Abott), which already passed numerous phase II trials as treatments against different kinds of cancer, either alone or in combination with chemotherapy, are two of them.

5 Aim of the Thesis

SET7/9 mono-methylates H3K4 as well as many non-histone proteins and controls numerous DNA damage response proteins such as p53, pRb and E2F1. We thus investigated whether the linker histone H1 is modified by SET7/9 and which amino acids are serving as methylation acceptor sites.

ARTD1 and the linker histone H1, two chromatin-associated proteins, affect many DNA-related processes. The second aim of this thesis was thus to investigate if and where H1 was modified by ARTD1 and how a possible ADP-ribosylation would affect SET7/9-mediated methylation.

6 Material und Methods

6.1 DNA based Methods

6.1.1 PCR: Site directed Mutagenesis

To create single lysine mutants in the H1.4 fragments 2 and 3, site directed mutagenesis was performed. Forward and reverse primers were designed to mutate the nucleotide sequence of specific lysines into the code for an arginine (AAG to AGG or AGA to AGG). Upstream and downstream of the mutation at least 12 correct nucleotides were attached to the primer to assure the correct binding. In the PCR reaction (100 ng template DNA, 1 µM of each primer, 200 µM of each nucleotide (dNTPs), 1x concentration of 10x Pfu buffer (Promega) and 1 unit of Pfu-polymerase (Promega), in 25 µl total volume), the plasmid served as template and was afterwards digested with DPN1 (NEB, according to manufacturer's protocol) to remove the non-amplified DNA. The remaining DNA was transformed into bacteria. The PCR program included the following steps: 2 min at 95°C, followed by 25 cycles of 30 s at 95°C, 1 min at 55°C, 14 min at 68°C, and a last step with 7 min at 68°C. Using a template with a single or double mutant in the reaction allowed to generate double and triple mutants, respectively.

6.1.2 PCR: Overlapping PCR

To create the cluster mutations in fragment 2 and 3, four different primers were designed for each cluster mutation. An outer forward primer and an outer reverse primer were designed to amplify the whole fragment, together with a reverse as well as a forward cluster primer, which encoded the desired mutation on the 5'-end (lysines mutated to arginine, AAG to AGG or AGA to AGG) and at least 18 nucleotides at the 3'-end, which allowed proper binding to the template. During the first PCR, two products were separately amplified using one flanking primer (e.g., outer forward/outer reverse) and one mutation primer (e.g., cluster reverse/cluster forward). The first PCR (100 ng template DNA, 1 µM of each primer, 200 µM of each nucleotide (dNTPs), 1x concentration of 10x Phusion buffer HF (NEB) and 1 unit of Phusion-polymerase (NEB), in 25 µl total volume) included following steps: 3 min at 98°C, followed by 25 cycles of 15 s at 98°C, 30 s at 55°C, 15 s at 75°C, and a last step with 7 min at 75°C. The separate products were then used together in a second overlapping PCR reaction as templates without primers. Due to the complementarity of the templates at the mutation site, the PCR fragments were initially combined in the first five cycles. After these

cycles, the flanking primers were added as described below to generate the desired full length PCR product. The second PCR (1 µl of both products from the first PCR, 1 µM of each flanking primer, 200 µM of each nucleotide (dNTPs), 1x concentration of 10x Phusion buffer HF (NEB) and 1 unit of Phusion-polymerase (NEB), in 50 µl total volume) included following steps: 3 min at 98°C, followed by 5 cycles of 15 s at 98°C, 30 s at 60°C, 20 min at 72°C, and a step with 3 min at 60°C, where the flanking primers were added, then the steps in the first cycle were repeated 25 times and a last step with 7 min at 72°C. The products were then loaded on a 1% agarose gel (Agarose from Promega) and separated with 90V in 1x TAE buffer (40 mM Tris acetate, 1 mM EDTA, 0,1% (v/v) acetic acid). The DNA from the PCR was subsequently cut out from the gel and isolated (according to 5.1.4).

6.1.3 Primers used

OTM	Primer name	5'-Sequence
1315	hH1.4_BamHI_for	GATCGGATCCATGTCCGAGACTGCGCCTG
1316	hH1.4_fl_XhoI_rev	GATCCTCGAGCTACTTTTTCTTGGCTGCCG
1317	hH1.4_a113_XhoI_rev	GATCCTCGAGCTAAGAGGCCGCCTTCTTGTTGAG
1318	hH1.4_a189_XhoI_rev	GATCCTCGAGCTACGCTGGGCTCTTGGGCGC
1319	hH1.4_a156_XhoI_rev	GATCCTCGAGCTACTTTGGGGTCTTCTTGGCG
1330	hH1.4_aa144_XhoI_rev	GATCCTCGAGCTACGCCCCCGTCGCCTTCTTG
1331	hH1.4_aa114_BamHI_for	AGCTGGATCCGGGGAAGCCAAGCCTAAGG
1332	hH1.4_aa145_BamHI_for	AGCTGGATCCGCCACCCCCAAGAAGAGCG
1333	hH1.4_aa190_BamHI_for	AGCTGGATCCAAGGCCAAAGCAGTTAAACCC
1443	hH1.4_aa113_XbaI_rev	GATCTCTAGACTAAGAGGCCGCCTTCTTGTTGAG
1444	hH1.4_fl_XbaI_rev	GATCTCTAGACTACTTTTTCTTGGCTGCCG
1445	hH1.4 Cluster1 for	AGGGCGAGGAGGCCGGCTGCAGCTGCTGG
1446	hH1.4 Cluster1 rev	CCTCCTCGCCCTCTTTGGGGTCTTCTTGG
1447	hH1.4 Cluster2 for	AGAAGAGCGAGAAGCCCGAGAAGGGCGAGAGCAGCCAAGCCAAAAAAGG
1448	hH1.4 Cluster2 rev	TCTCGCCCTTCTCGGGCTTCTCGCTCTTCTGGCTCCAGCAGCTGCAGC
1449	hH1.4 Cluster3 for	AGGCCAAGAAGGGCGCCCAGGAGCCCAGCGAAGGCCAAAGC
1450	hH1.4 Cluster3 rev	AGGCCAAGAAGGGCGCCCAGGAGCCCAGCGAAGGCCAAAGC
1451	hH1.4 Cluster4 for	AGGGCCAGAGCAGTTAGACCCAGGGCGGCTAAACCAAAGACC
1452	hH1.4 Cluster4 rev	CCTGGGTCTAACTGCTCTGGCCCTCGCTGGGCTCTTGGGCGC
1453	hH1.4 Cluster5 for	AGACCAAGGACCGCCAGGCCCAGGGCAGCCAAGCCAAAGAAGG
1454	hH1.4 Cluster5 rev	CCTGGGCCTGGCGGTCCTTGGTCTAGCCGCCTTGGGTTTAACTGC
1455	hH1.4 Cluster6 for	AGGCCAAGGAGGGCGGCAGCCAGGAGAAGGTAGCTCGAGCGGCCGCATCG
1456	hH1.4 Cluster6 rev	CCTTCTCCTGGCTGCCGCCCTCCTTGGCCTGGCTGCCTTGGGCTTGGCGG
1457	Outer ScaI for	TTGATAAGTACTTGAAATCCAGCAAG
1458	Outer ScaI rev	TCTGTGACTGGTGAGTACTCAACC
1473	hH1.4 Cluster4 rev new	CCTGGGTCTAACTGCTCTGGCCCTGGATCCAGATCCGCCCG
1474	hH1.4 Cluster1a for	AGGAGGAGCGCCAGGAGGACCCCAAGGAGGGCGAAGAAGCCGGCTGC
1475	hH1.4 Cluster1a rev	CCTCCTTGGGGTCCTCCTGGCGCTCCTCCTGGGGGTGGCGGATCCAG
1489	hH1.4 K157R for	CCAAAGAAGGCGAGGAAGCCGGCTGC

1490	hH1.4 K157R rev	GCAGCCGGCTTCCTCGCCTTCTTTGG
1491	hH1.4 K171R for	GAGCCAAAAAAGCGAGAAGCCCGAAAAAGGC
1492	hH1.4 K171R rev	GCCTTTTTCGGGCTTCTCGCTTTTTTGGCTC
1493	hH1.4 K177R for	CCGAAAAAGGCGAGAGCAGCCAAGCC
1494	hH1.4 K177R rev	GGCTTGGCTGCTCTCGCCTTTTTCGG
1495	hH1.4 K192R for	CTGGATCCAAGGCCAGAGCAGTTAAACCC
1496	hH1.4 K192R rev	GGGTTTAACTGCTCTGGCCTTGGATCCAG
1497	hH1.4 K197R for	GCAGTTAAACCCAGGGCGGCTAAACCAAAG
1498	hH1.4 K197R rev	CTTTGGTTTAGCCGCCCTGGGTTTAACTGC
1499	hH1.4 K212R for	GCAGCCAAGCCAAGGAAGGCGGCAGC
1500	hH1.4 K212R rev	GCTGCCGCCTTCCTTGGCTTGGCTGC
1501	hH1.4 K219R for	GGCAGCCAAGAAAAGGTAGCTCGAGCGG
1502	hH1.4 K219R rev	CCGCTCGAGCTACCTTTTCTTGGCTGCC
1511	hH1.4 K192R (fl) for	GAGCCCAGCGAAGGCCAGAGCAGTTAAACCC
1512	hH1.4 K192R (fl) rev	GGGTTTAACTGCTCTGGCCTTCGCTGGGCTC

6.1.4 Agarose Gel Extraction of DNA

Digested DNA and PCR products with the correct length were cut out from the gel (Agarose from Promega Corporation). Per 100 mg gel, 200 µl of NT-binding-buffer (MACHEREY-NAGEL, Switzerland) was added to dissolve the agarose gel and to equilibrate the purification columns. The sample was then heated to 50°C and mixed until the gel was solubilized. This solution was transferred onto a NucleoSpin column (MACHEREY-NAGEL, Switzerland) and centrifuged for 1 minute at 11000 rpm (12900 rcf) to bind the DNA to the silica-matrix of the column. The column was washed using 600 µl NT3 washing buffer (MACHEREY-NAGEL, Switzerland) and the centrifugation step was repeated (1 min, 11000 rpm, 12900 rcf). The washing buffer was discarded and the column dried by a 2 minute centrifugation step at 11000 rpm (12900 rcf). Then, the column was placed in a fresh Eppendorf tube and 30 µl sterile ddH_2O was added to the column. After 2 minutes of incubation at room temperature, the DNA was eluted from the column by another centrifugation step at 11000 rpm (12900 rcf) for 1 minute.

6.1.5 Restriction Endonuclease Digest

Restriction endonuclease digests were performed to prepare the ends of the amplified DNA fragments for cloning. DNAs (vector and insert) were digested with a single endonuclease or with two restriction enzymes simultaneously to generate the product ends of interest. All enzymes were purchased from New England Biolabs (NEB) and used according to NEB's protocols.

6.1.6 Ligation of DNA Fragments into a Vector

After the restriction digest, PCR products and the vector DNA were separately purified with NucleoSpin columns (as described in 5.1.4). For the ligation reaction, approximately 50 ng of linearized vector (pGEX-6PI, pEGFP-C1, pET28a), insert DNA in a molar ratio of 1:3 of vector to insert, 1µl of 10x T4-DNA-Ligase Buffer (Fermentas), and 1 Weiss Unit of T4-Ligase (Fermentas) were used. The ligation mix was incubated overnight at 16°C and inactivated at 65°C for 20 min the next day.

6.1.7 Small-scale Plasmid Isolation (Miniprep)

3 ml of an XL-10 *E. coli* overnight culture were grown under selection conditions and centrifuged for 5 minutes at 5000 rpm (2700 rcf). 300 µl RES-buffer (MARCHEREY-NAGEL, Switzerland) was used to resuspend the pellet. Then, 300 µl LYS-buffer (MARCHEREY-NAGEL, Switzerland) was added to lyse the bacteria. The samples were tilted 2-3 times and incubated 5 minutes at room temperature. Subsequently, 400 µl NEU-buffer (MARCHEREY-NAGEL, Switzerland) was added to stop the lysis. The samples were tilted twice, incubated on ice for 10 minutes, and centrifuged for 20 minutes at 14000 rpm (20800 rcf, 4°C). The supernatant, containing the extra chromosomal DNA, was transferred into a fresh tube and 700 µl isopropanol (100%, Sigma-Aldrich) was added to precipitate the DNA. Next, the samples were tilted and incubated for 10 minutes on ice. After centrifugation for 10 minutes at 14000 rpm (20800 rcf, 4°C), the supernatant was discarded and 200 µl of ice cold ethanol (70%) was added to wash the precipitated DNA. The DNA was incubated on ice for another 5 minutes, followed by centrifugation for 5 minutes at 14000 rpm (20800 rcf, 4°C). After that, the ethanol was discarded and the pellet was air-dried for 10 minutes at room temperature. The pellet containing the DNA was resuspended by adding 20 µl of sterile H_2O and gentle shaking for 20 minutes at room temperature.

6.2 Microbiological Methods

6.2.1 Transformation of Chemo-competent *E. coli*

Approximately 100 ng plasmid DNA and 90-120 µl competent *E. coli*, strain XL-10 for plasmid amplification or BL-21 for protein production, were incubated on ice for 10 minutes. Then, bacteria were heat shocked by exposing the mixture to 42°C for 45 seconds.

Subsequently, the samples were placed again on ice for 10 minutes. To allow the bacteria to recover and to express the selection markers, 1 ml of LB medium was added and the tubes were incubated while shaking for 60 minutes at 37°C. Samples were centrifuged for 1 minute at 11000 rpm (12900 rcf) to pellet the bacteria, the supernatant was discarded, the pellet resuspended in 100 µl LB medium and the cell suspension plated on a LB Agar-plate containing 50 µg/ml ampicillin or kanamycin, depending on the resistance marker of the plasmid. The plate was incubated overnight at 37°C. The next day, bacterial colonies were picked and inoculated into 3 ml LB-medium with 50 µg/ml antibiotics overnight at 37°C.

6.2.2 Expression of GST/His-tagged Histones in Bacteria

Plasmid-DNA was transformed into competent *E. coli* strain BL-21, according to 5.2.1. *E. coli* cells were grown at 37°C overnight in 20 ml LB medium containing 50 µg/ml ampicillin or kanamycin, depending on the plasmid's resistance marker. The next day, 5 ml of the bacterial culture was transferred into 120 ml LB medium containing antibiotics and grown at 37°C to an OD_{600}= 0.6. Addition of 1 mM IPTG induced the expression of the GST/His protein. After 4 hours incubation at 37°C, bacteria were centrifuged in a Sorvall RC 5C Plus centrifuge with a SLA-3000 rotor at 4000 rpm (2702 rcf) for 15 minutes at 4°C. The supernatant was discarded and the pellet was stored at -80°C until the purification was continued (see 5.3.1).

6.3 Protein based Methods

6.3.1 Purification of His/GST-tagged H1.4 Constructs

Tagged histone constructs were purified from frozen bacteria. The frozen pellets were thawed on ice and resuspended in 20 ml binding buffer (BB) (for content see below). Next, the solution was passed three times through a French® pressure cell press (SIM-AMINCO) with a maximum of 1500 psi and subsequently centrifuged in a Sorvall RC 5C Plus centrifuge with a SS-34 rotor for 30 minutes at 4°C and at 18000 rpm (38729 rcf). Meanwhile, 125-200 µl of a 50% (v/v) suspension Ni-Sepharose 6 Fast Flow beads (Amersham Bioscience) for His-tagged proteins, or Glutathione Sepharose 4B beads (GE Healthcare) for GST-tagged proteins, were equilibrated. The beads were washed twice with 1 ml BB and centrifuged at 2400 rcf for 1 minute after each washing step. Afterwards, the

cleared cell lysate (from above) was bound to the beads in a 50 ml falcon tube for 2 hours at 4°C while rolling.

The H1.2 cluster mutants were purified in a special manner. The bacterial pellets were initially resuspended in 15 ml EBC-buffer (for content see below) and processed as described above. After the first centrifugation, the pellet was resuspended in 500 µl 5% (v/v) perchloric acid and incubated in a Eppendorf tube for 2 hours at 4°C while rolling. Next, the suspension was centrifuged for 10 minutes at 4°C and 20800 rcf. After transferring the supernatant into a 15 ml falcon tube, 200 µl 3M Tris pH 9.5 were added. While shaking gently, 13,7 ml BB were slowly added and then the proteins were bound to the equilibrated beads for 2 hours at 4°C while shaking.

Later, all beads were collected by centrifugation (Hettich, 251 rcf, 5 minutes, 4°C) and were washed three times with 10 ml washing buffer (WB) (for content see below) for 10 minutes. The beads were transferred into a 1,5 ml Eppendorf tube and washed with 1 ml elution buffer (EB) (for content see below), without imidazole for His-tagged proteins or without glutathione for GST-tagged protein, and centrifuged at 2400 rcf for 1 minute at 4°C. Next, the purified proteins were eluted by twice adding 200-800 µl elution buffer with imidazole or with glutathione for 30 minutes at 4°C while rolling. Each time, the beads were collected by centrifugation (2400 rcf, 1 minute, 4°C) and the supernatant, containing the eluted proteins, was transferred into a fresh Eppendorf tube. Lastly, the eluted proteins were dialyzed overnight in 1 liter of dialysis buffer (for content see below) and a molecular porous membrane (MWCO: 6-8.000) (SPECTRA/POR®).

Composition of buffers used for the purification of GST-tagged proteins:

BB pH 7.3: 0.05 M Tris-HCl pH 7.4, 0.2 M NaCl, 0.1% (v/v) NP-40, 5% (v/v) glycerol, 1 mM DTT, 2 mM PMSF and 1 µl/ml pepstatin, bestatin and leupeptin.

WB pH 7.3: 0.05 M Tris-HCl pH 7.4, 0.5 M NaCl, 0.1% (v/v) NP-40, 5% (v/v) glycerol, 1 mM DTT, 2 mM PMSF and 1 µl/ml pepstatin, bestatin and leupeptin.

EB pH 8: 0.05 M Tris-HCl pH 7.4, 0.05 M NaCl, 0.04 M glutathione, 5% (v/v) glycerol, 1 mM DTT, 2 mM PMSF and 1 µl/ml pepstatin, bestatin and leupeptin.

Dialysis Buffer pH 7.4: 0.05 M Tris-HCl pH 7.4, 0.05 M NaCl, 20% (v/v) glycerol, 1 mM DTT, 2 mM PMSF and 1 µl/ml pepstatin, bestatin and leupeptin.

Composition of buffers used for the purification of GST-tagged proteins:

EBC: 0.05 M Tris-HCl pH 8, 0.12 M NaCl, 0.5% (v/v) NP-40, 5 mM DDT, 1 mM PMSF.

BB pH 7.4: 0.05 Tris-HCl pH 7.5, 0.5 M NaCl, 1% (v/v) triton, 5% (v/v) glycerol, 15 mM imidazole, 2 mM β-ME, 2 mM PMSF and 1 µl/ml pepstatin, bestatin and leupeptin

WB pH 7.4: 0.05 M Tris-HCl pH 7.5, 0.3 M NaCl, 1% (v/v) triton, 5% (v/v) glycerol, 15 mM imidazol, 2 mM β-ME, 2 mM PMSF and 1 µl/ml pepstatin, bestatin and leupeptin

EB pH 7.4: 0.05 M Tris-HCl pH 7.5, 0.05 M NaCl, 5% (v/v) glycerol, 0.5 M imidazol, 2 mM β-ME, 2 mM PMSF and 1 µl/ml pepstatin, bestatin and leupeptin.

Dialysis Buffer pH 7.4: 0.05 M Tris-HCl pH 7.4, 0.05 M NaCl, 20% (v/v) glycerol, 1 mM DTT, 2 mM PMSF and 1 µl/ml pepstatin, bestatin and leupeptin

6.3.2 Bradford Protein Concentration Measurement

To determine protein concentrations, the Bradford assay was performed. 5x BIO-RAD solution (BIO-RAD Protein assay, Bio-Rad Laboratories GmbH) was diluted to 1x concentration with ddH_2O. 5-15 µl of protein extract or 20 µl of BSA standard solutions (0.190 mg/ml, 0.328 mg/ml, 0.492 mg/ml and 0.643 mg/ml) were added to 1 ml of the 1x BIO-RAD solution. The absorbance was measured at 595 nm in a spectrometer and the protein concentrations were calculated based on the BSA standard curve.

6.3.3 Methylation Assay

1 µg purified protein was incubated with 1 µg SET7/9 and 30 nCi SAM or 20 mM cold SAM in methylation buffer (50 mM NaCl, 50 mM Tris pH 8 (pH 7.2 or pH 9 in experiments with H1.2), 10% (v/v) glycerol, 1 mM PMSF) in a total volume of 25 µl for 1 hour or 15 minutes at 30°C. The reaction was stopped by adding 3 µl of 10x SDS-sample buffer (600 mM Tris-HCl (pH 6.8), 20% (w/v) Na-dodecylsulfate, 20% (v/v) glycerol, 0.05% (w/v) bromphenol blue, 20% (v/v) mercaptoethanol, 25 mM DTT). The samples were subsequently boiled for 5 minutes at 95°C, followed by protein separation using a SDS-PAGE (as described in 5.3.6). The methylation assay was analyzed either by autoradiography or western blot.

6.3.4 PARylation Assay

1 µg purified protein was incubated with 10 pmol ARTD1 or ARTD10 in the presence or absence of 5 pmol activating EcoRI-linker DNA and 0.16 mM ^{32}P-NAD^+ or 10 mM cold NAD^+ in PARylation buffer (50 mM NaCl, 50 mM Tris pH 8, 4 mM $MgCl_2$, 250 µM DTT,

1 mg/ml pepstatin, 1 mg/ml bestatin, 1 mg/ml leupeptin) in a total volume of 25 µl for 10 minutes and at 30°C. The reaction was stopped by adding 3 µl of 10x SDS-sample buffer (600 mM Tris-HCl (pH 6.8), 20% (w/v) Na-dodecylsulfate, 20% (v/v) glycerol, 0.05% (w/v) bromphenol blue, 20% (v/v) mercaptoethanol, 25 mM DTT). The samples were subsequently boiled for 5 minutes at 95°C, followed by protein separation using SDS-PAGE (as described in 5.3.6). The PARylation assay was analyzed either by autoradiography or western blot.

6.3.5 Sequential ADP-Ribosylation and Methylation Assay

1 µg purified protein was incubated with 10 pmol ARTD1 in the presence of 5 pmol activating EcoRI-linker DNA and 160 µM NAD^+ in PARylation buffer (50 mM NaCl, 50 mM Tris pH 8, 4 mM $MgCl_2$, 250 µM DTT, 1 mg/ml pepstatin, 1mg/ml bestatin, 1mg/ml leupeptin) in a total volume of 25 µl for 15 minutes and at 30°C. 0.2 mM PJ-34 was used to inhibit PARylation by ARTD1 either before ADP-ribosylation or afterwards, always with 5 minutes incubation time. 1 µg SET7/9 and 0.03 µCi ^{14}C-SAM was then added to start the methylation (1 hour at 30°C). The reaction was stopped by adding 3 µl of 10x SDS-sample buffer (600 mM Tris-HCl (pH 6.8), 20% (w/v) Na-dodecylsulfate, 20% (v/v) glycerol, 0.05% (w/v) bromphenol blue, 20% (v/v) mercaptoethanol, 25 mM DTT). The samples were subsequently boiled for 5 minutes at 95°C, followed by protein separation using SDS-PAGE (as described in 5.3.6). The assays were analyzed by autoradiography.

6.3.6 Sodium Dodecyl Sulfate Polyacrylamide Gel Electrophoresis (SDS-PAGE)

The SDS-PAGE is used to separate proteins based on their molecular weight. Initially, a glass and a teflon plate (10 x 8.5 cm) were cleaned with Ethanol (70%) and laid on top of each other, separated by two spacers (10 x 0.15 cm). After assembling, the plates were placed into a gel preparation unit and 6 ml of separation gel solution was poured between the two plates (15% SDS-PAGE: 3 ml ddH_2O, 2 ml Solution B (1.5 M Tris-HCl pH 8.8, 0.4% (w/v) Na-dodecyl sulfate), 3 ml Acrylamide (Acrylamide-Bis solution (37.5:1), 40% (w/v), SERVA Electrophoresis GmbH), 80 µl APS (10%), 8 µl TEMED). Immediately after filling the chamber, the gel was overlaid with 1 ml of H_2O to obtain a sharp border of the gel. After polymerization (10 to 20 minutes), the water was replaced by 3 ml of stacking gel solution (3 ml of 4% (v/v) stacking solution (65 ml ddH_2O, 25 ml Solution C (0,5 M Tris-HCl pH 6.8, 0.4% (w/v) Na-dodecyl sulfate and a tip of Bromphenol blue), 10 ml of 40% (w/v)

Acrylamide), 30 µl APS (10%), 3 µl TEMED). Before polymerization, a comb containing 10 or 15 flaps was stuck into the stacking gel solution to generate the sample pockets. SDS-gels were either directly used 2 hours after pouring or stored at 4°C overnight. To run the gel, the comb was removed and the gel was placed into a running unit filled with 1x SDS running buffer (25 mM Tris base, 200 mM Glycine, 0.1% (w/v) Na-dodecyl sulfate). The sample pockets were rinsed with 1x SDS running buffer. Into one pocket, 3 µl of a pre-stained protein ladder (PageRuler™) as a marker with distinct molecular weights was loaded. The other pockets were loaded with different samples and run for 20 minutes at 70V, allowing proteins to stack and reach the beginning of the separation gel. Then, the voltage was raised to 120V until the sample buffer reached the end of the gel (1-2 hours). Finally, the gel was disassembled and either stained or blotted (as described in 5.3.7). For staining, the gel was soaked in Coomassie staining solution (0.25% (w/v) Coomassieblue R250, 40% (v/v) Methanol, 10% (v/v) Acetic acid) for at least 20 minutes. Destaining was performed with Fast Destain (12% (v/v) Methanol, 10% (v/v) Acetic acid) and the stained gel was dried in a gel dryer (Model 583, Bio Rad) at 70°C for 3 hours.

Gels containing radioactively marked proteins (^{14}C-SAM) were then exposed to a film (Typox TX-RP medical X-ray film, Raymed Imaging AG, Krauchthal), which was developed (Optimax, Raymed Imaging AG, Krauchtal) after 1-3 days of exposure.

6.3.7 Western Blot Analysis

After SDS-PAGE, proteins were transferred to a nitrocellulose membrane to specifically detect proteins or posttranslational modifications by western blotting. A western blot unit was assembled in a plastic frame in the following order: one wetted sponge, 3 pre-wetted Whatman papers, one PVDF membrane (Millipore, pore size 0.45 µm, first activated in 100% ethanol), the SDS-gel, 3 pre-wetted Whatman papers and one wetted sponge and subsequently put with an ice bloc into a western blot chamber filled with 1x transfer buffer (20% (v/v) methanol, 70% ddH_2O, 10% (v/v) 10x transfer buffer (25 mmol/l Tris-base, 192 mmol/l glycine, dissolved in ddH_2O)). Blotting was performed overnight at 32V and 4°C and the voltage was increased to 100V for the last 1 hour before processing the membrane. To confirm a successful blotting, the membrane was stained with Ponceau red (1% Ponceau S, 0.1% (v/v) acetic acid) and destained with deionized water. To avoid unspecific binding of the antibody, each membrane was incubated with 5 ml blocking solution for 1 hour on a shaker at room temperature. The blocking solution consisted of 5% skim milk or 3% BSA

(bovine serum albumin) in TBS-T (10 mmol/l Tris HCl pH 7.5,150 mmol NaCl, ddH_2O, 0.1% (v/v) tween 20) depending on the primary antibody. After blocking, the membrane was incubated with the primary antibody (anti-meARTD1, rabbit, 1:5000, Abcam or anti-PAR, rabbit, 1:3000, BD) in 1% skim milk or 3% BSA dissolved in TBS-T for 2 hours. After three washes with 5 ml TBS-T for 10 minutes each, the membrane was incubated with the secondary antibody in the presence of 1% skim milk or 3% BSA for 1 hour on a shaker at room temperature. The selection of the secondary antibody depended on the primary antibody (anti-rabbit or anti-mouse). At the end, the blot was washed again 3 times with 5 ml TBS-T for 10 minutes and analyzed with an Odyssey® Imager (Li-Cor Biosciences GmbH).

6.4 Cell Culture Methods

6.4.1 Cultivation

An aliquot of frozen U2OS cells, received from Ingrid Kassner (IVBMB, Zürich), was thawed at 37°C for 5 to 10 minutes. The cells were transferred to a 15 ml falcon tube and centrifuged at 251 rcf for 5 minutes. Afterwards, the cells were resuspended in fresh medium and seeded in a six well dish (TTP). U2OS cells were cultured in DMEM containing stable glutamine and supplemented with 10% fetal calf serum and 1% penicillin/streptomycin. Cells were grown in an incubator at 37°C, 5% CO_2. Before reaching confluency, cells were split. For splitting, plates containing cells were washed with PBS and then 1,5 ml trypsin-EDTA was added to a 10 cm plate. After 2 minutes incubation in the incubator, cells were collected from the plate with 3 ml DMEM and transferred to a 15 ml falcon tube. Cells were counted with the Casy Counter (Roche innovatis AG) and approximately $8x10^5$ cells were seeded again on a 10 cm plate.

6.4.2 Transient Cell Transfection

U2OS cells in six well dishes were grown until they reached a confluence of 80% and then transfected with transit LT1 (Mirus). A transfection solution was prepared (2 ml DMEM medium, 100 µl Opti-MEM (Invitrogen), 1,5 µg DNA and 4,5 µl transit LT1) and used according to the manufacturer's protocol.

6.4.3 Life Cell Imaging

Cells were analyzed by fluorescence microscopy (Leica, DMI6000 B) 3 days after transfection. U2OS cells, grown in six well dishes, were directly taken from the incubator to the microscope for the analysis, without removing the DMEM medium. After a short general inspection to evaluate the transfection rate, single clusters of cells were analyzed under fluorescent light (filter I3, 488 nm excitation laser light) or in phase contrast mode. A merged picture (fluorescence and phase contrast) was obtained by overlaying the single pictures.

7 Results

7.1 Published Results

7.1.1 Crosstalk between Set7/9-dependent Methylation and ARTD1-mediated ADP-ribosylation of Histone H1.4

Authors: Ingrid Kassner, Marc Barandun, Monika Fey, Michael O. Hottiger
Journal: Epigenetics Chromatin. 2013 Jan 5;6(1):1.
Contribution: Planning, performing (includes cloning and protein expression) and evaluating the experiments described in Figure 3A, F3C, F3D and supplementary Figure S2B, S2C and S2D

Kassner *et al. Epigenetics & Chromatin* 2013, **6**:1
http://www.epigeneticsandchromatin.com/content/6/1/1

Epigenetics & Chromatin

RESEARCH Open Access

Crosstalk between SET7/9-dependent methylation and ARTD1-mediated ADP-ribosylation of histone H1.4

Ingrid Kassner[1,2], Marc Barandun[1], Monika Fey[1], Florian Rosenthal[1,2] and Michael O Hottiger[1*]

Abstract

Background: Different histone post-translational modifications (PTMs) fine-tune and integrate different cellular signaling pathways at the chromatin level. ADP-ribose modification of histones by cellular ADP-ribosyltransferases such as ARTD1 (PARP1) is one of the many elements of the histone code. All 5 histone proteins were described to be ADP-ribosylated *in vitro* and *in vivo*. However, the crosstalk between ADP-ribosylation and other modifications is little understood.

Results: In experiments with isolated histones, it was found that ADP-ribosylation of H3 by ARTD1 prevents H3 methylation by SET7/9. However, poly(ADP-ribosyl)ation (PARylation) of histone H3 surprisingly allowed subsequent methylation of H1 by SET7/9. Histone H1 was thus identified as a new target for SET7/9. The SET7/9 methylation sites in H1.4 were pinpointed to the last lysine residues of the six KAK motifs in the C-terminal domain (K121, K129, K159, K171,
K177 and K192). Interestingly, H1 and the known SET7/9 target protein H3 competed with each other for SET7/9-dependent methylation.

Conclusions: The results presented here identify H1.4 as a novel SET7/9 target protein, and document an intricate crosstalk between H3 and H1 methylation and PARylation, thus implying substrate competition as a regulatory mechanism. Thereby, these results underline the role of ADP-ribosylation as an element of the histone code.

Keywords: PARP-1, SET7/9, Lysine methylation, Poly-ADP-ribosylation, Post-translational modification

Background

Histones are nuclear proteins that package and order the DNA into nucleosomes [1]. Five major families of histones exist: H1 (H5), H2A, H2B, H3, and H4. Two copies of the core histones H2A, H2B, H3 and H4 form the octameric nucleosome core particles [2]. Unlike the other histones, only one copy of the linker histone H1 is present and stabilizes the DNA, which is wrapped around the core nucleosome [3]. Linker histones bind to both the nucleosome and the linker DNA region (approximately 20 to 80 nucleotides in length) between nucleosomes. The interaction of H1 with the nucleosome and additional DNA stretches at the entry/exit of the nucleosome forms the chromatosome and leads to higher order chromatin structure [4]. Many experiments addressing H1 function have been performed with purified, processed chromatin under low-salt conditions, but the *in vivo* role of H1 is less clear. Cellular studies have shown that overexpression of H1 can cause aberrant nuclear morphology and chromatin structure and, depending on the gene, H1 can serve as either a positive or a negative regulator of transcription [5]. Similar to the core histones, H1 is composed of three domains [6]. The N-terminus is a short, flexible segment rich in basic amino acids, the central domain exhibits a globular structure composed of a winged helix motif [6] and the C-terminus is predominantly composed of lysine, alanine and proline residues and is the main determinant for H1 binding to chromatin [7]. Among the five histone families of the chromatosome, the linker histone H1 is the least conserved. In the human genome, 11 genes encoding H1 variants have been identified and

* Correspondence: hottiger@vetbio.uzh.ch
[1]Institute of Veterinary Biochemistry and Molecular Biology, University of Zurich, Winterthurerstrasse 190, Zurich 8057, Switzerland
Full list of author information is available at the end of the article

Kassner et al. Epigenetics & Chromatin 2013, 6:1
http://www.epigeneticsandchromatin.com/content/6/1/1

are transcribed either ubiquitously or in a cell type-specific manner [4,8]. The study described here focuses on histone H1.4, a histone variant that is expressed in somatic cells during S phase. Together with H1.2 it is the predominant histone variant in most cell types. Similar to the core histones, linker histones are subject to extensive post-translational modifications (PTMs), including phosphorylation, methylation and acetylation [9].

SET7/9 (also SET7, SET9, SETD7 or KMT7) is a mono-methyltransferase for the lysine residue at position 4 of histone H3 (H3K4) [10,11] that was linked to transcriptional activation. It methylates the consensus motif [K>R][S>KYARTPN][Kme] and prefers lysine residues within positively charged regions [12]. However, SET7/9 exhibits only weak lysine methyltransferase activity towards H3 in nucleosomes *in vitro*, suggesting that additional factors may affect SET7/9-dependent H3K4 methylation *in vivo*, or that histone proteins are not the main substrates of SET7/9. Lysine methylation can be reversed by demethylases of the lysine-specific demethylase (LSD) family or the Jumonji-C domain family of proteins [13,14].

In contrast to the canonical PTMs of the histone code, adenosine diphosphate (ADP)-ribosylation is much less studied. ADP-ribosylation comprises the transfer of the ADP-ribose moiety from the co-substrate nicotinamide adenine dinucleotide (NAD^+) onto specific amino acid side chains of acceptor proteins or to pre-existing protein-linked ADP-ribose units by ADP-ribosyltransferases (ARTs). Mammalian ARTs can be divided into two groups according to their similarity to the bacterial diphtheria and cholera toxins - the ARTDs (also known as poly(ADP-ribose) polymerases (PARPs)) and ARTCs, respectively [15]. ARTD1 (PARP1) is the best-studied member of the ARTD family and represents a highly abundant (on average 1×10^6 molecules per cell), chromatin-associated enzyme that is responsible for most (about 90%) of the cellular PAR generation [16,17]. It is implicated in many cellular processes such as the genotoxic stress response, cell cycle regulation, gene expression, differentiation and aging [18,19]. The major modification target of ARTD1 is ARTD1 itself, but it also modifies other nuclear proteins including all five histone proteins *in vitro* and *in vivo* [20]. In native chromatin, histone H1 is the main ADP-ribose acceptor, but depending on the chromatin composition and the accessibility of different histones, the ADP-ribosylation pattern of histones varies [21,22]. Mass spectrometry and electron-transfer dissociation (ETD) identified for the first time K13 of histone H2A, K30 of H2B, K27 and K37 of H3 as well as K16 of H4 as ADP-ribose acceptor sites (catalyzed by ARTD1) [23].

Crosstalk between different PTMs occurs directly by competition for acceptor sites or indirectly by changes in the accessibility of chromatin for modifying enzymes. The observation that specific lysine residues serve as ADP-ribose acceptors is important because the same amino acid residues are potential acetylation and methylation sites [24]. It is therefore likely that competition for acceptor sites between different histone PTMs such as ADP-ribosylation, acetylation, methylation and phosphorylation causes crosstalk [20]. This has been demonstrated by the finding that acetylation of lysine residue K16 of histone H4 inhibits ADP-ribosylation *in vitro* [23], which suggests that different crosstalk likely exists *in vivo* as well. Similarly, H1.4 K26 dimethylation and AuroraB-mediated phosphorylation of S27 have been reported to interfere with each other [25]. Whether or not other modifications of the histone code such as methylation or phosphorylation also crosstalk with ADP-ribosylation has not been studied before.

Here, we define the linker histone H1.4 as a novel target of SET7/9-dependent methylation, identify lysines K121, K129, K159, K171, K177 and K192 as methyl acceptor sites and describe crosstalk between H1.4 methylation and ADP-ribosylation as well as competition with histone H3 methylation.

Results and discussion

PARylation inhibits SET7/9-dependent methylation of histone H3

ADP-ribosylation is a PTM of a wide variety of target proteins, including histones [20,23,26]. However, since histone tails are subject to many types of PTMs, crosstalk between different modifications likely exists. Therefore, it was investigated whether histone PARylation by ARTD1 affects consecutive SET7/9-dependent H3 methylation. A histone mix was PARylated for different time periods and then subjected to methylation assays with SET7/9 and radio-labelled S-adenosyl-L-(methyl-^{14}C) methionine (^{14}C-SAM) as methyl donor. ARTD1 and histones were both strongly PARylated and the level of modification correlated with the reaction times (see Additional file 1). In the absence of PARylation, mainly core histones, which comprise H3, were methylated (time-point 0) (Figure 1A). However, after 1 minute of PARylation of the histones by ARTD1, the methylation of core histones was already strongly reduced.

As a control for these results, recombinant H3 was incubated with ARTD1, NAD^+ and with or without DNA (to stimulate ARTD1) and 3-AB (to inhibit ARTD1). H3 was methylated by SET7/9 if ARTD1 was inactive or inhibited (Figure 1B, lanes 1 and 4), but prevented in the samples containing activated ARTD1 (Figure 1B, lanes 2 and 3). PARylation of SET7/9 was not the cause for this effect, because the methyltransferase was only added after the PARylation reaction and

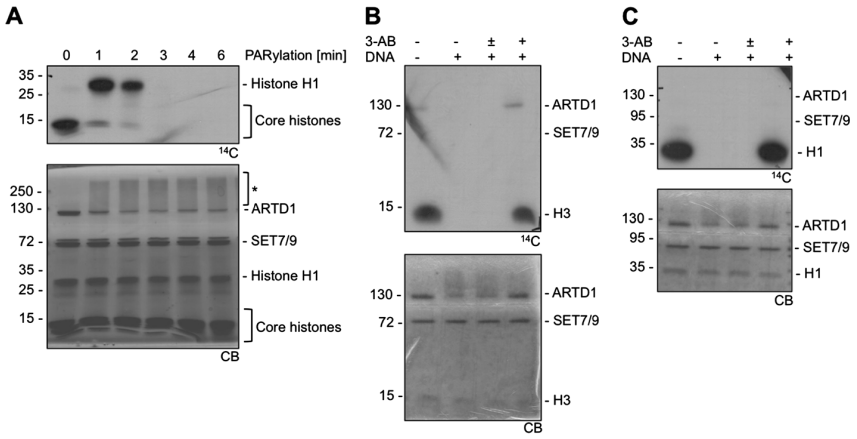

Figure 1 PARylation inhibits SET7/9-dependent methylation of histone H3 and H1. (**A**) ARTD1 was auto-modified for the indicated times and then inhibited by addition of PJ-34. A histone mix was added to the reaction either before or after the inhibition of ARTD1. Methylation was started after PJ-34 addition by adding SET7/9 and ^{14}C-SAM. Proteins were separated by SDS-PAGE, stained with Coomassie blue (CB, lower blot) and methylation was analyzed by autoradiography (^{14}C, upper blot). The asterisk marks the shift of automodified ARTD1. (**B**) H3 was incubated with ARTD1 and 160 μM NAD^+. Activating DNA and PARP inhibitor 3-AB were present during the reaction as indicated. Methylation was then started by addition of SET7/9 and ^{14}C-SAM ± 3-AB was added directly before addition of SET7/9 after the PAR reaction. (**C**) Influence of ARTD1 on H1 methylation as in (**B**). The approximate molecular weight is indicated on the left of each gel/blot.

addition or omission of 3-AB did not affect the result (Figure 1B, lanes 2 and 3).

PARylation of histone H3 allows methylation of H1 by SET7/9

Interestingly, ADP-ribosylation of H3 for 1 or 2 minutes and subsequent inhibition of its methylation resulted in an unexpected and strong H1 methylation (Figure 1A). In order to confirm H1 methylation by SET7/9, experiments with purified H1 were performed. As before, H1 was incubated with ARTD1, NAD^+ and with or without DNA and 3-AB. Similar to H3, histone H1 was methylated by SET7/9 in the absence of active ARTD1, but H1 methylation was completely inhibited by PARylation (Figure 1C). These results suggested that in addition to H3, histone H1 is a new methylation target of SET7/9 and that prior PARylation of H1 and H3 prevents consecutive methylation by SET7/9.

Histones H1 and H3 compete for SET7/9-dependent methylation

The results presented so far suggested that H1 and H3 are both methylated by SET7/9, but only in the absence of PARylation. ARTD1-dependent PARylation might thus modulate which histone protein is methylated. To test this hypothesis, *in vitro* competition experiments with or without PARylation of H1 and H3 were performed. H1 and H3 were strongly methylated by SET7/9 if present alone (Figure 2A, lanes 1 and 5). However, H1 and H3 competed with each other when present in the same reaction and thus lead to a reduced methylation signal (lanes 2 to 4). Prior PARylation of histone H3 completely abolished its competing activity for SET7/9-dependent H1 methylation (lanes 6 to 7). To further study and confirm this finding, a PARylation time course experiment with histone H1 or histone mix prior to SET7/9 methylation was performed. Set7/9-dependent methylation of H1 was abolished after 15 minutes of PARylation by ARTD1 (Figure 2B). In contrast, H3 methylation in a histone mix was already inhibited after 5 minutes of ARTD1 treatment, which lead to consecutive H1 methylation by Set7/9 (Figure 2C). In both cases, addition of the histones after the PARylation reaction did not influence consecutive Set7/9-dependent methylation (that is, H1 was methylated only if H3 was not present).

These results suggested that, in comparison to H1, H3 is preferentially modified by both, SET7/9 and ARTD1. In the short window when H1 methylation is inhibited due to PARylation but H3 is not yet fully ADP-ribosylated, SET7/9 dependent methylation of H3 is detectable. This example thus illustrates how different affinities for modifying enzymes can induce a switch of target proteins. These results suggest that differential PARylation of histone proteins by ARTD1 can indirectly influence histone methylation and thus the histone code by determining which target proteins are modified. In addition to crosstalk between PARylation and methylation, SET7/9 function is thus also subject to crosstalk between different substrates (for example, H3 and H1).

Kassner *et al. Epigenetics & Chromatin* 2013, **6**:1
http://www.epigeneticsandchromatin.com/content/6/1/1

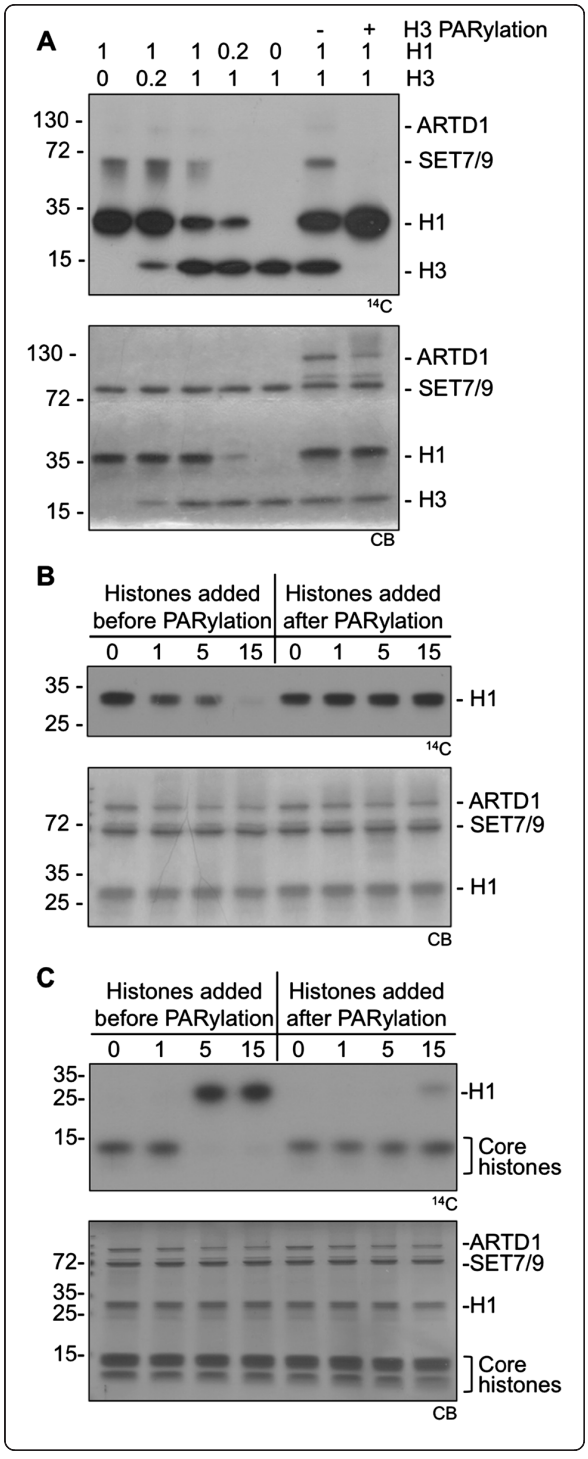

Figure 2 Histones H1 and H3 compete for SET7/9-dependent methylation. (**A**) H3 and H1 compete for methylation by SET7/9. H1 was methylated in presence of the indicated molar ratios of H3. In lanes 6 and 7, H3 was incubated with ARTD1 and NAD^+ in the presence or absence of 3-AB before addition of H1 and the methylation reaction. (**B**) ARTD1 was auto-modified for the indicated times and then inhibited by addition of PJ-34. H1 was added to the reaction either before or after the PARylation. Methylation was started after addition of PJ-34 by adding SET7/9 and ^{14}C-SAM. (**C**) As for (**B**), but a histone mix was used.

The C-terminus of linker histone H1.4 is methylated by SET7/9

In order to characterize the new SET7/9 methylation target H1, different fragments of H1.4 were created and their methylation was analyzed. Interestingly, full-length histone H1.4 was not methylated in the presence of plasmid DNA and neither was an H1.4 mutant lacking the C-terminus (ΔCT) (Figure 3A). These results suggested that H1.4 is methylated at the C-terminal domain (CTD), which has been reported to bind to DNA, and that SET7/9 likely methylates soluble H1.4 that is not part of the chromatin structure. In order to locate the methylation site in histone H1.4, recombinant, C-terminally truncated, HIS-tagged H1.4 fragments as well as short fragments of the CTD were analyzed (Figure 3B). Full length H1.4 (aa 1 to 219) was strongly methylated, while partial truncation of the CTD (1 to 189 or 1 to 156) caused reduced SET7/9-dependent methylation (Figure 3C). To further pinpoint the methylation sites in the H1.4 CTD, three H1.4 fragments covering the whole CTD were expressed as glutathione-S-transferase (GST)-fusion proteins (aa 114 to 144, 145 to 189, 190 to 219, Figure 3B) and used in methylation assays. All three fragments were methylated by SET7/9, albeit to different degrees (Figure 3D). Fragment 190 to 219 showed the strongest methylation, while the fragment from amino acids 114 to 144 was only weakly methylated, suggesting that multiple SET7/9-dependent methylation sites are present in the CTD of H1.4. These results demonstrated that the linker histone H1.4 is methylated by SET7/9 *in vitro*.

Linker histone H1.4 is methylated at six lysine residues of the C-terminal domain

In order to define all SET7/9-dependent methylation sites in the CTD of the H1.4, the C-terminal fragments (114 to 144, 145 to 189, 190 to 219) were further mutagenized. Since the strongest methylation was seen for fragments 145 to 189 and 190 to 219, these peptides were subjected to a cluster mutation approach. Seven lysine clusters that comprised all potential methylation sites were defined and in each of these clusters all lysine

Kassner *et al. Epigenetics & Chromatin* 2013, **6**:1
http://www.epigeneticsandchromatin.com/content/6/1/1

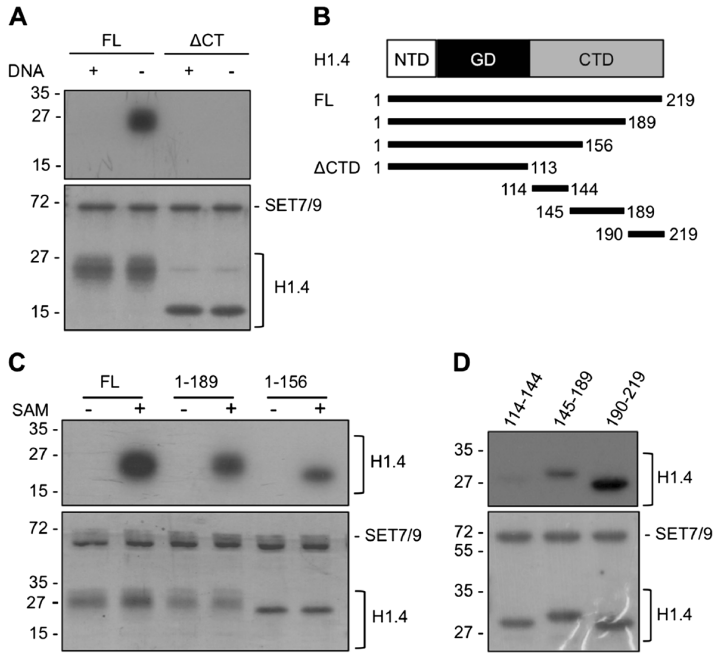

Figure 3 Linker histones are methylated by SET7/9. (**A**) HIS-tagged H1.4 FL and a deletion mutant without the CTD (ΔCTD) were *in vitro* methylated by SET7/9 in the presence or absence of plasmid DNA. (**B**) Schematic depiction of H1.4 wild-type (WT) protein and constructs. NTD, N-terminal domain; GD, globular domain; CTD, C-terminal domain; ΔCT, H1.4 construct completely lacking the C-terminus. (**C**) Recombinant HIS-tagged H1.4 full-length (FL) and deletion mutants were methylated *in vitro* by SET7/9. (**D**) H1.4 C-terminal fragments were expressed as GST fusion proteins and methylated *in vitro* by SET7/9. Methylation was analyzed by autoradiography.

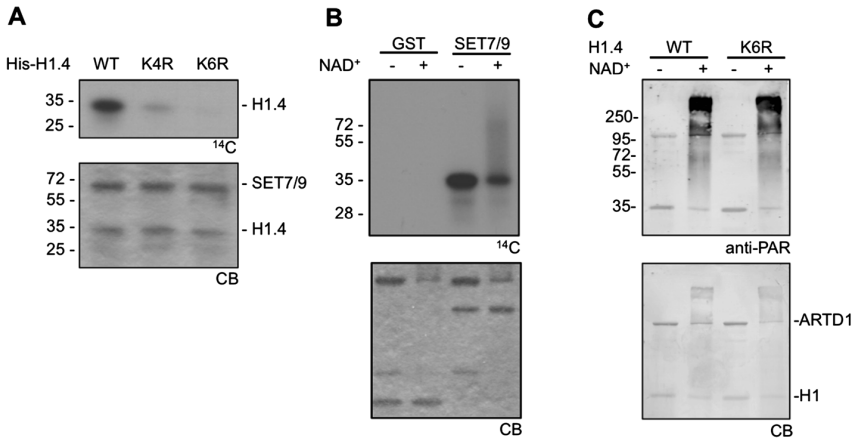

Figure 4 Full-length H1.4 is methylated at six lysine residues by SET7/9. (**A**) Mutation of the four lysine residues K159, K171, K177 and K192 (K4R) in wild-type (WT) H1.4 reduces SET7/9-dependent methylation. The additional mutation of K121 and K129 (K6R) abolishes methylation of full-length H1.4 by SET7/9. (**B**) H1.4 is efficiently PARylated after methylation by SET7/9. H1.4 was first incubated with S-adenosyl-L-(methyl-^{14}C) methionine (^{14}C-SAM) and glutathione-S-transferase (GST) or SET7/9 and then incubated with ADP-ribosyltransferase-D1 (ARTD1) in the presence or absence of cold nicotinamide adenine dinucleotide $(NAD)^+$. (**C**) H1.4 K6R is still modified by ARTD1. H1.4 WT and K6R were incubated with ARTD1 in the presence of 250 μM NAD^+. PARylation was analyzed by Western blotting.

Kassner et al. Epigenetics & Chromatin 2013, 6:1
http://www.epigeneticsandchromatin.com/content/6/1/1

residues were mutated to arginines (Additional file 2, Figure S2A). Mutation of cluster 4 and cluster 6 did not interfere with the methylation of the H1.4 fragments, indicating that the lysine residues located in these two clusters are not methylated by SET7/9 (Additional file 2: Figure S2B). The remaining cluster mutants 1, 2, 3, 5 and 7 were less methylated than the wild-type (WT) proteins (Additional file 2: Figure S2B). Computational analysis of these clusters as well as the fragment 114 to 144 identified six putative SET7/9 target sites matching the (KR)(STA)K consensus motif for SET7/9-dependent methylation [27]. These lysines at position 121, 129, 159, 171, 177 and 192 represent the last residues of the six KAK motifs in the CTD of H1.4 (Additional file 2, Figure S2A).

The corresponding lysine residues were then mutated individually and in combination. Only the mutation of all three lysines (K159, K171, K177) of the fragment 145 to 189 completely abolished the methylation of this peptide (Additional file 2, Figure S2C). Similarly, the K192R mutation abrogated the SET7/9-dependent methylation of fragment 190 to 219 (Additional file 2, Figure S2D). Interestingly, the combination of all four mutations (K159R, K171R, K177R and K192R) did not completely prevent the methylation of full-length H1.4 (Figure 4A). The additional mutation of K121 and K129 of the fragment 114 to 144 to arginines reduced the SET7/9-dependent methylation of full-length H1.4 most significantly, although a faint signal was sometimes observed even for this peptide (Figure 4A).

In summary, the mapping of the methylation sites in the H1.4 CTD thus identified the KAK motif and the six lysines K121, K129, K159, K171, K177 and K192 as the targets for SET7/9-dependent methylation of this linker histone variant.

Histones H1.4 and H3 methylation does not affect PARylation

The initial observation revealing H1 methylation by SET7/9 indicated crosstalk between PARylation and methylation as well as competition between H3 and H1.4. In order to elucidate the nature of this crosstalk, the influence of methylation on PARylation was studied and additional competition experiments with H1.4 and H3 were performed.

Prior methylation by SET7/9 did not prevent consecutive H1.4 PARylation, as observed by the shift of methylated H1 (Figure 4B). Similarly, the non-methylated H1.4 K6R mutant and WT H1.4 were modified by ARTD1 comparably (Figure 4C). These results clearly indicated that PARylation and SET7/9-dependent methylation of H3 and H1.4 do not crosstalk due to the same modification sites, even though prior PARylation does prevent methylation (Figures 2B, 2C). It is therefore likely that PARylation inhibits SET7/9 interaction with PARylated H3 or H1.4 and thereby prevents methylation.

Conclusions

This study describes the linker histone H1.4 as a new target for the H3K4 mono-methyltransferase SET7/9. Full-length histone H1.4 was methylated by SET7/9 at the lysine residues K121, K129, K159, K171, K177 and K192 of the KAK motifs of the CTD, which suggests a strong preference of SET7/9 for this recognition sequence. However, some of the KAK motifs seemed preferentially methylated, which may indicate a sequential modification or hint at differences in the accessibility of the different methylation sites.

The addition of plasmid DNA abolished SET7/9-dependent methylation of target proteins, indicating that incorporation into the nucleosome structure and DNA binding prevents methylation. This could be explained by DNA-induced conformational changes of the H1 CTD and by charge neutralization through DNA, as SET7/9 is known to prefer lysine residues in a positively charged context. Likewise, methylation may directly influence the binding of H1 to DNA and its function in chromatin compaction, especially as the six lysine residues targeted by SET7/9 all reside in the CTD of H1.4, which is important for chromatin binding [28]. These findings may indicate that SET7/9-dependent H1 methylation appears when H1 is not chromatin bound and possibly influences its turnover and exchange, which extends the scope of the histone code to the extra-chromatin realm.

Covalent histone modifications can alter chromatin structure and thereby define transcriptionally active or inactive chromatin states [29]. Compared with core histones, little is known about the modifications and the corresponding modifiers of the linker histones. One possible function of H1 methylation by SET7/9 might be the stimulation or repression of other post-translational modifications. Crosstalk between K26 dimethylation and AuroraB-mediated phosphorylation of S27 has been reported previously [25]. In addition, the H1.4 CTD is the target of acetylation, ADP-ribosylation and phosphorylation [30,31]. Interestingly, the four last KAK motifs, which displayed the strongest methylation *in vitro*, are located in close proximity to well known CDK phosphorylation sites (Figure 5A), which suggests a potential for significant crosstalk between acetylation, methylation and phosphorylation. Two of the sites in this region, S172 and S187, are not exclusively phosphorylated during mitosis and their phosphorylation in interphase correlated with transcription and chromatin relaxation [32]. Crosstalk between different histone modifications of H1.4 thus can fulfill important cellular functions. However, in most cases the modifying enzymes are currently not known and thus

Kassner *et al. Epigenetics & Chromatin* 2013, **6**:1
http://www.epigeneticsandchromatin.com/content/6/1/1

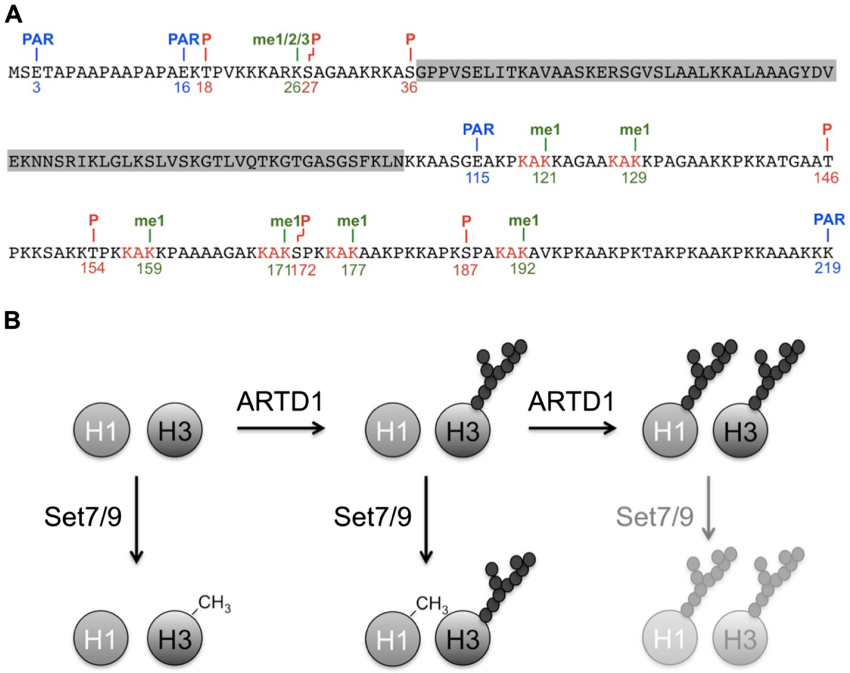

Figure 5 Crosstalk between adenosine diphosphate-ribosyltransferase (ARTD)-1 and SET7/9-dependent modification of linker and core histones. (**A**) Summary of known post-translational modification sites of H1.4. The grey box marks the central globular domain. The six newly identified KAK motifs that are methylated by SET7/9 are highlighted in red. Blue: PARylation (PAR), red: phosphorylation (P), green: methylation (me, number indicates methylation state). (**B**) Model of the sequential adenosine diphosphate (ADP)-ribosylation and methylation reactions on histone H3 and H1 by ARTD1 and SET7/9.

the biological and cellular functions of these modifications have not been elucidated in detail yet.

ARTD1 and histone ADP-ribosylation were previously suggested as components of the histone code [20,26]. The results described here provide a further line of evidence for this hypothesis. We show that ARTD1-dependent PARylation of histones influences their subsequent methylation by SET7/9. Compared to phosphorylation, which strongly reduces methylation if in proximity of SET7/9 target lysine residues [12], PARylation is a much more bulky modification with more negative charges and therefore also inhibited histone methylation by SET7/9. Based on the experiments shown here, SET7/9 methylates both H1 and H3, but prefers H3 if both substrates are present. Strikingly, PARylation did not merely inhibit SET7/9-dependent methylation of histones, but shifted its target from H3 to H1 (Figure 5B). These observations could be explained by sequential PARylation events, where ARTD1 modifies H3 before H1. PARylation of H3 would then inhibit its subsequent methylation by SET7/9 and its competition as a SET7/9 target with H1.

This ARTD1-dependent regulation of the substrate specificity of a histone modifying enzyme may be an exciting mechanism to explain how ARTD1 influences chromatin-associated processes such as transcription. It is also important to note that progressive PARylation of histones also inhibited the methylation of H1, documenting that different outcomes for SET7/9-dependent histone methylation can occur depending on the extent of ARTD1 activity.

The complexity of ARTD1-dependent histone modifications is increased by the facts that (1) ARTD1 can modify all core histones and the linker histones [23], and (2) the size and quality (for example, branching or length) of the polymers may differ under varying conditions and depending on the substrate histone. Therefore, future studies should not merely focus on the influence of ARTD1 and PARylation on other histone modifications but also on how ARTD1-dependent histone modification itself is regulated. In this regard, it will also be interesting to study specific ADP-ribose modifications and their effect on SET7/9 methylation. Although we have identified ADP-ribose acceptor sites in histones (for example, K37 of H3) it is not yet possible to chemically synthesize peptides with specific ADP-ribose modifications required for these studies. Furthermore, antibodies specific for a particular ADP-ribose modification have not been developed. In the future, such tools will allow study of the effect of SET7/9-dependent

Kassner *et al. Epigenetics & Chromatin* 2013, **6**:1
http://www.epigeneticsandchromatin.com/content/6/1/1

methylation on ARTD1 activity and modification sites in much more detail.

Methods

Plasmids and protein expression

pGEX-SET7/9 (52 to 366) and pET28b-H1.4 (fl) bacterial expression vectors were kind gifts from D Reinberg and R Schneider, respectively. H1.4 full-length and deletions mutants were subcloned into pET-28a to add the N-terminal HIS-tag. C-terminal H1.4 fragments were cloned into pGEX6P1. All point mutations were inserted by site-directed mutagenesis. Cluster mutants were created by overlapping PCR with the corresponding primers.

The baculovirus expression vector BacPak8 (Clontech, Mountain View, CA, USA) was used for the expression of recombinant ARTD1 in Sf21 insect cells, as described previously [33]. GST- and HIS-tagged histone proteins were expressed in *E.coli*. All recombinant proteins were purified by a one-step affinity chromatography using ProBond resin (Invitrogen, Paisley, UK) for HIS-tagged and glutathione sepharose (GE Healthcare, Uppsala, Sweden) for GST-tagged proteins, according to the manufacturer's recommendations. HIS-H1.4(fl) proteins were purified as described elsewhere [34].

Reagents

Lyophilized histones or H1 mix from calf thymus were purchased from Roche (Rotkreuz, Zug, Switzerland) and resolubilized in water. The 3-AB (Sigma-Aldrich, St. Louis, MO, USA) was freshly prepared in water.

In vitro methylation assays

If not stated otherwise, approximately 1 μg histone proteins were incubated with 1 μg bacterially purified GST-SET7/9 in the presence of 0.03 μCi ^{14}C-SAM (PerkinElmer, Boston, MA, USA) in methylation buffer (50 mM Tris–HCl pH8.0, 50 mM NaCl, 10% glycerol, 1 mM PMSF, 1 mM DTT) for 10 to 60 minutes at 30°C in a 25 μl reaction. For DNA inhibition assays, histones were preincubated with or without 0.5 μg plasmid DNA (pcDNA) and then methylated for 15 minutes. Reactions were stopped by addition of 10× SDS-loading buffer, boiled and separated by SDS-PAGE. Gels were stained with CB, incubated in 1 M sodium salicylate for 20 minutes, dried, and exposed on x-ray film at −80°C.

Sequential ADP-ribosylation and methylation assays

Sequential modification assays were performed in PAR buffer (50 mM Tris–HCl, 50 mM NaCl, 4 mM $MgCl_2$, 250 μM DTT, 1 mg/ml pepstatin, 1 mg/ml bestatin, 1 mg/ml leupeptin).

We incubated 10 pmol ARTD1, with or without 2.5 μg histone mix or 1 μg individual histones, in the presence or absence of 5 pmol activating DNA and 160 μM NAD^+ (Sigma-Aldrich, St. Louis, MO, USA) for 15 minutes at 30°C; 8 mM 3-AB or 0.2 mM PJ-34 were added to inhibit ARTD1 activity either before the ADP-ribosylation or afterwards, where indicated. The methylation was then started by addition of 1 μg SET7/9 and 0.03 μCi ^{14}C-SAM and allowed to proceed for 1 h at 30°C. Autoradiography was performed as described above. The activating DNA used in all assays was an annealed double-stranded oligomer (5'-GGAATTCC-3').

Additional files

Additional file 1: Figure S1. Time-dependent PARylation of adenosine diphosphate-ribosyltransferase (ARTD)-1 and histones. ARTD1 and a histone mix were modified for the indicated times. Proteins were separated by SDS-PAGE, stained with Coomassie blue (CB, upper blot) and adenosine diphosphate (ADP)-ribosylation was analyzed by autoradiography (^{32}P, lower blots showing a long and short exposure). The mobility shift of poly-ADP-ribosylated ARTD1 is marked in the SDS-PAGE gel.

Additional file 2: Figure S2. H1.4 C-terminal domain (CTD) is methylated at KAK* motifs. **(A)** Amino acid sequences of C-terminal H1.4 fragments. Boxes represent the lysine clusters which were mutated to arginines in (B). Grey boxes mark the clusters that markedly influence methylation. KAK motifs are highlighted in dark grey and the methylated lysines are bold. **(B)** Cluster mutant approach to identify methylation sites in H1.4 CTD, which contains 43 lysine residues as potential target sites. Clusters were mutated one by one in the corresponding C-terminal fragment and methylation efficiency by SET7/9 was tested *in vitro*. **(C)** Methylation of C-terminal fragments by SET7/9 was tested *in vitro* after mutation of single lysine residues in KAK* motifs. **(D)** Methylation of H1.4 (145–189) double and triple mutants by SET7/9.

Abbreviations

ADP: Adenosine diphosphate; ART: Adenosine diphosphate ribosyltransferase; CB: Coomassie blue; C-SAM: S-adenosyl-L-(methyl-^{14}C) methionine; CTD: C-terminal domain; ETD: Electron-transfer dissociation; GST: Glutathione-S-transferase; LSD: Lysine-specific demethylase; NAD: Nicotinamide adenine dinucleotide; PARP: Poly(ADP-ribose) polymerase; PCR: Polymerase chain reaction; PTM: Post-translational modification; WT: Wild-type.

Competing interests

The authors declare that they have no conflicts of interest.

Authors' contributions

IK and MOH designed the experiments; IK, MB, FR and MF performed experiments; MOH designed and supervised the study. IK and MOH wrote the manuscript. All the authors read and agreed with the manuscript.

Acknowledgements

We thank Danny Reinberg (Howard Hughes Medical Institute, NYU School of Medicine, New York, USA) for providing SET7/9, Timothey J. Richmond (Deportment of Biology, ETH Zurich, Switzerland) for providing purified histone H3 and Robert Schneider (Max-Planck Institute of Immunobiology and Epigenetics, Freiburg, Germany) for helpful advice. We are grateful to Florian Freimoser and all the members of the Institute of Veterinary Biochemistry and Molecular Biology (University of Zurich, Switzerland) for helpful advice and discussions. This work was supported by Swiss National Science Foundation Grants 31003A-122421 and 310030B-138667 (to MOH) and the Kanton of Zurich (to MOH).

Author details

[1]Institute of Veterinary Biochemistry and Molecular Biology, University of Zurich, Winterthurerstrasse 190, Zurich 8057, Switzerland. [2]Life Science Zurich Graduate School, Molecular Life Science Program, University of Zurich, Zurich, Switzerland.

Received: 12 December 2012 Accepted: 14 December 2012
Published: 5 January 2013

References

1. Campos E, Reinberg D: **Histones: annotating chromatin.** *Annu Rev Genet* 2009, **43:**559–599.
2. Kornberg RD, Lorch Y: **Twenty-five years of the nucleosome, fundamental particle of the eukaryote chromosome.** *Cell* 1999, **98:**285–294.
3. Annunziato AT: **DNA packaging: nucleosomes and chromatin.** *Nature Education* 2008, **1**(1). http://www.nature.com/scitable/topicpage/dna-packaging-nucleosomes-and-chromatin-310.
4. Happel N, Doenecke D: **Histone H1 and its isoforms: contribution to chromatin structure and function.** *Gene* 2009, **431:**1–12.
5. Shen X, Gorovsky MA: **Linker histone H1 regulates specific gene expression but not global transcription *in vivo*.** *Cell* 1996, **86:**475–483.
6. Ramakrishnan V, Finch JT, Graziano V, Lee PL, Sweet RM: **Crystal structure of globular domain of histone H5 and its implications for nucleosome binding.** *Nature* 1993, **362:**219–223.
7. Hendzel MJ, Lever MA, Crawford E, Th'ng JP: **The C-terminal domain is the primary determinant of histone H1 binding to chromatin *in vivo*.** *J Biol Chem* 2004, **279:**20028–20034.
8. Izzo A, Kamieniarz K, Schneider R: **The histone H1 family: specific members, specific functions?** *Biol Chem* 2008, **389:**333–343.
9. Raghuram N, Carrero G, Th'ng J, Hendzel MJ: **Molecular dynamics of histone H1.** *Biochem Cell Biol* 2009, **87:**189–206.
10. Wang H, Cao R, Xia L, Erdjument-Bromage H, Borchers C, Tempst P, Zhang Y: **Purification and functional characterization of a histone H3-lysine 4-specific methyltransferase.** *Mol Cell* 2001, **8:**1207–1217.
11. Nishioka K, Chuikov S, Sarma K, Erdjument-Bromage H, Allis CD, Tempst P, Reinberg D: **Set9, a novel histone H3 methyltransferase that facilitates transcription by precluding histone tail modifications required for heterochromatin formation.** *Genes Dev* 2002, **16:**479–489.
12. Dhayalan A, Kudithipudi S, Rathert P, Jeltsch A: **Specificity analysis-based identification of new methylation targets of the SET7/9 protein lysine methyltransferase.** *Chem Biol* 2011, **18:**111–120.
13. Klose RJ, Zhang Y: **Regulation of histone methylation by demethylimination and demethylation.** *Nat Rev Mol Cell Biol* 2007, **8:**307–318.
14. Mosammaparast N, Shi Y: **Reversal of histone methylation: biochemical and molecular mechanisms of histone demethylases.** *Annu Rev Biochem* 2010, **79:**155–179.
15. Hottiger MO, Hassa PO, Lüscher B, Schüler H, Koch-Nolte F: **Toward a unified nomenclature for mammalian ADP-ribosyltransferases.** *Trends Biochem Sci* 2010, **35:**208–219.
16. Yamanaka H, Penning CA, Willis EH, Wasson DB, Carson DA: **Characterization of human poly(ADP-ribose) polymerase with autoantibodies.** *J Biol Chem* 1988, **263:**3879–3883.
17. D'Amours D, Desnoyers S, D'Silva I, Poirier GG: **Poly(ADP-ribosyl)ation reactions in the regulation of nuclear functions.** *Biochem J* 1999, **342**(Pt 2):249–268.
18. Gibson BA, Kraus WL: **New insights into the molecular and cellular functions of poly(ADP-ribose) and PARPs.** *Nat Rev Mol Cell Biol* 2012, **13:**411–424.
19. Altmeyer M, Hottiger MO: **Poly(ADP-ribose) polymerase 1 at the crossroad of metabolic stress and inflammation in aging.** *Aging* 2009, **1:**458–469.
20. Hottiger MO: **ADP-ribosylation of histones by ARTD1: an additional module of the histone code?** *FEBS Lett* 2011, **585:**1595–1599.
21. Huletsky A, de Murcia G, Muller S, Hengartner M, Ménard L, Lamarre D, Poirier G: **The effect of poly(ADP-ribosyl)ation on native and H1-depleted chromatin. A role of poly(ADP-ribosyl)ation on core nucleosome structure.** *J Biol Chem* 1989, **264:**8878–8886.
22. Adamietz P, Hilz H: **Poly(adenosine diphosphate ribose) is covalently linked to nuclear proteins by two types of bonds.** *Hoppe Seylers Z Physiol Chem* 1976, **357:**527–534.
23. Messner S, Altmeyer M, Zhao H, Pozivil A, Roschitzki B, Gehrig P, Rutishauser D, Huang D, Caflisch A, Hottiger MO: **PARP1 ADP-ribosylates lysine residues of the core histone tails.** *Nucleic Acids Res* 2010, **38:**6350–6362.
24. Kouzarides T: **Chromatin modifications and their function.** *Cell* 2007, **128:**693–705.
25. Hergeth SP, Dundr M, Tropberger P, Zee BM, Garcia BA, Daujat S, Schneider R: **Isoform-specific phosphorylation of human linker histone H1.4 in mitosis by the kinase Aurora B.** *J Cell Sci* 2011, **124:**1623–1628.
26. Messner S, Hottiger MO: **Histone ADP-ribosylation in DNA repair, replication and transcription.** *Trends Cell Biol* 2011, **21:**534–542.
27. Couture JF, Collazo E, Hauk G, Trievel RC: **Structural basis for the methylation site specificity of SET7/9.** *Nat Struct Mol Biol* 2006, **13:**140–146.
28. Caterino TL, Hayes JJ: **Structure of the H1 C-terminal domain and function in chromatin condensation.** *Biochem Cell Biol* 2011, **89:**35–44.
29. Jenuwein T, Allis CD: **Translating the histone code.** *Science* 2001, **293:**1074–1080.
30. Ogata N, Ueda K, Kagamiyama H, Hayaishi O: **ADP-ribosylation of histone H1. Identification of glutamic acid residues 2, 14, and the COOH-terminal lysine residue as modification sites.** *J Biol Chem* 1980, **255:**7616–7620.
31. Wisniewski JR, Zougman A, Kruger S, Mann M: **Mass spectrometric mapping of linker histone H1 variants reveals multiple acetylations, methylations, and phosphorylation as well as differences between cell culture and tissue.** *Mol Cell Proteomics* 2007, **6:**72–87.
32. Zheng Y, John S, Pesavento JJ, Schultz-Norton JR, Schiltz RL, Baek S, Nardulli AM, Hager GL, Kelleher NL, Mizzen CA: **Histone H1 phosphorylation is associated with transcription by RNA polymerases I and II.** *J Cell Biol* 2010, **189:**407–415.
33. Hassa PO, Buerki C, Lombardi C, Imhof R, Hottiger MO: **Transcriptional coactivation of nuclear factor-κB-dependent gene expression by p300 is regulated by poly(ADP)-ribose polymerase-1.** *J Biol Chem* 2003, **278:**45145–45153.
34. Weiss T, Hergeth S, Zeissler U, Izzo A, Tropberger P, Zee BM, Dundr M, Garcia BA, Daujat S, Schneider R: **Histone H1 variant-specific lysine methylation by G9a/KMT1C and Glp1/KMT1D.** *Epigenetics Chromatin* 2010, **3:**7.

doi:10.1186/1756-8935-6-1
Cite this article as: Kassner *et al.*: Crosstalk between SET7/9-dependent methylation and ARTD1-mediated ADP-ribosylation of histone H1.4. *Epigenetics & Chromatin* 2013 **6**:1.

LEGENDS OF SUPPLEMENTARY FIGURES

Figure S1. Time-dependent PARylation of ARTD1 and histones. ARTD1 and a histone mix were modified for the indicated times. Proteins were separated by SDS-PAGE, stained with Coomassie blue (CB, upper blot) and ADP-ribosylation was analyzed by autoradiography (^{32}P, lower blots showing a long and short exposure). The mobility shift of poly-ADP-ribosylated ARTD1 is marked in the SDS-PAGE gel.

Figure S2. H1.4 CTD is methylated at KAK* motifs. (A) Amino acid sequences of C-terminal H1.4 fragments. Boxes represent the lysine clusters which were mutated to arginines in (B). Grey boxes mark the clusters that markedly influence methylation. KAK* motifs are highlighted in dark grey and the methylated lysines are bold. **(B)** Cluster mutant approach to identify methylation sites in H1.4 CTD which contains 43 lysine residues as potential target sites. Clusters were mutated one by one in the corresponding C-terminal fragment and methylation efficiency by SET7/9 was tested *in vitro*. **(C)** Methylation of C-terminal fragments by SET7/9 was tested *in vitro* after mutation of single lysine residues in KAK* motifs. **(D)** Methylation of H1.4 (145-189) double and triple mutants by SET7/9.

Kassner et al. Supplementary Figure 1

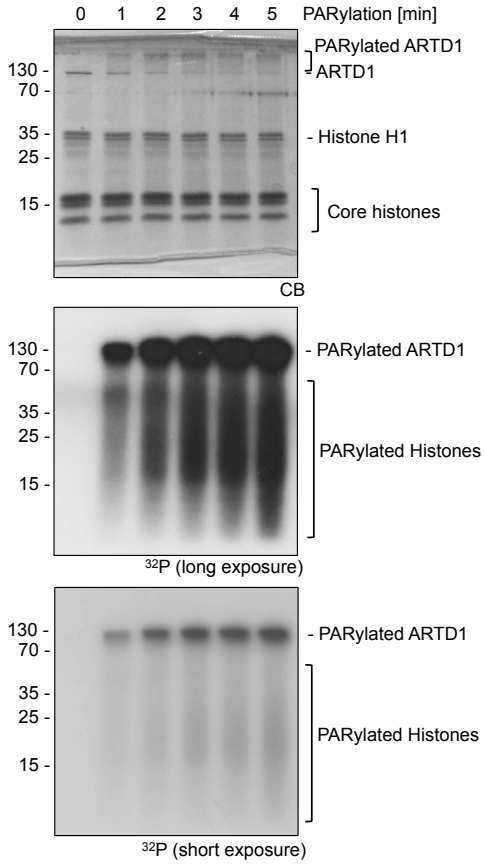

Kassner et al. Supplementary Figure 2

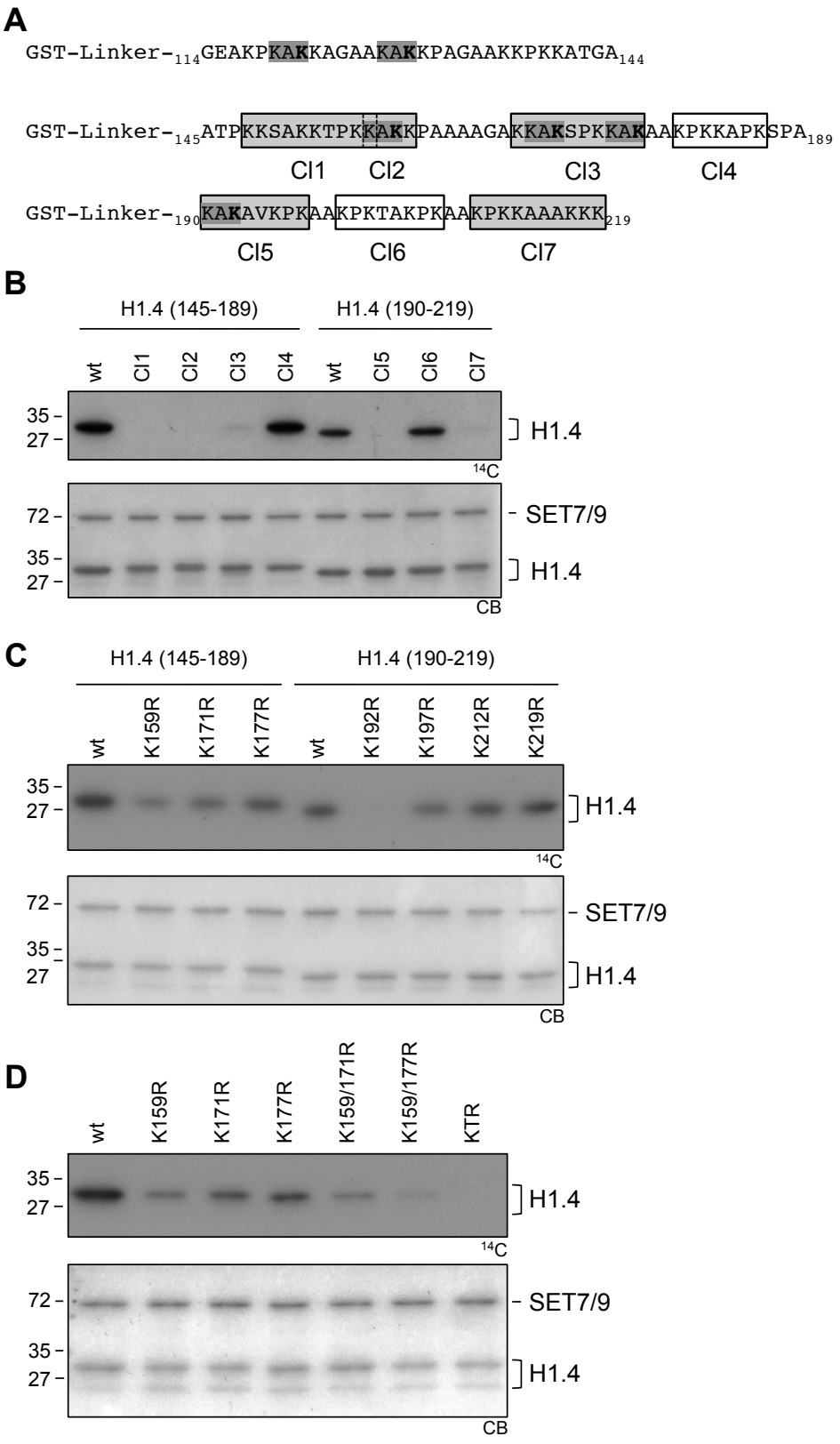

7.2 Unpublished Results

7.2.1 DNA inhibits Methylation of full-length or the Histone H1.4 Deletion Mutants

To investigate whether the addition of DNA alters the methylation of H1.4 by SET7/9, the same constructs as described in section 6.1 (H1.4 full-length (amino acids 1-210) C-terminal mutant 1 (1-189), the C-terminal mutant 2 (1-156) and the C-terminal mutant 3 (1-113)) were incubated with SET7/9 and 30nCi SAM in the presence or absence of 0.5 µg DNA (Fig 14A and B).

A

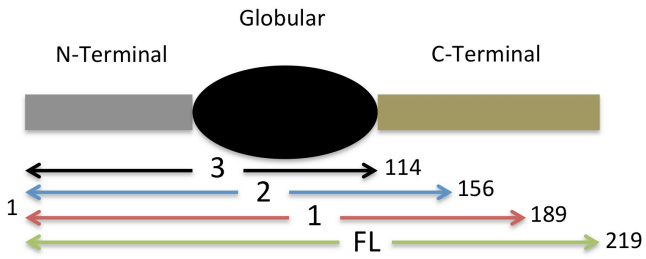

B

MSETAPAAPAAPAPAEKTPVKKKARKSAGAAKRKASGPPVSELITKAVAASKERSGVSLAALKKALAAAGYDVEK
NNSRIKLGLKSLVSKGTLVQTKGTGASGSFKLNKKAASGEAKPKAKKAGAAKAKKPAGAAKKPKKATGAATPKKS
AKKTPKKAKKPAAAAGAKKAKSPKKAKAAKPKKAPKSPAKAKAVKPKAAKPKTAKPKAAKPKKAAAKKK

Figure 14: Structural features of H1.4. **A:** Histone H1.4 is comprised of an N-terminal, a globular and a C-terminal domain. We have created deletion mutants lacking parts of their C-terminus. **B:** Amino acid sequence of H1.4 colored accordingly to the domain they represent (N-terminal tail: grey, globular domain: black, C-terminal domain: brownish) with the potential methylated lysine residues in red.

After the incubation, the reaction was stopped and the proteins were separated by SDS-PAGE. The gel was stained with Coomassie, vacuum dried and then exposed to a film (Fig. 15).

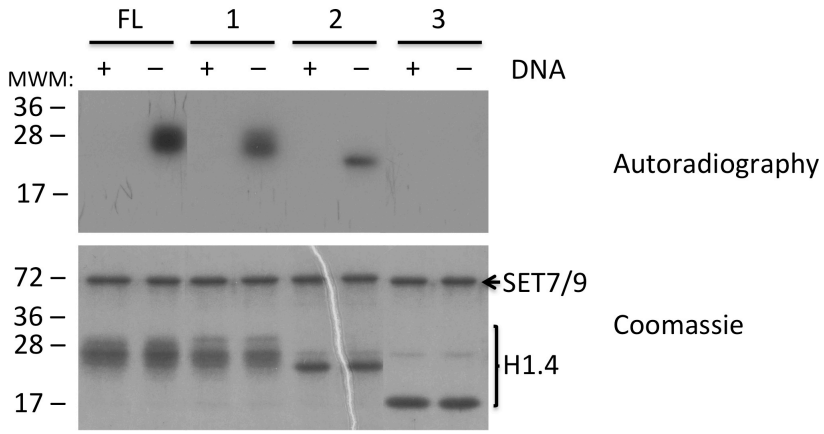

Figure 15: SET7/9-induced methylation of full-length and different H1.4 deletion mutants in the presence or absence of pcDNA. Autoradiography of a 15% SDS-PAGE after methylation and separation of the different proteins (3 days exposure; upper panel). The lower panel shows the Coomassie stained gel to visualize the protein levels of SET7/9, full-length H1.4 (FL) and different H1.4 deletion mutant (1, 2 or 3).

The presence of DNA inhibited the methylation of full-length and H1.4 deletion mutants 1 and 2. The deletion mutant 3 was not methylated and thus not inhibited. Even after long exposure of the x-ray film, no radioactive signal could be detected, suggesting that the methylation of linker histone H1.4 and of its C-terminal fragments is completely inhibited by DNA under these conditions.

7.2.2 Different H1.2 C-terminal Domain Cluster Mutants are methylated by SET7/9 to the same Extent

Before focusing on H1.4, a cluster mutation approach for H1.2 was performed to further investigate potential modification sites. Therefore, several lysine residues were deleted together in clusters. Hereby, it was helpful that cluster mutants in the entire C-terminal tail were already available from Robert Schneider (MPI Freiburg, Germany), who used these mutants to characterize the methylation site of other methyltransferases such as G9a/KMT1C and Glp1/KMT1D in H1.2 [177]. We therefore decided to analyze the SET7/9-induced methylation pattern of these H1.2 cluster mutants with the expectation to identify conserved lysine residue(s) not only present in H1.2 but also in H1.4.

The C-terminal domain of H1.2 contained 10 clusters (Cl1-Cl10) that comprised all 40 potential lysine acceptors for the methylation by SET7/9. Different constructs containing either single or multiple mutations were cloned into the pET expression vector replacing the original amino acid sequence of each cluster with a lysine free amino acid sequence. The 10

C-terminal polypeptides were expressed in *E. coli* and purified by using perchloric acid to dissolve the inclusion bodies, which contained the His-tagged proteins (see also Materials and Methods) (Fig. 16).

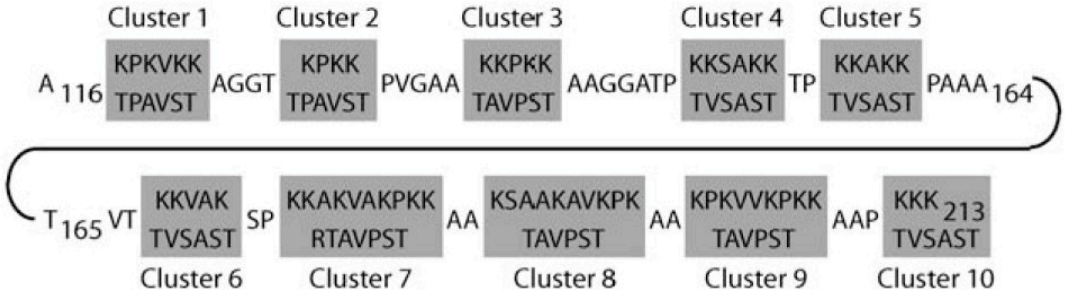

Figure 16: Amino acid sequence of the histone H1.2 cluster mutants.

To analyze whether one of the cluster mutants is no longer methylated, the purified polypeptides were separately incubated for 1 hour at 30°C with SET7/9 and 30 nCi SAM. After terminating the reaction, the proteins were analyzed by SDS-PAGE and subsequent exposure of the gel to an X-ray film (Fig. 17A and B).

A:

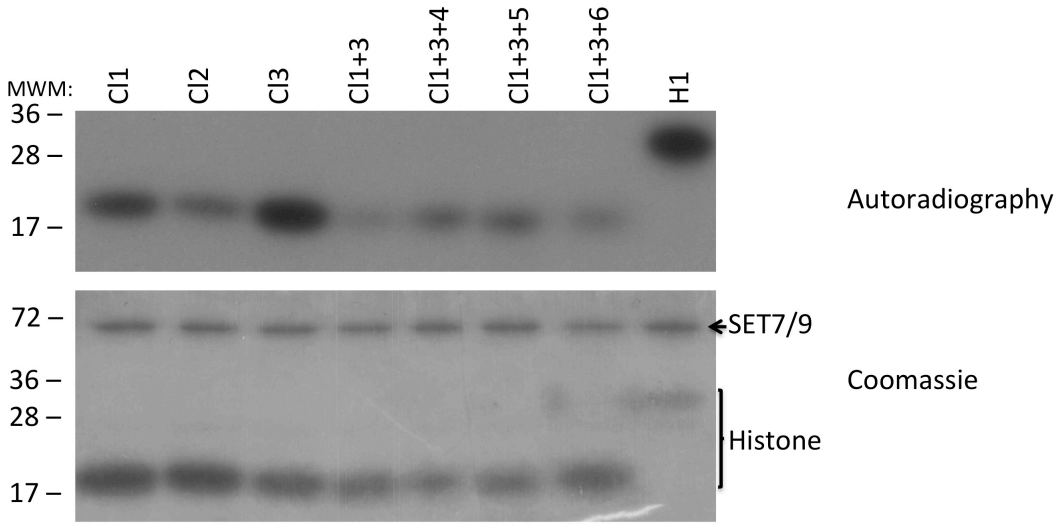

B:

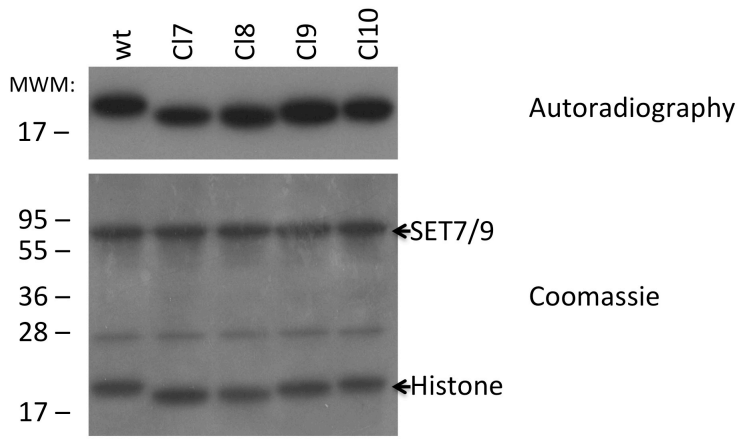

Figure 17: **A:** SET7/9-induced methylation of the H1.2 cluster mutants. Autoradiography of a 15% SDS-PAGE after methylation and separation of the different proteins (3 days of exposure; upper panel). H1 mix from Roche was included as a control (wt). The lower panel shows the Coomassie stained gel to visualize the protein levels of SET7/9 and the H1.2 cluster mutants (Cl1-Cl1+3+5). **B:** SET7/9-induced methylation of H1.2 cluster mutants. Autoradiography of a 15% SDS-PAGE after methylation and separation of the different proteins (4 days exposure; upper panel). The C-terminal domain of H1.2 with an additional linker was included as positive control (wt). The lower panel shows the Coomassie stained gel to visualize the protein levels of SET7/9 and the cluster mutants of H1.2 (Cl7-Cl10).

As a positive methylation control, a commercial histone H1 from Roche or the wt C-terminus was used. As observed for H1.4, the C-terminus of H1.2 was also methylated by SET7/9. The tested clusters in Figure 17A showed differential methylation. Unfortunately, none of the tested cluster mutants showed a complete loss of the radioactive signal. The Cl2 mutant and combinations of multiple cluster mutants (e.g., Cl1 and Cl3) seemed less methylated than Cl3 alone, indicating that there are possibly several methylation sites, which are located in different parts of the C-terminal tail of H1.2. On the other hand, the strong reduction observed for mutant Cl1+Cl3 could not be explained by an additive effect of the single clusters and furthermore indicates that this approach was subjected to a certain fluctuation. This was supported by the fact, that constructs with an additional cluster (e.g., Cl1, Cl3 and Cl5) were stronger methylated than the construct with only Cl1 and Cl3.

None of the clusters Cl7 to Cl10 showed any reduction in methylation when compared to the wt control, indicating that either this part of the C-terminus is not methylated or that mutating only one cluster is not enough to observe reduced methylation.

7.2.3 Changing the pH from 8 to 7.2 or 9 does not alter Methylation of H1.2 by SET7/9

As there were no strong differences in methylation of the H1.2 cluster mutants by SET7/9 under the standard conditions, the reaction was repeated at different pHs in order to increase the specificity of the methylation. The pH for the reaction was either decreased from pH 8 to pH 7.2 (Fig. 18) or increased to pH 9 (Fig. 19).

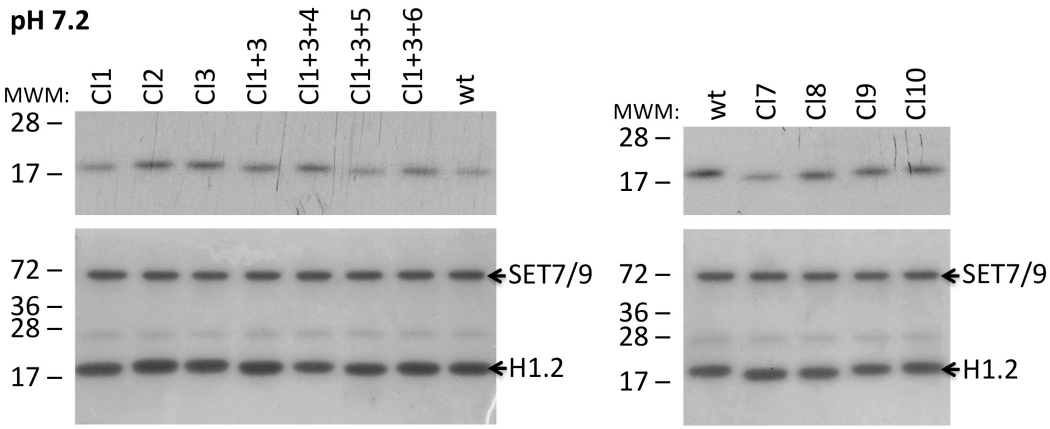

Figure 18: SET7/9-induced methylation of H1.2 cluster mutants at pH 7.2. Autoradiography of a 15% SDS-PAGE after methylation and separation of the different proteins (3 days exposure; upper panel). Coomassie stained gel to visualize the protein levels of SET7/9, the cluster mutants of H1.2 (Cl1-Cl1+3+5 and Cl7-10) and the C-terminal tail as control (wt) is shown in the lower panel.

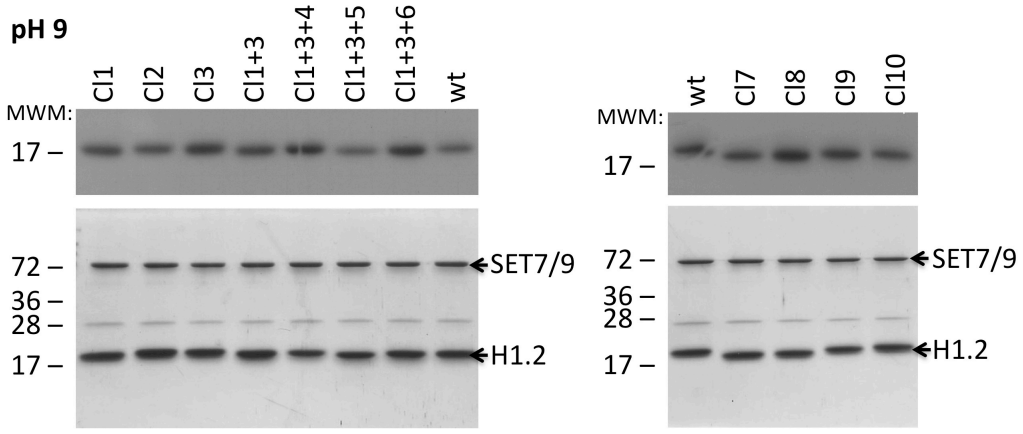

Figure 19: SET7/9-induced methylation of H1.2 cluster mutants at pH 9. Autoradiography of a 15% SDS-PAGE after methylation and separation of the different proteins (overnight exposure; upper panel). Coomassie stained gel to visualize the protein levels of SET7/9, the cluster mutants of H1.2 (Cl1-Cl1+3+5 and Cl7-10) and the wt C-terminal tail (wt) is shown in the lower panel.

Moreover, the incubation time with SET7/9 and 30nCi SAM was reduced from 1 hour to only 15 minutes, which was the standard incubation time for the later experiments.

The variable SET7/9-induced methylation was even weaker under the new conditions and the strongly decreased methylation of cluster 3 seen in Figure 17A was no longer observed. Overall, the variability of the methylation intensity was rather low (equal methylation), which could also be caused by uneven amounts of proteins used in the experiments. Interestingly, the methylation was significantly stronger at pH 9 as compared to pH 7.2. While it took 3 days for a strong signal of the proteins methylated at pH 7.2, for pH 9 a comparable signal was obtained already after overnight exposure, which implied a higher efficiency of SET7/9-induced methylation at pH 9.

At pH 7.2, Cl1 was stronger methylated than Cl2 and wt, which were both comparably methylated (Fig. 18), while at pH 9 Cl2 was stronger methylated than Cl1 and wt (Fig. 19). The variation of the pH seemed to affect the specificity and efficiency of SET7/9 for these two clusters. Overall, the changing the pH did not improve the specificity of SET7/9 for the purified cluster mutants and did not allow the identification of a lysine acceptor site.

7.2.4 Increasing the NaCl Concentration up to 120 mM does not affect the Methylation of H1.2 by SET7/9

Since changing the pH and using an incubation time of 15 minutes was not enough to significantly increase the specificity of SET7/9-induced methylation of H1.2, different NaCl concentrations (50 mM and 120 mM, respectively) were next tested with a selected number of cluster mutants. Increasing the NaCl concentration was expected to affect the affinity of SET7/9 to the target proteins and to favor the transfer of methyl groups only to high affinity sites. The methylation assay was performed with the two mentioned NaCl concentrations and at pH 8 (Fig. 20), 7.2 or 9 (Fig 21) as previously described.

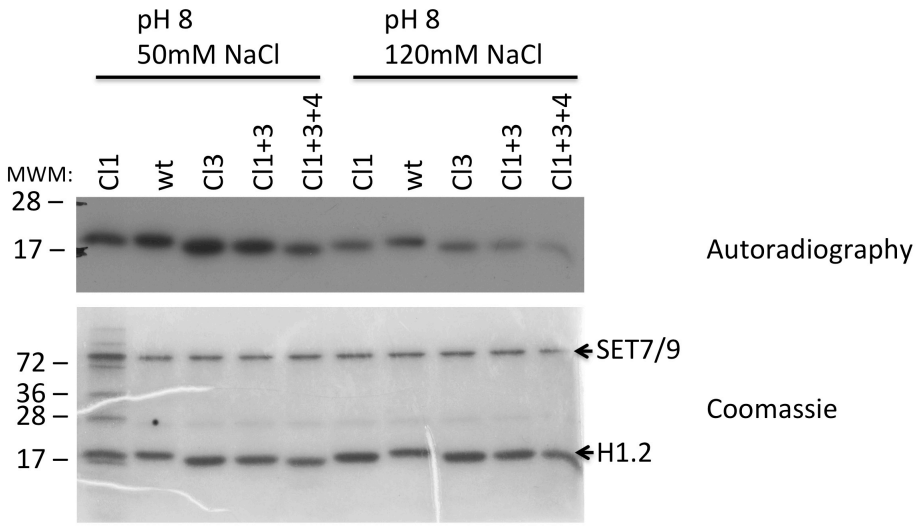

Figure 20: SET7/9-induced methylation of H1.2 cluster mutants at pH 8 with 50 mM NaCl or 120 mM NaCl. Autoradiography of a 15% SDS-PAGE after methylation and separation of the different proteins (2 days exposure; upper panel). The lower panel shows the Coomassie stained gel to visualize the protein levels of SET7/9, the cluster mutants of H1.2 (Cl1, Cl1+3, Cl1+3+4, Cl1+3+5) and the C-terminal tail of H1.2 (wt).

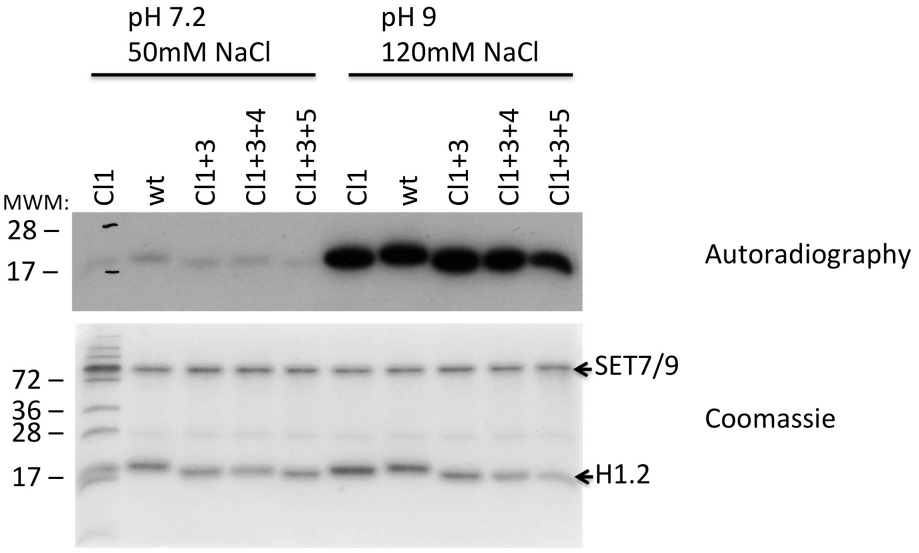

Figure 21: SET7/9-induced methylation of H1.2 cluster mutants at pH 7.2 or pH 9 with 50 mM NaCl or 120 mM NaCl. Autoradiography of a 15% SDS-PAGE after methylation and separation of the different proteins (1 day exposure; upper panel). The lower panel shows the Coomassie stained gel to visualize the protein levels of SET7/9, the cluster mutants of H1.2 (Cl1, Cl1+3, Cl1+3+4, Cl1+3+5) and the C-terminal tail of H1.2 (wt).

Overall, increasing the NaCl concentration reduced the intensity of the methylation (Fig. 20). Again, increasing the pH to 9 resulted in stronger methylation of the proteins, even in the presence of higher NaCl (Fig. 21). Irrespective of the pH and NaCl concentration, H1.2

wt was methylated to the same extent, indicating that increasing the pH or NaCl concentration does not affect the specificity of SET7/9. The reduced methylation of Cl1 and Cl1+3+5 was again observed under the tested conditions (Fig. 20 and 21). Methylation of the Cl1 mutant showed a noteworthy decrease in methylation compared to the tested wt, while only Cl1+3+5 reduced the methylation of the C-terminus further, suggesting that the SET7/9 methylation sites are located in different clusters. However, none of the tested conditions affected specificity of SET7/9 to such a degree that a single cluster could be identified as the main acceptor site.

Together, the cluster mutation approach using the entire C-terminal domain failed to identify the SET7/9-induced methylation of H1.2. This was mainly due to the fact that most probably several acceptors do exist and that these sites are distributed throughout the C-terminal end of H1.2

7.2.5 The GFP-tagged full length H1.4, C-terminus, and N-terminus of H1.4 translocate to the Nucleus

To gain more insight into the cellular localization of H1.4 and to establish a readout for the investigation of the methylation sites of H1.4 in cells, the H1.4 N-terminal domain (1-36), the C-terminal domain (114-219) or the full-length protein (1-219) was cloned as a GFP-fusion protein into the pEGFP-C1 vector (Fig. 22).

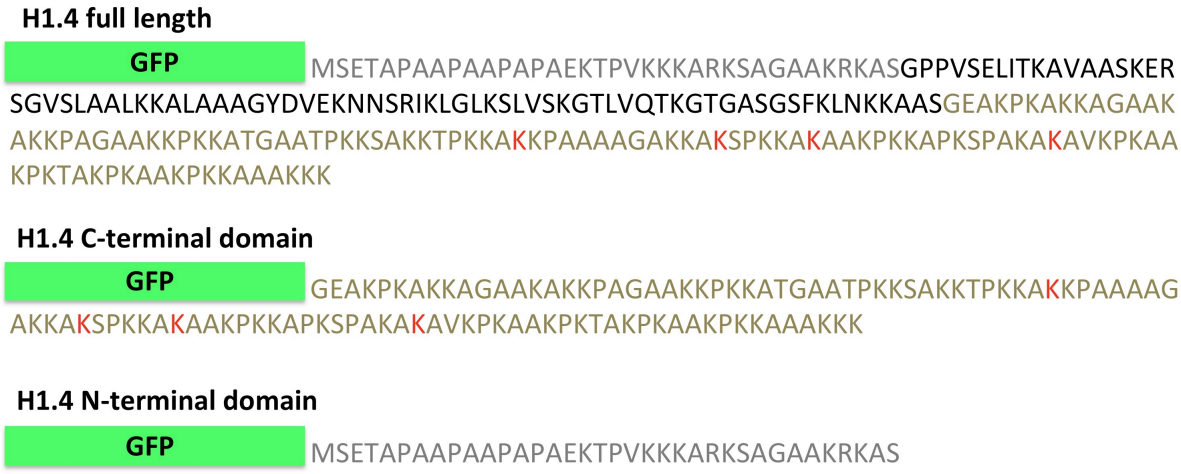

Figure 22: Amino acid sequence of the GFP-fusion H1.4 constructs (Fl, C-tail, N-tail) and the newly identified methylation acceptor sites marked in red.

The different constructs were transfected into U2OS cells (as described in Material and Methods). The cells were analyzed by fluorescence microscopy three days after transfection (Fig. 23).

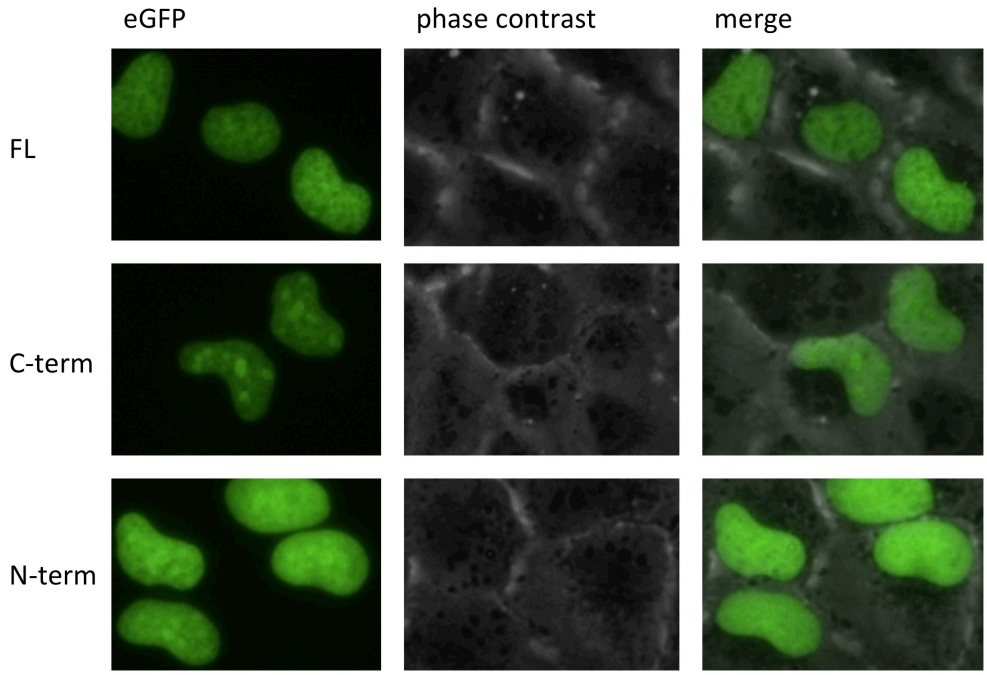

Figure 23: U2OS cells 3 days after transfection of the GFP-constructs. Fluorescence microscope and phase contrast analysis of the three eGFP-tagged H1.4 constructs transfected into U2OS cells.

The analysis revealed that all three protein constructs are expressed. Although none of the constructs contained a nuclear localization signal (NLS), all three proteins were observed in the nucleus, indicating that an amino acid sequence of the C-terminus as well as the N-terminus might serve as a NLS. Alternatively, the fusion proteins may have translocated to the nucleus by a co-carrier transport with a so far unknown protein.

Due to time constraints, the methylation-deficient mutants of H1.4 could not be tested in the established readout. It would, however, be interesting to study the localization of wild type or the methylation-deficient histone H1.4 mutants under different conditions, including LPS stimulation or H_2O_2 treatment.

7.2.6 ARTD1 modifies mainly the C-terminal Domain of H1.4

To elucidate a possible modification of H1.4 by ARTD1 *in vitro*, the same constructs as in 6.2.1 where used in a PAR-assay. PARylation of the purified, His-tagged H1.4 proteins was determined by incubating with recombinant ARTD1 in the presence of ^{32}P-NAD$^+$ and

activating EcoRI-linker DNA in PAR-Buffer. The reaction was stopped and the proteins were separated and analyzed by SDS-PAGE. After Coomassie staining, the gel was vacuum dried and exposed to an x-ray film. The incorporated radioactivity correlated with the methylation of the His-tagged protein (Fig. 24).

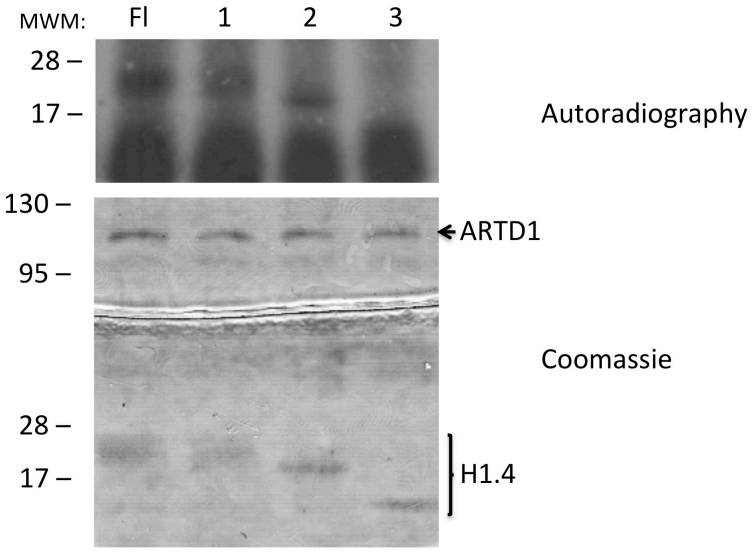

Figure 24: ARTD1-induced ADP-ribosylation of full-length and different H1.4 deletion mutants. Autoradiography of a 15% SDS-PAGE after ADP-ribosylation and separation of the different proteins (1 day exposure; upper panel). The lower panel shows the Coomassie stained gel to visualize the protein levels of ARTD1, full-length H1.4 (FL) and different H1.4 deletion mutants (1, 2 or 3).

While ARTD1 was able to PARylate full-length H1.4 and the C-terminal deletion mutants 1 and 2 in the presence of NAD^+ and DNA, the modification of the deletion mutant 3 expressing only the core domain and the N-terminal domain was weak. This result implied that ARTD1 modifies H1.4 mainly in the C-terminal domain. The intensity of the detected radioactivity correlated with the length of the H1.4 histone tail, suggesting multiple acceptor sites in the C-terminal domain of H1.4.

7.2.7 Acceptor Sites for PARylation by ARTD1 on the C-terminal Tail of H1.4

To further investigate the PARylated acceptor sites of H1.4, the C-terminal fragments described in 6.1 were used (fragment 1 (Fr1): expressing amino acids 114-144, fragment 2 (Fr2): expressing amino acids 145-189, and fragment 3 (Fr3): expressing amino acids 190-210) (Fig. 26).

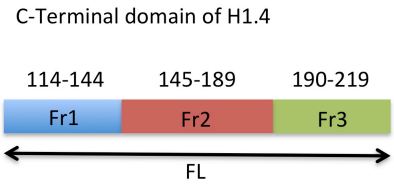

Figure 26: Scheme of the H1.4 C-terminal domain showing the cloned fragments

These fragments and a full-length (FL) C-terminal domain (expressing amino acids 114-210) were cloned into a pGEX-6P1 vector as GST fusions (linked by GGS amino acid repeats to minimize the steric influence of the GST-tag on the interaction of SET7/9 with the polypeptide). The constructs were transformed and the proteins were expressed and subsequently purified from *E.coli* according to the description in the Materials and Methods.

While all three deletion mutants (Fr1, 2 and 3) could be purified, the full-length C-terminal domain could not be eluted from the beads and thus the assay was performed with the protein still bound to the beads. The GST-tagged proteins were incubated with recombinant ARTD1 in the presence of ^{32}P-NAD^{+} and activating EcoRI-linker DNA. The reaction was stopped and proteins were separated by SDS-PAGE. After Coomassie staining, the gel was vacuum dried and exposed to an x-ray film as described before (Fig. 27).

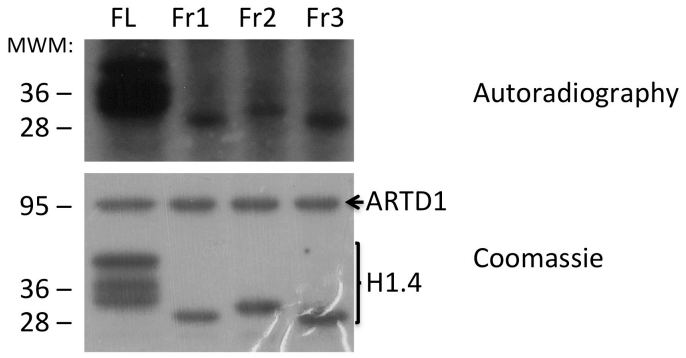

Figure 27: ARTD1-induced ADP-ribosylation of full length and different fragments of the H1.4 C-terminal domain. The upper panel shows the x-ray film (1 day exposure) to identify radiolabeled proteins and the lower panel shows the Coomassie stained gel to visualize the protein levels of ARTD1, the full length (FL) and different fragments (Fr1, Fr2, Fr3) of the H1.4 C-terminal domain.

All three deletion mutants were strongly PARylated, although Fr1 and Fr3 stronger than Fr2, indicating that this fragment either has a different affinity for ARTD1 or contains a

lower number of acceptor sites. Even though the full-length C-terminus was still bound to the beads, it was strongly PARylated by ARTD1. In contrast, SET7/9 was not able to methylate the bound C-terminal domain, which could be due to steric hindrance or the inaccessibility of the polypeptides for SET7/9.

According to this experiment the C-terminal domain of H1.4 has multiple acceptor sites for ARTD1 induced ADP-ribosylation.

7.2.8 ARTD1- and ARTD10-dependent PARylation of H1.4 Fragments 2 and 3

The lysines of fragment 2 and fragment 3 have already been further mutagenized for the determination of the methylation sites of SET7/9 in H1.4 and are thought to be one of the main acceptors for ARTD-induced PARylation. In order to identify PARylation sites, these deletion mutants were modified. Fr2 was split into four clusters (Cl1-4) and Fr3 into three clusters (Cl5-7). These clusters comprised all lysines and therefore many possible PARylation acceptor site in this region of H1.4. By overlapping PCR, all lysines in each cluster were mutated to arginines (Fig. 28). The new constructs were then cloned into pGEX-6PI vector, expressed and purified.

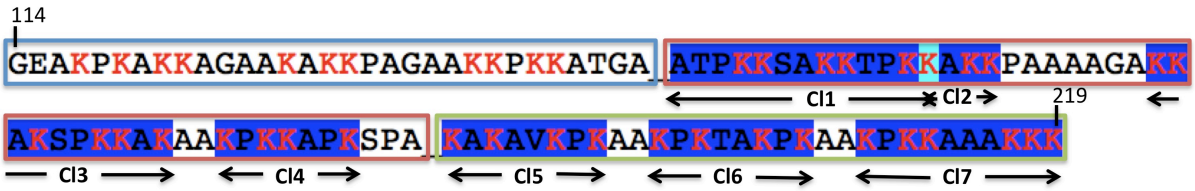

Figure 28: Amino acid sequence of the C-terminal tail of histone H1.4. The C-terminal domain is divided into the three fragments (Fr1 framed blue, Fr2 framed red, Fr3 framed green), Fr2 is split into Cl1-4 (highlighted in blue) (Cl1 and Cl2 share the turquois highlighted lysine), and Fr3 into Cl5-7 (highlighted in blue). The lysines, which were mutated to arginines, are marked in red.

The wt fragments (Fr2 and 3, as positive control) as well as the cluster mutants were incubated with ARTD1 or ARTD10, which is a mono-APD-ribosyltransferas and thus may possess a different spezification, in the presence of ^{32}P-NAD^{+} and activating EcoRI-linker DNA for 10 minutes and protein PARylation was analyzed by separating the proteins by SDS-PAGE (Fig. 29A and B).

A

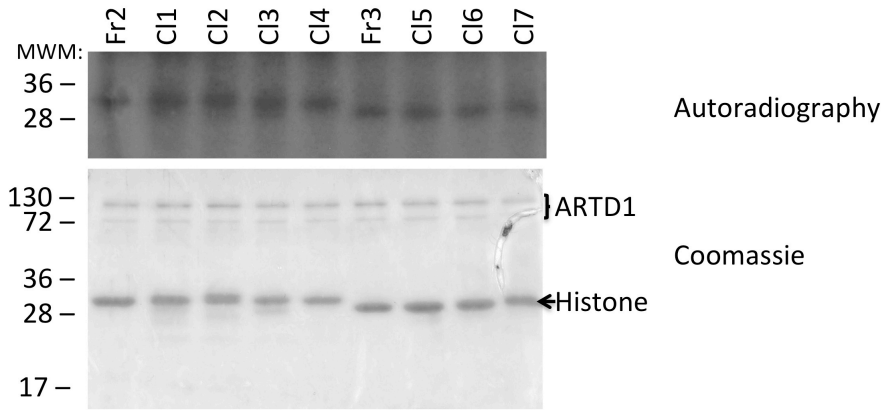

B

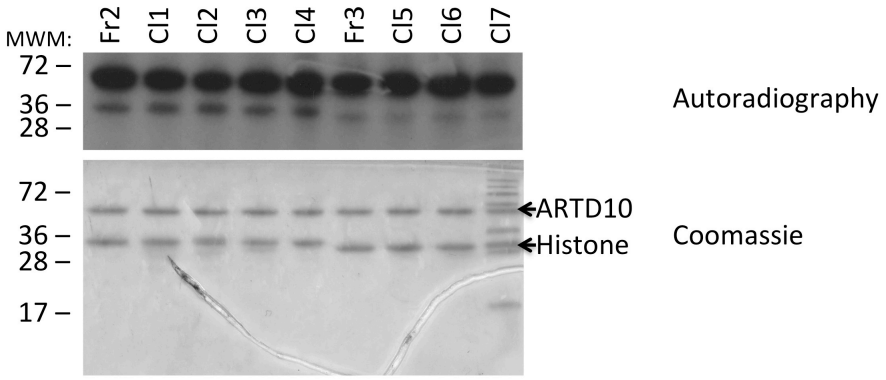

Figure 29: ARTD1 and 10 induced ADP-ribosylation of wt and cluster mutants of fragments 2 and 3. **A**: Autoradiography of a 15% SDS-PAGE after ADP-ribosylation by ARTD1 and separation of the different proteins (10 hours exposure; upper panel). The lower panel shows the Coomassie stained gel to visualize the protein levels of SET7/9, the wild-type fragments (Fr2, Fr3) and the cluster mutants (Cl1-7). **B:** Autoradiography of a 15% SDS-PAGE after ADP-ribosylation by ARTD10 and separation of the different proteins (2 days exposure; upper panel). The lower panel shows the Coomassie stained gel to visualize the protein levels of SET7/9, the wild-type fragments (Fr2, Fr3) and the cluster mutants (Cl1-7).

Interestingly, all cluster mutants were ADP-ribosylated to the same extent by ARTD1 and ARTD10 as the wt counterpart (Fr2 and Fr3), suggesting that in these fragments lysine residues do not serve as acceptor sites. Unfortunately, the arginine residues, which replaced the lysines, could also serve as targets for ARTD1- or ARTD10-induced PARylation.

A consolidated view of the results indicates that there are multiple acceptor sites for ADP-ribosylation in the C-terminal domain of H1.4 and that it is not possible to further determine these sites with our cluster mutation approach and our experimental setup.

7.2.9 Cluster 2 of Fragment 2 and Cluster 7 of Fragment 3 are less modified by ARTD1 in the Presence of high NAD^+ Concentrations

To confirm these result, the same ADP-ribosylation reactions as shown in 6.2.8 were performed in the presence or absence of 10 nM cold (non-radioactive) NAD^+ to analyze PARylation by western blot analysis using an antibody able to detect PAR residues (anti-PAR, BD). The reaction was stopped and proteins were separated by SDS-PAGE. After transferring the proteins onto a nitrocellulose membrane, the membrane was incubate with the anti-PAR antibody, a secondary anti-rabbit antibody and then analyzed with the Odyssey Imager (Fig. 30 A and B)

A

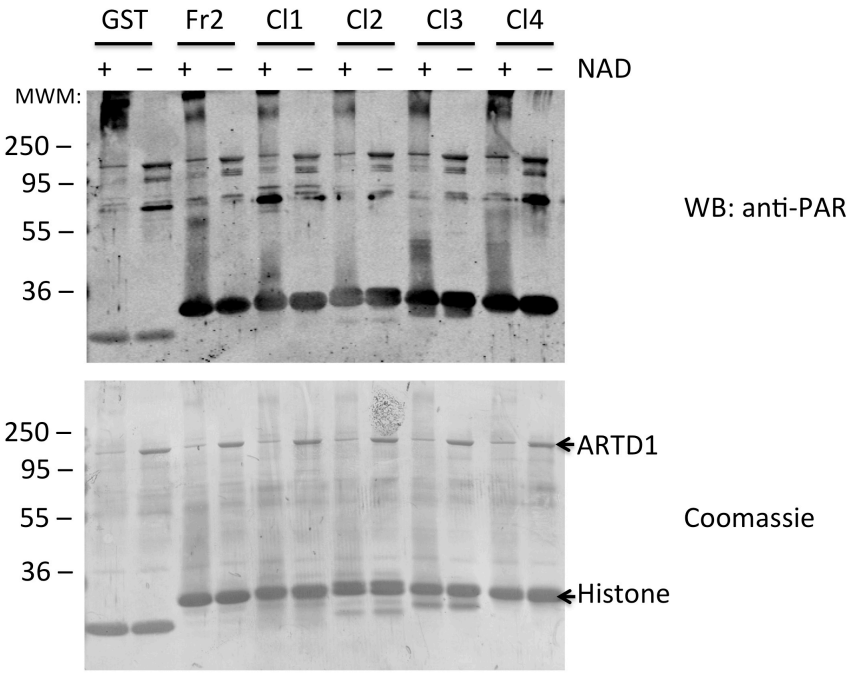

B

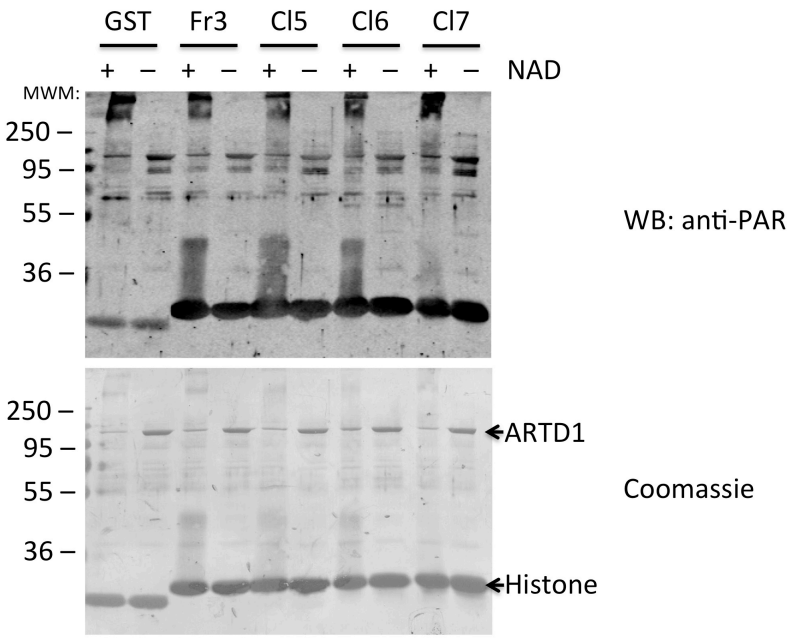

Figure 30: ARTD1-induced ADP-ribosylation of wt and cluster mutants of fragments 2 and 3. Western blot analysis of 15% SDS-PAGE using an anti-PAR antibody (upper part of panel). 1 µg GST-linker protein was included as control (GST). The reaction was performed in the presence or absence of NAD^+. The lower panel shows the Coomassie stained membrane. **A**: GST-linker, Fr2 wt and Cl1-Cl4. **B**: GST-linker, Fr3 wt and Cl5-CL7.

The western blot analysis revealed that the presence of high NAD^+ caused a strong shift of ARTD1 due to its auto-PARylation. Remarkably, this shift was similarly observed in both wt fragments (Fr2 and Fr3) and in Cl3-6, but not or to a lesser extent in Cl1, Cl2 and Cl7. These clusters thus likely contain lysine residues, which are targeted by ARTD1-induced ADP-ribosylation. Hence, these lysines could be the main acceptor for PARylation in the C-terminal domain of H1.4, which supports the idea of multiple target sites. Nevertheless, further studies would be needed to confirm these findings.

7.2.10 PARylation by ARTD1 inhibits Methylation by SET7/9

To study the crosstalk of posttranscriptional ADP-ribosylation and methylation, a sequential ADP-ribosylation and methylation assay was performed.

H1.4 fl and the wt of fragment 3 (Fr3) were both incubated with either wt ARTD1 or with an enzymatically inactive ARTD1 mutant in the presence of cold NAD^+ and activating EcoRI-linker DNA (15 minutes, 30°C). PJ-34 was added either before or after ADP-ribosylation to inhibit PARylation (5 minutes incubation time). Next, SET7/9 and ^{14}C-SAM

were added and the reaction was incubated for 1 hour at 30°C. Protein methylation was analyzed by separating the proteins by SDS-PAGE (Fig. 25).

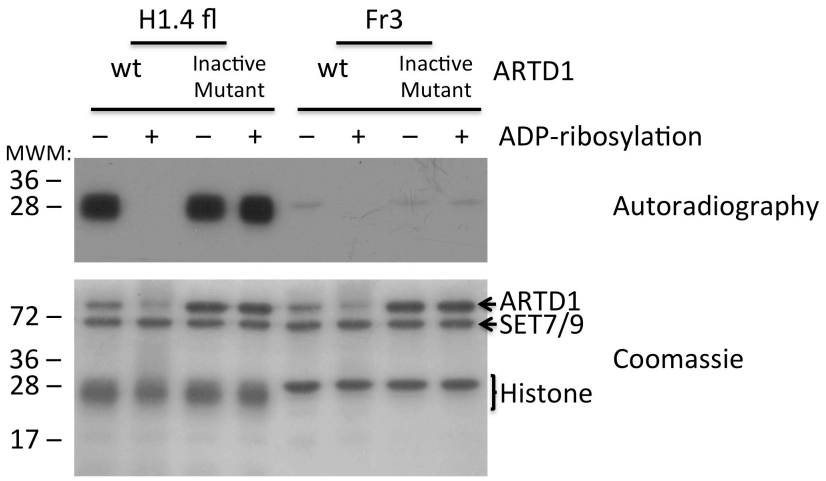

Figure 25: SET7/9 induced methylation of H1.4 fl and wt fragment 3 in the presence or absence of ADP-ribosylation. Autoradiography of a 15% SDS-PAGE after methylation and separation of the different proteins (2 days exposure; upper panel). The lower panel shows the Coomassie stained gel to visualize the protein levels of SET7/9, ARTD1, full length H1.4 and the wild-type fragment (Fr3).

As shown in the autoradiography, Set7/9-dependent methylation is prevented by ARTD1-dependent ADP-ribosylation of H1.4. This result could imply a structural proximity of the methylated lysine residues and the ADP-ribosylation acceptor site, which leads to steric hindrance. This crosstalk of ADP-ribosylation and methylation in H1.4 strengthens the importance of histone modifications and is an additional interaction in the “histone code”.

8 Discussion

8.1 Linker Histone H1 Methylation by SET7/9

SET7/9 was identified as a mono-methyltransferase for H3K4 [73,167]. In the course of our studies, SET7/9 was found to methylate the C-terminal fragment of linker histone H1.4, while neither the globular nor the N-terminal part were modified. Methylation was abolished by the addition of DNA to the methylation reaction. In order to identify the methyl acceptor sites in the lysine rich C-terminus, a cluster mutation approach was pursued. Since different cluster mutants of the entire histone H1.2 C-terminus were already available [177] and the sequence of the H1 variants is rather conserved, these constructs were chosen for the initial analysis. The variability of the methylation intensity of the cluster mutants was weak and adjustments in pH and the NaCl concentration did not increase the specificity of SET7/9 for H1.2. At pH 9, the methylation efficiency was strongly increased. However, the cluster mutation approach was not successful for H1.2, since methylation by SET7/9 could not be ascribed to only one cluster, indicating that SET7/9 methylates several lysine residues, which are distributed throughout the entire C-terminal domain of H1.2. To increase the chance to identify the methylation sites, the C-terminus of H1.4 was divided into three C-terminal fragments. SET7/9 mainly methylated H1.4 in fragment 2 (amino acids 145-189) and 3 (amino acids 190-219), whereas fragment 1 (amino acids 114-144) was only weakly methylated. A cluster mutation approach then identified six KAK sites, which were methylated *in vitro* at the last lysine residue by recombinant SET7/9. The second cluster approach was likely successful because the analyzed H1.4 fragments were smaller (in average 35 amino acids) as compared to the fragments investigated for H1.2 (full length C-terminus, 98 amino acids).

It is striking that SET7/9-induced methylation was strongly enhanced at a higher pH (9 versus 7.2). This might be due to the different pKa's of lysine (2.18, 8.95 and 10.53), which would lead to the deprotonation of lysines at higher pH, indicating that a fully protonated lysine is not a good methyl group acceptor.

The C-terminal domain of H1.4 acquires a specific secondary structure when bound to DNA [40], stabilizes the folding of the nucleosome array into chromatin fibers, and is needed for the high affinity binding to chromatin [41]. Addition of DNA to the methylation reaction abrogated the methylation of SET7/9 completely. It is thus tempting to speculate that SET7/9-induced methylation of the C-terminal domain affects the binding to DNA or even

the stabilization of the nucleosome arrays, leading to less compact chromatin and increasing the accessibility for other proteins to the DNA.

The binding affinity of the different H1 subtypes correlates with the length of the C-terminal domain, with H1.4 and H1.5 having the highest affinity [45]. Modifications such as SET7/9-induced methylation of the C-terminal domain might thus modulate the kinetics of H1 chromatin exchange by altering the interaction of H1 with other structural protein components of chromatin. For example, it was shown that ongoing phosphorylation is needed for histone H1 mobility [48].

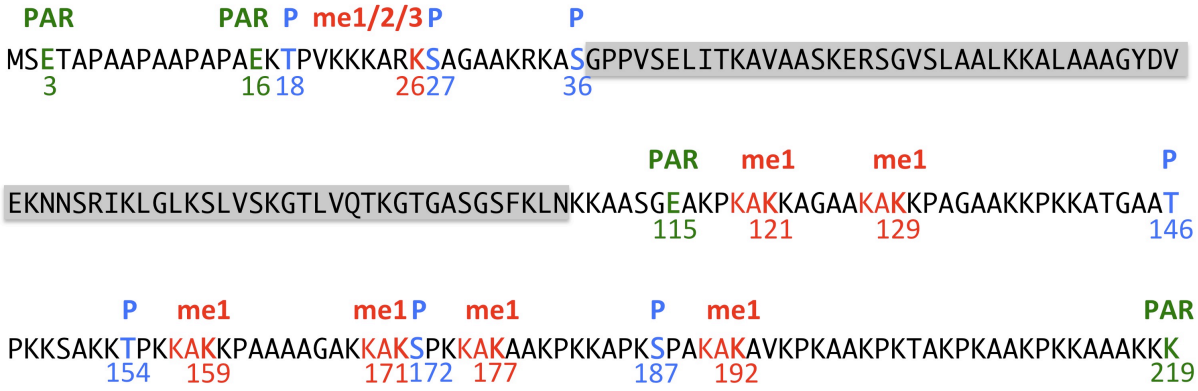

Figure 31: Amino acid sequence of the human linker histone H1.4 with the so far known post-translational modification sites. PARylation (PAR) is marked in green and phosphorylation (P) in blue. Methylation (me) sites with the number indicating the methylation state, as well as the six newly identified KAK motifs, are indicated in red.

The biological relevance and *in vivo* function of methylation by SET7/9 is still unclear. However, stimulation and repression of other post-translational modifications might be one possible function. In comparison to core histones, very little is known about the modifications and consequent modifiers of the linker histones. For example, the four last lysine residues, which showed the strongest modification by SET7/9, are located very close to already known CDK phosphorylation sites. In addition, interactions between K26 dimethylation and AuroraB-mediated phosphorylation of S27 have been shown earlier [173]. A comparable interaction could exist between phosphorylation by CDKs and SET7/9-induced methylation of H1.4. For example, S172 and S187 are not only phosphorylated during mitosis and their modification in interphase is associated with transcription and chromatin relaxation [176]. The close proximity of these post-translational modifications could implie a possible crosstalk.

The first H1.4 methylation site to be discovered was K26, which is catalyzed by Enhancer of zeste homolog 2 (Ezh2). Heterochromatin protein 1 (HP1) binding to this methyl-group induces transcriptional repression, whereas phosphorylation of H1.4 on S27 abolishes HP1 binding [60]. H1.4K26 methylation increases the residence time of H1.4 at the chromatin [178]. Furthermore, due to technical improvements in mass spectrometry, new H1 modification sites of different PTMs have lately been identified, but the function of the majority of these modifications is still unknown. One of them is H1.2K187, which is methylated by the histone lysine methyltransferases G9a and Glp1 [177], but its function is still unknown.

In vitro experiments identified H3K4 as a hindrance for repressive histone modifiers, so that H3K4 modification by SET7/9 was associated with transcriptional activation [75]. However, the global H3K4 methylation levels are not changed in SET7/9 knockout mice [179]. A prerequisite to test a similar gene-specific function for H1 methylation by SET7/9 is the availability of an antibody exclusive for this modification. Such an H3K4-specific antibody would allow an in-depth analysis of the impact of SET7/9-dependent methylation on individual genes and promoters. Since variant H1.4 has one of the strongest affinities for chromatin [45] and the C-terminal domain was described to interact with HP1, one might be tempted to propose that the methylation of H1.4 by SET7/9 leads to an even stronger binding of H1.4 to chromatin [41]. Therefore, SET7/9 methylation could potentially be a major player in the repression of transcription, but this has to be a topic of further studies.

The nuclear distribution and mobility of wt GFP-H1.4 and the K6R mutant was compared by live-cell imaging and FRAP experiments, respectively, by Ingrid Kassner. We neither observed a difference in the localization nor in the mobility under the tested conditions. It is possible that variations in mobility can only be seen in cells overexpressing or lacking SET7/9, as it is the case for ARTD1 methylation [180]. The H1.4 fusion proteins with photoactivatable GFP, which have been used to determine the nuclear localization of full length, C-terminal and N-terminal tails of H1.4 in U2OS cells on both eu- and heterochromatin, may be used in future studies. It would be interesting to monitor the dynamics of H1.4 as a function of SET7/9-induced methylation in specific nuclear regions and under defined conditions.

Genome-wide binding studies identified H1 to reside mainly on inactive genes, whereas ARTD1 showed reciprocal binding to chromatin [128]. Hence, it is interesting to speculate that the exchange of H1 and ARTD1 on their target promoters during gene

activation is regulated by SET7/9 induced methylation. Other chromatin binding factors, which assist in accumulation and displacement of H1 and ARTD1 from chromatin, could be regulated by methylation and thus induce adjustments in chromatin structures.

8.2 Linker Histone H1 Modification by ARTD1

ADP-ribosylation by ARTD1 affects inter- and intracellular signaling, cell cycle regulation, chromatin remodeling, DNA replication, transcription, DNA repair, somatic recombination, regulation of telomere length, inflammation and cell death via apoptosis or necrosis, and thus plays a critical role in many cellular processes [105,120].

In this study we identified the acceptor site for ARTD1-induced modification in linker histone H1. It was shown, that ADP-ribosylation is mainly found in the C-terminal domain of H1.4 and that there have to be multiple acceptor sites for this modification. An exact identification of the amino acid residues was not possible. There was also no significant difference in ARTD1- and ARTD10-induced modification in H1.4. It may have been impossible to identify the acceptor sited due to the cluster mutation approach itself, which may not be suited for the amount of target sites. In addition, the arginines, which replaced the lysines, could potentially also serve as acceptors for ADP-ribose.

However, in a PAR-assay with increased NAD^+ concentrations, a reduced shift of mutated H1.4 (Cl1, Cl2 and Cl7) was observed. This could indicate, that the arginines, which were thought to be acceptor sites, are not ADP-ribosylated in H1.4 and lysines are the main target of ARTD1-induced modification. Due to time restrictions, this has to be the focus of further studies.

8.3 Crosstalk of ARTD1 and SET7/9 on H1.4

Epigenetics is known as heritable changes in gene expression or cellular phenotypes that occur without changes in the underlying DNA sequence. DNA methylation, histone modification and chromatin alterations thus comprise epigenetic modifications. The results described in this study further strengthen the importance of ARTD1 and histone ADP-ribosylation as components of the histone code [171]. ARTD1-induced PARylation of linker histone H1 impacts subsequent methylation by SET7/9. ADP-ribosylation is a bulky modification with strong, negative charges, which most likely inhibits H1 modification by

SET7/9. This is comparable to phosphorylation, which reduces methylation of close SET7/9 target lysine residues [76].

The facts that ARTD1 is able to ADP-ribosylate all core histones and the linker histones [112] and that the size and branching of the polymers can vary under different conditions, increase the complexity of ARTD1-induced histone modification even more. Hence, it is important for future studies to not only concentrate on the impact of ADP-ribosylation on other histone modifications, but moreover on the regulation of ARTD1-dependent histone modification itself.

9 References

1. Lodish, H., Berk, A., Kaiser, C. A., Krieger, M., Scott, M. P., Bretscher, A., Ploegh, H. and Matsudaira, P. *Molecular cell biology*, 973 (W.H. Freeman, New York, 2008).
2. Rouleau, M., Aubin, R.A. & Poirier, G.G. Poly(ADP-ribosyl)ated chromatin domains: access granted. *Journal of cell science* **117**, 815-25 (2004).
3. Felsenfeld, G. & Groudine, M. Controlling the double helix. *Nature* **421**, 448-53 (2003).
4. Kouzarides, T. Chromatin modifications and their function. *Cell* **128**, 693-705 (2007).
5. Kass, S.U. & Wolffe, A.P. DNA methylation, nucleosomes and the inheritance of chromatin structure and function. *Novartis Foundation symposium* **214**, 22-35; discussion 36-50 (1998).
6. Happel, N. & Doenecke, D. Histone H1 and its isoforms: contribution to chromatin structure and function. *Gene* **431**, 1-12 (2009).
7. Wolffe, A.P. Histone H1. *The international journal of biochemistry & cell biology* **29**, 1463-6 (1997).
8. Belmont, A.S., Dietzel, S., Nye, A.C., Strukov, Y.G. & Tumbar, T. Large-scale chromatin structure and function. *Current opinion in cell biology* **11**, 307-11 (1999).
9. Earnshaw, W.C. & Mackay, A.M. Role of nonhistone proteins in the chromosomal events of mitosis. *The FASEB journal : official publication of the Federation of American Societies for Experimental Biology* **8**, 947-56 (1994).
10. Kasinsky, H.E., Lewis, J.D., Dacks, J.B. & Ausio, J. Origin of H1 linker histones. *The FASEB journal : official publication of the Federation of American Societies for Experimental Biology* **15**, 34-42 (2001).
11. Arents, G. & Moudrianakis, E.N. The histone fold: a ubiquitous architectural motif utilized in DNA compaction and protein dimerization. *Proceedings of the National Academy of Sciences of the United States of America* **92**, 11170-4 (1995).
12. Luger, K., Mader, A.W., Richmond, R.K., Sargent, D.F. & Richmond, T.J. Crystal structure of the nucleosome core particle at 2.8 A resolution. *Nature* **389**, 251-60 (1997).
13. Shechter, D., Dormann, H.L., Allis, C.D. & Hake, S.B. Extraction, purification and analysis of histones. *Nature protocols* **2**, 1445-57 (2007).
14. Oohara, I. & Wada, A. Spectroscopic studies on histone-DNA interactions. I. The interaction of histone (H2A, H2B) dimer with DNA: DNA sequence dependence. *Journal of molecular biology* **196**, 389-97 (1987).
15. Wyrick, J.J. & Parra, M.A. The role of histone H2A and H2B post-translational modifications in transcription: a genomic perspective. *Biochimica et biophysica acta* **1789**, 37-44 (2009).
16. Svotelis, A., Gevry, N. & Gaudreau, L. Regulation of gene expression and cellular proliferation by histone H2A.Z. *Biochemistry and cell biology = Biochimie et biologie cellulaire* **87**, 179-88 (2009).
17. Li, B., Carey, M. & Workman, J.L. The role of chromatin during transcription. *Cell* **128**, 707-19 (2007).
18. Polo, S.E. & Almouzni, G. Chromatin assembly: a basic recipe with various flavours. *Current opinion in genetics & development* **16**, 104-11 (2006).
19. Bassing, C.H. *et al.* Histone H2AX: a dosage-dependent suppressor of oncogenic translocations and tumors. *Cell* **114**, 359-70 (2003).
20. Stucki, M. & Jackson, S.P. gammaH2AX and MDC1: anchoring the DNA-damage-response machinery to broken chromosomes. *DNA repair* **5**, 534-43 (2006).
21. Doyen, C.M. *et al.* Mechanism of polymerase II transcription repression by the histone variant macroH2A. *Molecular and cellular biology* **26**, 1156-64 (2006).
22. Campos, E.I. & Reinberg, D. Histones: annotating chromatin. *Annual review of genetics* **43**, 559-99 (2009).
23. Guillemette, B. *et al.* Variant histone H2A.Z is globally localized to the promoters of inactive yeast genes and regulates nucleosome positioning. *PLoS biology* **3**, e384 (2005).
24. Zhang, H., Roberts, D.N. & Cairns, B.R. Genome-wide dynamics of Htz1, a histone H2A variant that poises repressed/basal promoters for activation through histone loss. *Cell* **123**, 219-31 (2005).
25. Schwartz, B.E. & Ahmad, K. Transcriptional activation triggers deposition and removal of the histone variant H3.3. *Genes & development* **19**, 804-14 (2005).
26. Caterino, T.L. & Hayes, J.J. Structure of the H1 C-terminal domain and function in chromatin condensation. *Biochemistry and cell biology = Biochimie et biologie cellulaire* **89**, 35-44 (2011).
27. Maresca, T.J., Freedman, B.S. & Heald, R. Histone H1 is essential for mitotic chromosome architecture and segregation in Xenopus laevis egg extracts. *The Journal of cell biology* **169**, 859-69 (2005).
28. Sancho, M., Diani, E., Beato, M. & Jordan, A. Depletion of human histone H1 variants uncovers specific roles in gene expression and cell growth. *PLoS genetics* **4**, e1000227 (2008).

29. Parseghian, M.H., Newcomb, R.L., Winokur, S.T. & Hamkalo, B.A. The distribution of somatic H1 subtypes is non-random on active vs. inactive chromatin: distribution in human fetal fibroblasts. *Chromosome research : an international journal on the molecular, supramolecular and evolutionary aspects of chromosome biology* **8**, 405-24 (2000).
30. Meergans, T., Albig, W. & Doenecke, D. Varied expression patterns of human H1 histone genes in different cell lines. *DNA and cell biology* **16**, 1041-9 (1997).
31. Izzo, A., Kamieniarz, K. & Schneider, R. The histone H1 family: specific members, specific functions? *Biological chemistry* **389**, 333-43 (2008).
32. Happel, N., Schulze, E. & Doenecke, D. Characterisation of human histone H1x. *Biological chemistry* **386**, 541-51 (2005).
33. Zlatanova, J. & Doenecke, D. Histone H1 zero: a major player in cell differentiation? *The FASEB journal : official publication of the Federation of American Societies for Experimental Biology* **8**, 1260-8 (1994).
34. Lin, Q., Sirotkin, A. & Skoultchi, A.I. Normal spermatogenesis in mice lacking the testis-specific linker histone H1t. *Molecular and cellular biology* **20**, 2122-8 (2000).
35. Rabini, S. *et al.* Spermatogenesis in mice is not affected by histone H1.1 deficiency. *Experimental cell research* **255**, 114-24 (2000).
36. Fan, Y., Sirotkin, A., Russell, R.G., Ayala, J. & Skoultchi, A.I. Individual somatic H1 subtypes are dispensable for mouse development even in mice lacking the H1(0) replacement subtype. *Molecular and cellular biology* **21**, 7933-43 (2001).
37. Fan, Y. *et al.* H1 linker histones are essential for mouse development and affect nucleosome spacing in vivo. *Molecular and cellular biology* **23**, 4559-72 (2003).
38. Fan, Y. *et al.* Histone H1 depletion in mammals alters global chromatin structure but causes specific changes in gene regulation. *Cell* **123**, 1199-212 (2005).
39. Brown, D.T., Izard, T. & Misteli, T. Mapping the interaction surface of linker histone H1(0) with the nucleosome of native chromatin in vivo. *Nature structural & molecular biology* **13**, 250-5 (2006).
40. Roque, A., Iloro, I., Ponte, I., Arrondo, J.L. & Suau, P. DNA-induced secondary structure of the carboxyl-terminal domain of histone H1. *The Journal of biological chemistry* **280**, 32141-7 (2005).
41. Hendzel, M.J., Lever, M.A., Crawford, E. & Th'ng, J.P. The C-terminal domain is the primary determinant of histone H1 binding to chromatin in vivo. *The Journal of biological chemistry* **279**, 20028-34 (2004).
42. Catez, F., Ueda, T. & Bustin, M. Determinants of histone H1 mobility and chromatin binding in living cells. *Nature structural & molecular biology* **13**, 305-10 (2006).
43. Buttinelli, M., Panetta, G., Rhodes, D. & Travers, A. The role of histone H1 in chromatin condensation and transcriptional repression. *Genetica* **106**, 117-24 (1999).
44. Nightingale, K.P., Pruss, D. & Wolffe, A.P. A single high affinity binding site for histone H1 in a nucleosome containing the Xenopus borealis 5 S ribosomal RNA gene. *The Journal of biological chemistry* **271**, 7090-4 (1996).
45. Th'ng, J.P., Sung, R., Ye, M. & Hendzel, M.J. H1 family histones in the nucleus. Control of binding and localization by the C-terminal domain. *The Journal of biological chemistry* **280**, 27809-14 (2005).
46. Vogler, C. *et al.* Histone H2A C-terminus regulates chromatin dynamics, remodeling, and histone H1 binding. *PLoS genetics* **6**, e1001234 (2010).
47. Misteli, T., Gunjan, A., Hock, R., Bustin, M. & Brown, D.T. Dynamic binding of histone H1 to chromatin in living cells. *Nature* **408**, 877-81 (2000).
48. Lever, M.A., Th'ng, J.P., Sun, X. & Hendzel, M.J. Rapid exchange of histone H1.1 on chromatin in living human cells. *Nature* **408**, 873-6 (2000).
49. Wood, C. *et al.* Post-translational modifications of the linker histone variants and their association with cell mechanisms. *The FEBS journal* **276**, 3685-97 (2009).
50. Jenuwein, T. & Allis, C.D. Translating the histone code. *Science* **293**, 1074-80 (2001).
51. Spannhoff, A., Hauser, A.T., Heinke, R., Sippl, W. & Jung, M. The emerging therapeutic potential of histone methyltransferase and demethylase inhibitors. *ChemMedChem* **4**, 1568-82 (2009).
52. Nightingale, K.P., O'Neill, L.P. & Turner, B.M. Histone modifications: signalling receptors and potential elements of a heritable epigenetic code. *Current opinion in genetics & development* **16**, 125-36 (2006).
53. Jiang, T., Zhou, X., Taghizadeh, K., Dong, M. & Dedon, P.C. N-formylation of lysine in histone proteins as a secondary modification arising from oxidative DNA damage. *Proceedings of the National Academy of Sciences of the United States of America* **104**, 60-5 (2007).
54. Suzuki, M. SPKK, a new nucleic acid-binding unit of protein found in histone. *The EMBO journal* **8**, 797-804 (1989).

55. Sarg, B., Helliger, W., Talasz, H., Forg, B. & Lindner, H.H. Histone H1 phosphorylation occurs site-specifically during interphase and mitosis: identification of a novel phosphorylation site on histone H1. *The Journal of biological chemistry* **281**, 6573-80 (2006).
56. Boggs, B.A., Allis, C.D. & Chinault, A.C. Immunofluorescent studies of human chromosomes with antibodies against phosphorylated H1 histone. *Chromosoma* **108**, 485-90 (2000).
57. Alexandrow, M.G. & Hamlin, J.L. Chromatin decondensation in S-phase involves recruitment of Cdk2 by Cdc45 and histone H1 phosphorylation. *The Journal of cell biology* **168**, 875-86 (2005).
58. Hale, T.K., Contreras, A., Morrison, A.J. & Herrera, R.E. Phosphorylation of the linker histone H1 by CDK regulates its binding to HP1alpha. *Molecular cell* **22**, 693-9 (2006).
59. Vaquero, A. *et al.* Human SirT1 interacts with histone H1 and promotes formation of facultative heterochromatin. *Molecular cell* **16**, 93-105 (2004).
60. Daujat, S., Zeissler, U., Waldmann, T., Happel, N. & Schneider, R. HP1 binds specifically to Lys26-methylated histone H1.4, whereas simultaneous Ser27 phosphorylation blocks HP1 binding. *The Journal of biological chemistry* **280**, 38090-5 (2005).
61. Zhang, Y. & Reinberg, D. Transcription regulation by histone methylation: interplay between different covalent modifications of the core histone tails. *Genes & development* **15**, 2343-60 (2001).
62. Martin, C. & Zhang, Y. The diverse functions of histone lysine methylation. *Nature reviews. Molecular cell biology* **6**, 838-49 (2005).
63. Santos-Rosa, H. *et al.* Active genes are tri-methylated at K4 of histone H3. *Nature* **419**, 407-11 (2002).
64. Smith, B.C. & Denu, J.M. Chemical mechanisms of histone lysine and arginine modifications. *Biochimica et biophysica acta* **1789**, 45-57 (2009).
65. Bedford, M.T. & Richard, S. Arginine methylation an emerging regulator of protein function. *Molecular cell* **18**, 263-72 (2005).
66. Klose, R.J. & Zhang, Y. Regulation of histone methylation by demethylimination and demethylation. *Nature reviews. Molecular cell biology* **8**, 307-18 (2007).
67. Shi, Y. *et al.* Histone demethylation mediated by the nuclear amine oxidase homolog LSD1. *Cell* **119**, 941-53 (2004).
68. Tochio, N. *et al.* Solution structure of the SWIRM domain of human histone demethylase LSD1. *Structure* **14**, 457-68 (2006).
69. Lee, M.G., Wynder, C., Cooch, N. & Shiekhattar, R. An essential role for CoREST in nucleosomal histone 3 lysine 4 demethylation. *Nature* **437**, 432-5 (2005).
70. Karytinos, A. *et al.* A novel mammalian flavin-dependent histone demethylase. *The Journal of biological chemistry* **284**, 17775-82 (2009).
71. Shi, Y. & Whetstine, J.R. Dynamic regulation of histone lysine methylation by demethylases. *Molecular cell* **25**, 1-14 (2007).
72. Tsukada, Y. *et al.* Histone demethylation by a family of JmjC domain-containing proteins. *Nature* **439**, 811-6 (2006).
73. Wang, H. *et al.* Purification and functional characterization of a histone H3-lysine 4-specific methyltransferase. *Molecular cell* **8**, 1207-17 (2001).
74. Brasacchio, D. *et al.* Hyperglycemia induces a dynamic cooperativity of histone methylase and demethylase enzymes associated with gene-activating epigenetic marks that coexist on the lysine tail. *Diabetes* **58**, 1229-36 (2009).
75. Deering, T.G., Ogihara, T., Trace, A.P., Maier, B. & Mirmira, R.G. Methyltransferase Set7/9 maintains transcription and euchromatin structure at islet-enriched genes. *Diabetes* **58**, 185-93 (2009).
76. Dhayalan, A., Kudithipudi, S., Rathert, P. & Jeltsch, A. Specificity analysis-based identification of new methylation targets of the SET7/9 protein lysine methyltransferase. *Chemistry & biology* **18**, 111-20 (2011).
77. Yang, J. *et al.* Reversible methylation of promoter-bound STAT3 by histone-modifying enzymes. *Proceedings of the National Academy of Sciences of the United States of America* **107**, 21499-504 (2010).
78. Dillon, S.C., Zhang, X., Trievel, R.C. & Cheng, X. The SET-domain protein superfamily: protein lysine methyltransferases. *Genome biology* **6**, 227 (2005).
79. Chuikov, S. *et al.* Regulation of p53 activity through lysine methylation. *Nature* **432**, 353-60 (2004).
80. Kouskouti, A., Scheer, E., Staub, A., Tora, L. & Talianidis, I. Gene-specific modulation of TAF10 function by SET9-mediated methylation. *Molecular cell* **14**, 175-82 (2004).
81. Kurash, J.K. *et al.* Methylation of p53 by Set7/9 mediates p53 acetylation and activity in vivo. *Molecular cell* **29**, 392-400 (2008).
82. Couture, J.F., Collazo, E., Hauk, G. & Trievel, R.C. Structural basis for the methylation site specificity of SET7/9. *Nature structural & molecular biology* **13**, 140-6 (2006).

83. Ea, C.K. & Baltimore, D. Regulation of NF-kappaB activity through lysine monomethylation of p65. *Proceedings of the National Academy of Sciences of the United States of America* **106**, 18972-7 (2009).
84. Munro, S., Khaire, N., Inche, A., Carr, S. & La Thangue, N.B. Lysine methylation regulates the pRb tumour suppressor protein. *Oncogene* **29**, 2357-67 (2010).
85. Pagans, S. *et al.* The Cellular lysine methyltransferase Set7/9-KMT7 binds HIV-1 TAR RNA, monomethylates the viral transactivator Tat, and enhances HIV transcription. *Cell host & microbe* **7**, 234-44 (2010).
86. Subramanian, K. *et al.* Regulation of estrogen receptor alpha by the SET7 lysine methyltransferase. *Molecular cell* **30**, 336-47 (2008).
87. Wang, J. *et al.* The lysine demethylase LSD1 (KDM1) is required for maintenance of global DNA methylation. *Nature genetics* **41**, 125-9 (2009).
88. Kontaki, H. & Talianidis, I. Lysine methylation regulates E2F1-induced cell death. *Molecular cell* **39**, 152-60 (2010).
89. Hottiger, M.O., Hassa, P.O., Luscher, B., Schuler, H. & Koch-Nolte, F. Toward a unified nomenclature for mammalian ADP-ribosyltransferases. *Trends in biochemical sciences* **35**, 208-19 (2010).
90. Messner, S. & Hottiger, M.O. Histone ADP-ribosylation in DNA repair, replication and transcription. *Trends in cell biology* **21**, 534-42 (2011).
91. Hilz, H. ADP-ribosylation of proteins--a multifunctional process. *Hoppe-Seyler's Zeitschrift fur physiologische Chemie* **362**, 1415-25 (1981).
92. Wielckens, K., Bredehorst, R., Adamietz, P. & Hilz, H. Protein-bound polymeric and monomeric ADP-ribose residues in hepatic tissues. Comparative analyses using a new procedure for the quantification of poly(ADP-ribose). *European journal of biochemistry / FEBS* **117**, 69-74 (1981).
93. Chambon, P., Weill, J.D. & Mandel, P. Nicotinamide mononucleotide activation of new DNA-dependent polyadenylic acid synthesizing nuclear enzyme. *Biochemical and biophysical research communications* **11**, 39-43 (1963).
94. Kim, M.Y., Zhang, T. & Kraus, W.L. Poly(ADP-ribosyl)ation by PARP-1: 'PAR-laying' NAD+ into a nuclear signal. *Genes & development* **19**, 1951-67 (2005).
95. Altmeyer, M., Messner, S., Hassa, P.O., Fey, M. & Hottiger, M.O. Molecular mechanism of poly(ADP-ribosyl)ation by PARP1 and identification of lysine residues as ADP-ribose acceptor sites. *Nucleic acids research* **37**, 3723-38 (2009).
96. Alvarez-Gonzalez, R. & Jacobson, M.K. Characterization of polymers of adenosine diphosphate ribose generated in vitro and in vivo. *Biochemistry* **26**, 3218-24 (1987).
97. Koch-Nolte, F., Kernstock, S., Mueller-Dieckmann, C., Weiss, M.S. & Haag, F. Mammalian ADP-ribosyltransferases and ADP-ribosylhydrolases. *Frontiers in bioscience : a journal and virtual library* **13**, 6716-29 (2008).
98. Oka, S., Kato, J. & Moss, J. Identification and characterization of a mammalian 39-kDa poly(ADP-ribose) glycohydrolase. *The Journal of biological chemistry* **281**, 705-13 (2006).
99. Koh, D.W. *et al.* Failure to degrade poly(ADP-ribose) causes increased sensitivity to cytotoxicity and early embryonic lethality. *Proceedings of the National Academy of Sciences of the United States of America* **101**, 17699-704 (2004).
100. Di Girolamo, M., Dani, N., Stilla, A. & Corda, D. Physiological relevance of the endogenous mono(ADP-ribosyl)ation of cellular proteins. *The FEBS journal* **272**, 4565-75 (2005).
101. Ahel, I. *et al.* Poly(ADP-ribose)-binding zinc finger motifs in DNA repair/checkpoint proteins. *Nature* **451**, 81-5 (2008).
102. Karras, G.I. *et al.* The macro domain is an ADP-ribose binding module. *The EMBO journal* **24**, 1911-20 (2005).
103. Pleschke, J.M., Kleczkowska, H.E., Strohm, M. & Althaus, F.R. Poly(ADP-ribose) binds to specific domains in DNA damage checkpoint proteins. *The Journal of biological chemistry* **275**, 40974-80 (2000).
104. Milne, J.C. & Denu, J.M. The Sirtuin family: therapeutic targets to treat diseases of aging. *Current opinion in chemical biology* **12**, 11-7 (2008).
105. Hassa, P.O., Haenni, S.S., Elser, M. & Hottiger, M.O. Nuclear ADP-ribosylation reactions in mammalian cells: where are we today and where are we going? *Microbiology and molecular biology reviews : MMBR* **70**, 789-829 (2006).
106. Yamanaka, H., Penning, C.A., Willis, E.H., Wasson, D.B. & Carson, D.A. Characterization of human poly(ADP-ribose) polymerase with autoantibodies. *The Journal of biological chemistry* **263**, 3879-83 (1988).
107. D'Amours, D., Desnoyers, S., D'Silva, I. & Poirier, G.G. Poly(ADP-ribosyl)ation reactions in the regulation of nuclear functions. *The Biochemical journal* **342 (Pt 2)**, 249-68 (1999).

108. Citarelli, M., Teotia, S. & Lamb, R.S. Evolutionary history of the poly(ADP-ribose) polymerase gene family in eukaryotes. *BMC evolutionary biology* **10**, 308 (2010).
109. Kleine, H. *et al.* Substrate-assisted catalysis by PARP10 limits its activity to mono-ADP-ribosylation. *Molecular cell* **32**, 57-69 (2008).
110. Marsischky, G.T., Wilson, B.A. & Collier, R.J. Role of glutamic acid 988 of human poly-ADP-ribose polymerase in polymer formation. Evidence for active site similarities to the ADP-ribosylating toxins. *The Journal of biological chemistry* **270**, 3247-54 (1995).
111. Ruf, A., Rolli, V., de Murcia, G. & Schulz, G.E. The mechanism of the elongation and branching reaction of poly(ADP-ribose) polymerase as derived from crystal structures and mutagenesis. *Journal of molecular biology* **278**, 57-65 (1998).
112. Messner, S. *et al.* PARP1 ADP-ribosylates lysine residues of the core histone tails. *Nucleic acids research* **38**, 6350-62 (2010).
113. Rulten, S.L. *et al.* PARP-3 and APLF function together to accelerate nonhomologous end-joining. *Molecular cell* **41**, 33-45 (2011).
114. Boulikas, T. DNA strand breaks alter histone ADP-ribosylation. *Proceedings of the National Academy of Sciences of the United States of America* **86**, 3499-503 (1989).
115. Kawaichi, M., Ueda, K. & Hayaishi, O. Initiation of poly(ADP-ribosyl) histone synthesis by poly(ADP-ribose) synthetase. *The Journal of biological chemistry* **255**, 816-9 (1980).
116. Huletsky, A. *et al.* The effect of poly(ADP-ribosyl)ation on native and H1-depleted chromatin. A role of poly(ADP-ribosyl)ation on core nucleosome structure. *The Journal of biological chemistry* **264**, 8878-86 (1989).
117. Nolan, N.L., Butt, T.R., Wong, M., Lambrianidou, A. & Smulson, M.E. Characterization of poly(ADP-ribose)--histone H1 complex formation in purified polynucleosomes and chromatin. *European journal of biochemistry / FEBS* **113**, 15-25 (1980).
118. Minaga, T., Romaschin, A.D., Kirsten, E. & Kun, E. The in vivo distribution of immunoreactive larger than tetrameric polyadenosine diphosphoribose in histone and non-histone protein fractions of rat liver. *The Journal of biological chemistry* **254**, 9663-8 (1979).
119. Hassa, P.O. & Hottiger, M.O. The diverse biological roles of mammalian PARPS, a small but powerful family of poly-ADP-ribose polymerases. *Frontiers in bioscience : a journal and virtual library* **13**, 3046-82 (2008).
120. Hassa, P.O. & Hottiger, M.O. The functional role of poly(ADP-ribose)polymerase 1 as novel coactivator of NF-kappaB in inflammatory disorders. *Cellular and molecular life sciences : CMLS* **59**, 1534-53 (2002).
121. Wang, Z.Q. *et al.* PARP is important for genomic stability but dispensable in apoptosis. *Genes & development* **11**, 2347-58 (1997).
122. Masutani, M. *et al.* Function of poly(ADP-ribose) polymerase in response to DNA damage: gene-disruption study in mice. *Molecular and cellular biochemistry* **193**, 149-52 (1999).
123. Trucco, C., Oliver, F.J., de Murcia, G. & Menissier-de Murcia, J. DNA repair defect in poly(ADP-ribose) polymerase-deficient cell lines. *Nucleic acids research* **26**, 2644-9 (1998).
124. Kraus, W.L. & Lis, J.T. PARP goes transcription. *Cell* **113**, 677-83 (2003).
125. Hassa, P.O. & Hottiger, M.O. A role of poly (ADP-ribose) polymerase in NF-kappaB transcriptional activation. *Biological chemistry* **380**, 953-9 (1999).
126. de Murcia, G. *et al.* Modulation of chromatin superstructure induced by poly(ADP-ribose) synthesis and degradation. *The Journal of biological chemistry* **261**, 7011-7 (1986).
127. Timinszky, G. *et al.* A macrodomain-containing histone rearranges chromatin upon sensing PARP1 activation. *Nature structural & molecular biology* **16**, 923-9 (2009).
128. Krishnakumar, R. *et al.* Reciprocal binding of PARP-1 and histone H1 at promoters specifies transcriptional outcomes. *Science* **319**, 819-21 (2008).
129. Hassa, P.O., Covic, M., Bedford, M.T. & Hottiger, M.O. Protein arginine methyltransferase 1 coactivates NF-kappaB-dependent gene expression synergistically with CARM1 and PARP1. *Journal of molecular biology* **377**, 668-78 (2008).
130. Hassa, P.O., Buerki, C., Lombardi, C., Imhof, R. & Hottiger, M.O. Transcriptional coactivation of nuclear factor-kappaB-dependent gene expression by p300 is regulated by poly(ADP)-ribose polymerase-1. *The Journal of biological chemistry* **278**, 45145-53 (2003).
131. Krishnakumar, R. & Kraus, W.L. The PARP side of the nucleus: molecular actions, physiological outcomes, and clinical targets. *Molecular cell* **39**, 8-24 (2010).
132. Mortusewicz, O., Ame, J.C., Schreiber, V. & Leonhardt, H. Feedback-regulated poly(ADP-ribosyl)ation by PARP-1 is required for rapid response to DNA damage in living cells. *Nucleic acids research* **35**, 7665-75 (2007).

133. Haince, J.F. *et al.* PARP1-dependent kinetics of recruitment of MRE11 and NBS1 proteins to multiple DNA damage sites. *The Journal of biological chemistry* **283**, 1197-208 (2008).
134. Ahel, D. *et al.* Poly(ADP-ribose)-dependent regulation of DNA repair by the chromatin remodeling enzyme ALC1. *Science* **325**, 1240-3 (2009).
135. Dantzer, F. *et al.* Base excision repair is impaired in mammalian cells lacking Poly(ADP-ribose) polymerase-1. *Biochemistry* **39**, 7559-69 (2000).
136. Pachkowski, B.F. *et al.* Cells deficient in PARP-1 show an accelerated accumulation of DNA single strand breaks, but not AP sites, over the PARP-1-proficient cells exposed to MMS. *Mutation research* **671**, 93-9 (2009).
137. Le Page, F., Schreiber, V., Dherin, C., De Murcia, G. & Boiteux, S. Poly(ADP-ribose) polymerase-1 (PARP-1) is required in murine cell lines for base excision repair of oxidative DNA damage in the absence of DNA polymerase beta. *The Journal of biological chemistry* **278**, 18471-7 (2003).
138. Allinson, S.L., Dianova, II & Dianov, G.L. Poly(ADP-ribose) polymerase in base excision repair: always engaged, but not essential for DNA damage processing. *Acta biochimica Polonica* **50**, 169-79 (2003).
139. Sanderson, R.J. & Lindahl, T. Down-regulation of DNA repair synthesis at DNA single-strand interruptions in poly(ADP-ribose) polymerase-1 deficient murine cell extracts. *DNA repair* **1**, 547-58 (2002).
140. Vodenicharov, M.D., Sallmann, F.R., Satoh, M.S. & Poirier, G.G. Base excision repair is efficient in cells lacking poly(ADP-ribose) polymerase 1. *Nucleic acids research* **28**, 3887-96 (2000).
141. Wang, Z.Q. *et al.* Mice lacking ADPRT and poly(ADP-ribosyl)ation develop normally but are susceptible to skin disease. *Genes & development* **9**, 509-20 (1995).
142. Berger, N.A., Sims, J.L., Catino, D.M. & Berger, S.J. Poly(ADP-ribose) polymerase mediates the suicide response to massive DNA damage: studies in normal and DNA-repair defective cells. *Princess Takamatsu symposia* **13**, 219-26 (1983).
143. Hassa, P.O. The molecular "Jekyll and Hyde" duality of PARP1 in cell death and cell survival. *Frontiers in bioscience : a journal and virtual library* **14**, 72-111 (2009).
144. Wang, Y. *et al.* Poly(ADP-ribose) (PAR) binding to apoptosis-inducing factor is critical for PAR polymerase-1-dependent cell death (parthanatos). *Science signaling* **4**, ra20 (2011).
145. Herceg, Z. & Wang, Z.Q. Failure of poly(ADP-ribose) polymerase cleavage by caspases leads to induction of necrosis and enhanced apoptosis. *Molecular and cellular biology* **19**, 5124-33 (1999).
146. Petrilli, V. *et al.* Noncleavable poly(ADP-ribose) polymerase-1 regulates the inflammation response in mice. *The Journal of clinical investigation* **114**, 1072-81 (2004).
147. Kauppinen, T.M. *et al.* Direct phosphorylation and regulation of poly(ADP-ribose) polymerase-1 by extracellular signal-regulated kinases 1/2. *Proceedings of the National Academy of Sciences of the United States of America* **103**, 7136-41 (2006).
148. Zhang, S. *et al.* c-Jun N-terminal kinase mediates hydrogen peroxide-induced cell death via sustained poly(ADP-ribose) polymerase-1 activation. *Cell death and differentiation* **14**, 1001-10 (2007).
149. Walker, J.W., Jijon, H.B. & Madsen, K.L. AMP-activated protein kinase is a positive regulator of poly(ADP-ribose) polymerase. *Biochemical and biophysical research communications* **342**, 336-41 (2006).
150. Beckert, S. *et al.* IGF-I-induced VEGF expression in HUVEC involves phosphorylation and inhibition of poly(ADP-ribose)polymerase. *Biochemical and biophysical research communications* **341**, 67-72 (2006).
151. Hassa, P.O. *et al.* Acetylation of poly(ADP-ribose) polymerase-1 by p300/CREB-binding protein regulates coactivation of NF-kappaB-dependent transcription. *The Journal of biological chemistry* **280**, 40450-64 (2005).
152. Messner, S. *et al.* Sumoylation of poly(ADP-ribose) polymerase 1 inhibits its acetylation and restrains transcriptional coactivator function. *FASEB journal : official publication of the Federation of American Societies for Experimental Biology* **23**, 3978-89 (2009).
153. Bryant, H.E. *et al.* Specific killing of BRCA2-deficient tumours with inhibitors of poly(ADP-ribose) polymerase. *Nature* **434**, 913-7 (2005).
154. Farmer, H. *et al.* Targeting the DNA repair defect in BRCA mutant cells as a therapeutic strategy. *Nature* **434**, 917-21 (2005).
155. Gottipati, P. *et al.* Poly(ADP-ribose) polymerase is hyperactivated in homologous recombination-defective cells. *Cancer research* **70**, 5389-98 (2010).
156. Tulin, A. Re-evaluating PARP1 inhibitor in cancer. *Nature biotechnology* **29**, 1078-9 (2011).
157. Veuger, S.J., Hunter, J.E. & Durkacz, B.W. Ionizing radiation-induced NF-kappaB activation requires PARP-1 function to confer radioresistance. *Oncogene* **28**, 832-42 (2009).

158. Hunter, J.E. *et al.* NF-kappaB mediates radio-sensitization by the PARP-1 inhibitor, AG-014699. *Oncogene* **31**, 251-64 (2012).
159. Hamby, A.M., Suh, S.W., Kauppinen, T.M. & Swanson, R.A. Use of a poly(ADP-ribose) polymerase inhibitor to suppress inflammation and neuronal death after cerebral ischemia-reperfusion. *Stroke; a journal of cerebral circulation* **38**, 632-6 (2007).
160. Giansanti, V., Dona, F., Tillhon, M. & Scovassi, A.I. PARP inhibitors: new tools to protect from inflammation. *Biochemical pharmacology* **80**, 1869-77 (2010).
161. Javle, M. & Curtin, N.J. The role of PARP in DNA repair and its therapeutic exploitation. *British journal of cancer* **105**, 1114-22 (2011).
162. Kornberg, R.D. & Lorch, Y. Twenty-five years of the nucleosome, fundamental particle of the eukaryote chromosome. *Cell* **98**, 285-94 (1999).
163. AT, A. DNA Packaging: nucleosomes and chromatin. *Nature Education* (2008).
164. Shen, X. & Gorovsky, M.A. Linker histone H1 regulates specific gene expression but not global transcription in vivo. *Cell* **86**, 475-83 (1996).
165. Ramakrishnan, V., Finch, J.T., Graziano, V., Lee, P.L. & Sweet, R.M. Crystal structure of globular domain of histone H5 and its implications for nucleosome binding. *Nature* **362**, 219-23 (1993).
166. Raghuram, N., Carrero, G., Th'ng, J. & Hendzel, M.J. Molecular dynamics of histone H1. *Biochemistry and cell biology = Biochimie et biologie cellulaire* **87**, 189-206 (2009).
167. Nishioka, K. *et al.* Set9, a novel histone H3 methyltransferase that facilitates transcription by precluding histone tail modifications required for heterochromatin formation. *Genes & development* **16**, 479-89 (2002).
168. Mosammaparast, N. & Shi, Y. Reversal of histone methylation: biochemical and molecular mechanisms of histone demethylases. *Annual review of biochemistry* **79**, 155-79 (2010).
169. Gibson, B.A. & Kraus, W.L. New insights into the molecular and cellular functions of poly(ADP-ribose) and PARPs. *Nature reviews. Molecular cell biology* **13**, 411-24 (2012).
170. Altmeyer, M. & Hottiger, M.O. Poly(ADP-ribose) polymerase 1 at the crossroad of metabolic stress and inflammation in aging. *Aging* **1**, 458-69 (2009).
171. Hottiger, M.O. ADP-ribosylation of histones by ARTD1: an additional module of the histone code? *FEBS letters* **585**, 1595-9 (2011).
172. Adamietz, P. & Hilz, H. Poly(adenosine diphosphate ribose) is covalently linked to nuclear proteins by two types of bonds. *Hoppe-Seyler's Zeitschrift fur physiologische Chemie* **357**, 527-34 (1976).
173. Hergeth, S.P. *et al.* Isoform-specific phosphorylation of human linker histone H1.4 in mitosis by the kinase Aurora B. *Journal of cell science* **124**, 1623-8 (2011).
174. Ogata, N., Ueda, K., Kagamiyama, H. & Hayaishi, O. ADP-ribosylation of histone H1. Identification of glutamic acid residues 2, 14, and the COOH-terminal lysine residue as modification sites. *The Journal of biological chemistry* **255**, 7616-20 (1980).
175. Wisniewski, J.R., Zougman, A., Kruger, S. & Mann, M. Mass spectrometric mapping of linker histone H1 variants reveals multiple acetylations, methylations, and phosphorylation as well as differences between cell culture and tissue. *Molecular & cellular proteomics : MCP* **6**, 72-87 (2007).
176. Zheng, Y. *et al.* Histone H1 phosphorylation is associated with transcription by RNA polymerases I and II. *The Journal of cell biology* **189**, 407-15 (2010).
177. Weiss, T. *et al.* Histone H1 variant-specific lysine methylation by G9a/KMT1C and Glp1/KMT1D. *Epigenetics & chromatin* **3**, 7 (2010).
178. Trojer, P. *et al.* Dynamic Histone H1 Isotype 4 Methylation and Demethylation by Histone Lysine Methyltransferase G9a/KMT1C and the Jumonji Domain-containing JMJD2/KDM4 Proteins. *The Journal of biological chemistry* **284**, 8395-405 (2009).
179. Wang, P. *et al.* Global analysis of H3K4 methylation defines MLL family member targets and points to a role for MLL1-mediated H3K4 methylation in the regulation of transcriptional initiation by RNA polymerase II. *Molecular and cellular biology* **29**, 6074-85 (2009).
180. Kassner, I. University of Zürich (2012).

Acknowledgement

I am very thankful to everyone who helped and supported me during my studies and while working on this Doctoral thesis.

First of all, I want to thank Prof. Dr. Dr. Michael Hottiger for giving me the opportunity to work in his group and sharing his knowledge with me. His continuous support and motivation helped me to accomplish this thesis. Thanks for the carrot and the stick.

I would also like to thanks Prof. Dr. Hans-Peter Nägeli for agreeing to review my thesis.

My special thanks goes to Ingrid Kassner for leading me through this whole project. She always had time for me, solved all my little problems and never lost her patience. She was the best possible supervisor for me.

Thanks to Monika Fey for all the solution I could "borrow" from her and all the help she offered. Further, I would like to thank Florian Freienmoser for correcting my thesis.

Many thanks to the whole Hottiger group and all other members of the institute, without you it would not have been so much fun to stick around all day long in the lab. The nice atmosphere, the jokes (even the ones at my expense), the good vibes and your support made it an enjoyable experience. Thanks for the funny, motivating and never boring coffee breaks.

Last but not least I want to thank my family: my parents; who support me in everything I do, my sisters; who bring me back to earth when it is needed and always stick with me no matter what, my one and only Raja; for taking me out for a walk and all the patience she needed. Finally, a special thank to my friends and roommates for all the support (especially Reto Mühlemann, layout guy), for being how they are and for the food they cooked. Thanks to Jäcqui for bearing me and bringing all this pleasure into my life.

Curriculum Vitae

Vorname Name	Marc André Barandun
Geburtsdatum	13/07/1986
Geburtsort	Frauenfeld
Nationalität	Schweiz
Heimatort bei Schweizern	Feldis GR
Schulausbildung	08/2002 – 07/2006 Kantonsschule, Frauenfeld, Schweiz
Höchster Schulabschluss	07/2006 Matura, Kantonsschule, Frauenfeld, Schweiz
Studium	09/2007 – 01/2013 Veterinärmedizin, Universität Zürich, Schweiz
Abschlussprüfung vet. med.	31/01/2013 Universität Zürich, Schweiz
Anfertigung der Dissertation	09/2011 – 07/2014 unter Leitung von Prof. Dr. Dr. Michael O. Hottiger am Institut für Veterinärchemie und Molekularbiologie der Vetsuisse Fakultät, Universität Zürich
Fachrelevante Anstellungen	08/2013 – 07/2014 Internship, Bessy's Kleintierklinik, Watt, Schweiz